IAEA-TECDOC-1687

Fuel Modelling at Extended Burnup (FUMEX-II)

Report of a Coordinated Research Project 2002–2007

IAEA
International Atomic Energy Agency

Fuel Modelling at Extended Burnup (FUMEX-II)

The following States are Members of the International Atomic Energy Agency:

AFGHANISTAN
ALBANIA
ALGERIA
ANGOLA
ARGENTINA
ARMENIA
AUSTRALIA
AUSTRIA
AZERBAIJAN
BAHRAIN
BANGLADESH
BELARUS
BELGIUM
BELIZE
BENIN
BOLIVIA
BOSNIA AND HERZEGOVINA
BOTSWANA
BRAZIL
BULGARIA
BURKINA FASO
BURUNDI
CAMBODIA
CAMEROON
CANADA
CENTRAL AFRICAN REPUBLIC
CHAD
CHILE
CHINA
COLOMBIA
CONGO
COSTA RICA
CÔTE D'IVOIRE
CROATIA
CUBA
CYPRUS
CZECH REPUBLIC
DEMOCRATIC REPUBLIC OF THE CONGO
DENMARK
DOMINICA
DOMINICAN REPUBLIC
ECUADOR
EGYPT
EL SALVADOR
ERITREA
ESTONIA
ETHIOPIA
FINLAND
FRANCE
GABON
GEORGIA
GERMANY
GHANA
GREECE
GUATEMALA
HAITI
HOLY SEE
HONDURAS
HUNGARY
ICELAND
INDIA
INDONESIA
IRAN, ISLAMIC REPUBLIC OF
IRAQ
IRELAND
ISRAEL
ITALY
JAMAICA
JAPAN
JORDAN
KAZAKHSTAN
KENYA
KOREA, REPUBLIC OF
KUWAIT
KYRGYZSTAN
LAO PEOPLE'S DEMOCRATIC REPUBLIC
LATVIA
LEBANON
LESOTHO
LIBERIA
LIBYA
LIECHTENSTEIN
LITHUANIA
LUXEMBOURG
MADAGASCAR
MALAWI
MALAYSIA
MALI
MALTA
MARSHALL ISLANDS
MAURITANIA
MAURITIUS
MEXICO
MONACO
MONGOLIA
MONTENEGRO
MOROCCO
MOZAMBIQUE
MYANMAR
NAMIBIA
NEPAL
NETHERLANDS
NEW ZEALAND
NICARAGUA
NIGER
NIGERIA
NORWAY
OMAN
PAKISTAN
PALAU
PANAMA
PAPUA NEW GUINEA
PARAGUAY
PERU
PHILIPPINES
POLAND
PORTUGAL
QATAR
REPUBLIC OF MOLDOVA
ROMANIA
RUSSIAN FEDERATION
RWANDA
SAUDI ARABIA
SENEGAL
SERBIA
SEYCHELLES
SIERRA LEONE
SINGAPORE
SLOVAKIA
SLOVENIA
SOUTH AFRICA
SPAIN
SRI LANKA
SUDAN
SWEDEN
SWITZERLAND
SYRIAN ARAB REPUBLIC
TAJIKISTAN
THAILAND
THE FORMER YUGOSLAV REPUBLIC OF MACEDONIA
TUNISIA
TURKEY
UGANDA
UKRAINE
UNITED ARAB EMIRATES
UNITED KINGDOM OF GREAT BRITAIN AND NORTHERN IRELAND
UNITED REPUBLIC OF TANZANIA
UNITED STATES OF AMERICA
URUGUAY
UZBEKISTAN
VENEZUELA
VIETNAM
YEMEN
ZAMBIA
ZIMBABWE

The Agency's Statute was approved on 23 October 1956 by the Conference on the Statute of the IAEA held at United Nations Headquarters, New York; it entered into force on 29 July 1957. The Headquarters of the Agency are situated in Vienna. Its principal objective is "to accelerate and enlarge the contribution of atomic energy to peace,

IAEA-TECDOC-1687

FUEL MODELLING AT EXTENDED BURNUP (FUMEX-II)

REPORT OF A COORDINATED RESEARCH PROJECT 2002–2007

INTERNATIONAL ATOMIC ENERGY AGENCY
VIENNA, 2012

For further information on this publication, please contact:

Nuclear Power and Technology Development Section
International Atomic Energy Agency
Vienna International Centre
PO Box 100
1400 Vienna, Austria
Email: Official.Mail@iaea.org

Printed by the IAEA in Austria
August 2012

IAEA Library Cataloguing in Publication Data

Fuel modelling at extended burnup (FUMEX-II) :
report of a coordinated research project 2002 – 2007. – Vienna : International Atomic Energy Agency, 2012.
p. ; 30 cm. – (IAEA-TECDOC series, ISSN 1011-4289 ; no. 1687)
ISBN 978-92-0-133810-5
Includes bibliographical references.

1. Nuclear reactors – Safety measures. 2. Fuel burnup (Nuclear engineering) – Mathematical models – Data processing. 3. Nuclear power plants – Power distribution. I. International Atomic Energy Agency. II. Series.

IAEAL 12-00768

FOREWORD

It is fundamental to the future of nuclear power that reactors can be run safely and economically to compete with other forms of power generation. As a consequence, it is essential to develop the understanding of fuel performance and to embody that knowledge in codes to provide best estimate predictions of fuel behaviour. This, in turn, leads to a better understanding of fuel performance, a reduction in operating margins, flexibility in fuel management and unproved operating economics.

Reliable prediction of fuel behaviour constitutes a basic demand for safety based calculations, for design purposes and for fuel performance assessments. Owing to the large number of interacting physical, chemical and thermomechanical phenomena occurring in the fuel rod during irradiation, it is necessary to perform calculations using computer codes. The ultimate goal is a description of fuel behaviour in both normal and abnormal conditions. From this knowledge, operating rules can be derived to prevent fuel failures and the release of fission products to the environment, and also, in extreme cases, to prevent escalation of fuel and core damage and the consequential hazards.

The IAEA has therefore embarked on a series of programmes addressing different aspects of fuel behaviour modelling with the following objectives:

- To assess the maturity and prediction capabilities of fuel performance codes, and support interaction and information exchange between countries with code development and application needs (FUMEX series);
- To build a database of well-defined experiments suitable for code validation in association with the OECD/NEA;
- To transfer a mature fuel modelling code to developing countries, to support teams in these countries in their efforts to adapt the code to the requirements of particular reactors, and to give guidance on applying the code to reactor operation and safety assessments;
- To provide guidelines for code quality assurance, code licensing and code application to fuel licensing.

This report describes the results of the coordinated research project on fuel modelling at extended burnup (FUMEX-II). This programme was initiated in 2000 and completed in 2006. It followed previous programmes on fuel modelling, D-COM which was conducted between 1982 and 1984, and the FUMEX programme which was conducted between 1993 and 1996.

The participants used a mixture of data, derived from actual irradiation histories, in particular those with PIE measurements from high burnup commercial and experimental fuels, combined with idealized power histories intended to represent possible future extended dwell, commercial irradiations, to test code capabilities at high burnup. All participants have carried out calculations on the six priority cases selected from the 27 cases identified to them at the first research coordination meeting (RCM). At the second RCM, three further priority cases were identified and have been modelled. These priority cases have been chosen as the best available to help determine which of the many high burnup models used in the codes best reflect reality. The participants are using the remaining cases for verification and validation purposes as well as inter-code comparisons.

The codes participating in the exercise have been developed for a wide variety of purposes, including predictions for fuel operation in PWR, BWR, WWER, the pressurized HWR type, CANDU and other reactor types. They are used as development tools as well as for routine licensing calculations, where code configuration is strictly controlled.

FUMEX-II was made possible as a result of the support and dedication of many organizations and individuals. The IAEA would like to thank the International Working Group on Fuel Performance and Technology (IWGFPT) for suggesting and supporting the programme, the OECD Halden Reactor Project for providing experimental data and the participants for performing the calculations and submission of summaries and meeting contributions. During the course of FUMEX-II, the IAEA was

advised by experts who also prepared the intermediate working material and the final report. They were led by J.A. Turnbull (United Kingdom). The IAEA officer responsible for this publication was J. Killeen.

EDITORIAL NOTE

The use of particular designations of countries or territories does not imply any judgement by the publisher, the IAEA, as to the legal status of such countries or territories, of their authorities and institutions or of the delimitation of their boundaries.

The mention of names of specific companies or products (whether or not indicated as registered) does not imply any intention to infringe proprietary rights, nor should it be construed as an endorsement or recommendation on the part of the IAEA.

CONTENTS

1. INTRODUCTION

The coordinated research programme (CRP) on Fuel Modelling at Extended Burnup (FUMEX-II) was initiated by the IAEA following a recommendation of the International Working Group on Fuel Performance and Technology (IWGFPT). It was conducted over the period 2002–2006. Seventeen countries took part. The FUMEX-II programme continued the work of the former CRP on The Development of Computer Models for Fuel Element Behaviour in Water Reactors (D-COM), which started in 1982 and was terminated in 1984, and the FUMEX CRP Fuel Modelling at Extended Burnup which started in 1993 and concluded in 1996.

The participants and codes used in the three code comparison exercises, D-COM Blind, FUMEX-I and FUMEX-II are given in Tables 1, 2 and 3 respectively.

1.1. THE D-COM BLIND EXERCISE

The list of participants in the D-COM blind exercise is given in Table 1. The detailed consultants' report presenting the state of the art in modelling the fuel rod behaviour and including a comprehensive review of fuel rod computer codes at that time is given in Refs [1, 2].

TABLE 1. PARTICIPANTS IN THE D-COM BLIND PROBLEM

Country	Organization	Code
Denmark	RISC	Experiment
Argentina	CNEA	BACO
Belgium	BN	COMETHE III-L
Canada	AECL	ELESIM2.MOD10
Czechoslovakia	Rez	PIN/RELA
F.R. Germany/CEC	TU-Darmstadt/ITU	URANUS
Finland	VTT	FRAPCON-2
France	CEA-Grenoble	CREOLE
France	EdF	CYRANO-2
France	CEN-Saclay	RESTA
India	BARC	PROFESS
Japan	CRIEPI	FEMAXI-III
Sweden	Studsvik	GAPCON-SV
United Kingdom	BNFL	HOTROD
United Kingdom	UKAEA	MIN1PAD-E
United States of America	Exxon	RAMPX2

As part of this programme, a code exercise was conducted [3], where the objective was to investigate the capability of fuel performance codes to predict fission gas release. The test cases to be calculated by the codes consisted of three mini pins irradiated together (test HP 096) in the Danish DR 3 test reactor to a burnup of 32 MW·d/kgU. Two of the pins were finally bumped together with average heat ratings of 33.7 and 36.2 kW/m respectively at the end of bump. The blind code predictions were presented at the OECD/NEA/CSNI/IAEA Specialists Meeting on Water Reactor Fuel Safety and Fission Product Release in Off-Normal and Accident Conditions, Risø National Laboratory, 1983 [4]. However, the results were not included in the proceedings of the meeting, but some are given in Ref. [5].

The main conclusions from the D-COM exercise were as follows:

- Temperature: Temperature predictions showed a large spread.
- Fission gas release: Fission gas release during the base irradiation was in fair agreement with experimental values. The fission gas release during the transient (bump test) was under-predicted by most of the codes.
- Mechanical behaviour: Since the exercise concentrated on the thermal behaviour and gas release, many participants did not provide dimensional data. Of those codes which submitted mechanical data most codes predicted the cladding creep down reasonably well, mechanical data during the ramp were scarce and showed considerable spread.

The D-COM blind code exercise was considered by participants as being very valuable in promoting discussions among modellers. A better knowledge of the centre line temperature during base irradiation was identified as an area of further development. It was also stated in the conclusions that basic phenomena such as gaseous swelling, transient gas release and grain growth should be better known during transients.

The subsequent experimental programmes both at Halden and Risø addressed these requests. Within these projects it was demonstrated that the fuel thermal conductivity degrades with burnup and can be modelled by an additional phonon contribution. The effect of this degradation is a higher fuel temperature which partially explains the general under-prediction of fission gas release in the transient of the D-COM blind prediction. It is of interest to note that some modelling groups that participated in the D-COM exercise also participated in the FUMEX blind exercise. This list is shown in Table 2.

1.2. THE FUMEX BLIND EXERCISE

Following the D-COM exercise, the IAEA initiated a second code comparison exercise in 1993 addressing fuel thermal performance and fission gas release at high burnup as well as aspects of pellet-cladding mechanical interaction. There were a total of six cases, FUMEX 1–6 including 10 rods, which represented actual irradiations in the OECD Halden heavy water reactor in Norway.

The FUMEX CRP was initiated by the IAEA following a recommendation of the IWGFPT. It was conducted over the period 1993–1996. Fifteen countries took part. The FUMEX programme continued the work of the former CRP on The Development of Computer Models for Fuel Element Behaviour in Water Reactors (D-COM), which started in 1982 and was terminated in 1984. The participants are shown in Table 2.

The elements of the CRP were defined as follows:

- A blind prediction carried out by the participants on data provided by the Halden Project, Norway, in the form of irradiation histories, in-pile measurements and post irradiation examination (PIE) of six experiments involving 10 fuel rods. Only after all the predictions were submitted were the measurements released.
- A comparison of calculations carried out after code improvement on the 10 rods of the FUMEX blind exercise.
- The definition of eight simplified cases, to assess code response to changes of single parameters such as internal gas composition, burnup, power steps, and a statistical analysis of two of the simplified cases.
- Follow-up of code status, progress in modelling and modification made at research coordination meetings (RCMs), also providing a forum for discussion and interaction among participants.

TABLE 2. PARTICIPANTS IN THE FUMEX EXERCISE

Country	Organization	Code
Norway/OECD	Halden	Experimental data provider
Argentina	CNEA	BACO
Bulgaria	INRNE	PIN micro
Canada	AECL	ELESIM.MOD11
CEC	ITU	TRANSURANUS
China	CIAE	FRAPCON-2
Czech Republic	NRI Rez	PIN/W
Finland	VTT	ENIGMA 5. 8f
France	CEA/DRN	METEOR-TRANSURANUS
France	EdF	TRANSURANUS-EdF 1.01
India	BARC	PROFESS
India	BARC	FAIR
India	NPC	FUDA
Japan	CRIEPI	EIMUS
Japan	NNFD	TRUST Ib
Romania	INR	ROFEM-1B
Russian Federation	IIM	START 3
Switzerland	PSI	TRANSURANUS-PSI
United Kingdom	BNFL	ENIGMA 5.2
United Kingdom	NE	ENIGMA 5.8 D

Note: Turkey joined the CRP at the time of the 3rd RCM in Bombay. Turkey used a version of FRAPCON-2.

In early 1993 the specifications of six experiments performed at the Halden Project (Norway) were distributed to the participants. The first research coordination meeting took place in Halden, 28 June–1 July 1993. During this meeting a description of the 19 codes was given and the preliminary results were released.

The second RCM took place on 15–16 September 1994 in Windermere (United Kingdom). Here, the outcome of the code predictions was discussed along with the future actions to be taken by the participants in code development and improvements. There was a general agreement that each participant should rerun the original FUMEX study, conduct a new study on simplified cases and a limited sensitivity study based on agreed uncertainties of power and dimensions to investigate the sensitivity of predictions.

The third RCM was held in Mumbai (India), 1–5 April 1996. The meeting focused on elementary model improvement, the impact of the FUMEX programme and the recommendations from the participating countries. In this meeting the role of quality assurance in developing and maintaining fuel performance codes was also introduced. The final report [6] provides a description of the experiments chosen, an overview of the codes used by participants in the exercise, and the improvements implemented as a consequence of FUMEX. A commentary is given regarding the various aspects of fuel behaviour tested and a detailed quantitative comparison is made between experimental data and code predictions. The report concludes with a discussion of the main findings of the exercise, the identified improvements and shortcomings in codes and modelling, and outstanding technical issues that require further attention.

1.2.1. Description of the codes used in the FUMEX exercise

Within the FUMEX exercise, blind predictions were submitted from 15 countries employing 19 codes or code variants. All the codes in the exercise used an axi-symmetric fuel rod representation and consisted of three main parts:

- Thermal analysis including gap conductance models which account for different pin pressures, gas compositions and gap sizes; standard correlations for the thermal conductivity of fuel and cladding are used. Standard numerical techniques such as finite difference (FD) and finite element (FE) methods are applied.
- Mechanical analysis including cracking and relocation of fuel pellets; in a few cases a simplified mechanical treatment of the fuel is adopted. However, most codes are based on an axi-symmetric, modified plane strain assumption. Two codes offer the capability of a two dimensional treatment. FD and FE methods are used.
- A variety of physical models or empirical correlations are used for densification, swelling, fission gas release, grain growth, etc. The number of executable statements ranges from 2000 up to 30 000 and all the code descriptions claimed that the codes represented state of the art modelling. Two codes were specifically designed and validated for heavy water reactors (HWR) with a collapsible cladding. As to be expected, these codes showed some deficiencies in predicting an open gap situation, and modifications were necessary when applied to the Halden irradiated rods.

1.2.2. Experimental data used for the comparison exercise

The FUMEX irradiations were all provided by the OECD Halden Reactor Project. They represented a selection of experiments from the Halden Project fuel testing programme, which focussed on the consequences of extended burnup on fuel operation. The six cases can be summarized briefly as follows:

FUMEX 1 This data set represents the irradiation of production line pressurised water reactor (PWR) type fuel under benign conditions. Temperatures remained low but increased slightly with burnup.

FUMEX 2 This was a small diameter rod designed to achieve rapid accumulation of burnup. Temperatures were estimated to remain low. The internal pin pressure was measured in-pile and an assessment of fission gas release (FGR) was also provided by PIE.

FUMEX 3 This case consisted of 3 short rods equipped with centreline thermocouples each with a different gap and fill gas composition. After steady state irradiation to approximately 30 $MW \cdot d/kgUO_2$, they were given a severe increase in power (power ramp).

FUMEX 4 Two rods filled with 3 bar He and 1 bar He/Xe mixture were irradiated to approximately 33 $MW \cdot d/kgUO_2$. Both rods experienced a period of increased power part way through the irradiation.

FUMEX 5 The test case comprised a single rod base irradiated at low power to 16 $MW \cdot d/kgUO_2$ with a power ramp and a hold period at the end of life. The main purpose of this case was to assess pellet clad mechanical interaction (PCMI) and FGR under ramp conditions.

FUMEX 6 Two rods were base irradiated at low power. The rods were refabricated to include pressure transducers. Rod internal pressure was monitored during power ramps, one fast, one slow.

The response to the FUMEX programme was very encouraging with a high degree of participation from Member States. All agreed that it was a worthwhile exercise and that the cases chosen were stringent tests of model and code performance. The exercise was useful in demonstrating the strong points of the codes as well as highlighting deficiencies where improvements were necessary. As a

consequence most of the codes underwent some development during the programme. It was also apparent that many of the codes had been developed on only a limited database and that the FUMEX cases provided a valuable addition. As a result of the FUMEX exercise, the following points were noted. It was universally recognized that the fuel conductivity decreased significantly with burnup, and at the end of the exercise, all codes included a treatment of this phenomena. It was in the area of thermal performance that the greatest improvements were made.

- The exercise showed that difficulties still remained with modelling fission gas release. However, through refining existing models and the introduction of new models there was a general improvement in predictive capabilities;
- It was apparent that the major lack of progress was in the area of mechanical interaction. This was considered to be an important omission with adverse consequences on many aspects of fuel modelling;
- The exercise showed that modern codes could be run on state of the art PCs without difficulty. Despite the complexity and degree of difficulty of the experimental cases chosen for the comparison, in general, the codes could handle the volume of data and required mathematical convergence without difficulty;
- QA was recognized as an essential part of the code development process.

A further conclusion was that there was a need for technical meetings or workshops on specific technical issues, and over the next few years, these were held at CEA Cadarache as follows:

- Thermal Performance in Light Water (High Burnup) Fuels, 3–6 March 1998, Ref. [7];
- Seminar on Fission Gas Behaviour in Water Reactor Fuels, 26–29 September 2000, Ref. [8];
- Pellet-Clad Interaction in Water Reactor Fuels (PCI-2004), 9–11 March 2004, Ref. [9].

1.3. THE FUEL PERFORMANCE EXPERIMENTS DATABASE

Running concurrent with the FUMEX exercise, the OECD/NEA Nuclear Science Committee (NSC) Task Force had recommended the compilation of a public domain database on fuel performance for the express purpose of fuel performance code development and validation. In the light of the experience during the FUMEX exercise, The IAEA actively supported this initiative and made available both data and funds for what is now known as the International Fuel Performance Experiments (IFPE) Database.

2. COORDINATED RESEARCH PROJECT, FUMEX-II

The FUMEX-II coordinated research project was initiated by the IAEA following a recommendation of the IWGFPT. It was conducted over the period 2002–2006 and seventeen Member States took part. The first RCM was held in Vienna 16–19 December 2002, the second was held at Halden, Norway, 7–10 September 2004 and the final meeting in Vienna, December 5–8 2005.

A seminar on PCI, which had been proposed at the end of the previous FUMEX CRP, was held as part of the discussions of FUMEX-II under the auspices of the OECD/NEA, Cadarache. This meeting took place in Aix-en-Provence, France from 9–11 March 2004. At the same location, consultants meetings were also held on the IFPE Database and FUMEX-II on 8 March 2004.

Further consultants meetings were held in Kendal (UK) in September 2005, Mumbai (India) in December 2006 and Vienna in November 2001 and in June 2006.

2.1. REQUIREMENTS FOR FUMEX-II

In response to requests from participants of the earlier code comparison exercises, a new CRP, FUMEX-II was launched in December 2002. The general purpose of this exercise was to expose code developers to a wide ranging database of information, namely, the IFPE database, and, through a large

number of participants, to assist compilers of the IFPE database to correct errors, detect missing data and search for additional datasets. More specifically, it was agreed that this new FUMEX-II CRP would concentrate on the predictive capabilities of codes at extended burnup, i.e. under conditions where restructuring of the pellet rim had been observed by PIE. Unlike the former exercises which required 'blind' predictions, all of the data were released at the start of FUMEX-II.

The nineteen participants of the FUMEX CRP exercise were requested to prioritize the topics they wished for inclusion in the new CRP. Fifteen answers were received with the following topics identified as important points for code improvement:

TABLE 3. QUESTIONNAIRE FOR PREFERRED TOPICS FOR FUMEX-II CRP

	Topic	Number of answers
A.	Availability of a comprehensive database for code validation	15
B.	Influence of the high burnup 'rim' structure on thermal performance and fission gas release	13
C.	Transient data on reactivity insertion accidents (RIA) and loss of coolant accidents (LOCA)	13
D.	The influence of densification and swelling on thermal performance	11
E.	Mechanical treatment of fuel pellets and PCMI	10
F.	Data on mixed oxide (MOX) fuel	10
G.	Data on intra-granular microstructure	10

2.2. DESCRIPTION OF FUMEX-II

The key elements of the FUMEX-II CRP were defined by a panel of experts at a meeting held in Vienna 26–29 November 2001. This group drew up a list of potential cases for participants to use to calibrate and compare their predictions. The original list of cases is given in the notes of the first RCM, Annex I. From this list, participants in FUMEX-II were to be requested to perform calculations for the six cases identified as high priority and a minimum of a further 4 cases at their discretion.

Subsequent to constructing the list of cases given in Annex I, it was found that a number of cases were not available. In particular, the CEA GONCOR dataset was not available. The participants agreed at the first RCM that data for the HATAC and REGATE experiments which were offered as substitutes should be used instead. These are both cases where fuel had been base irradiated in French commercial reactors before ramping in the CENG Siloe reactor. The data they provided were: FGR, cladding diameter measurements, electron probe microanalysis (EPMA) of fission product distributions and further PIE. It was agreed that both experiments should be included in the FUMEX-II list of cases and the datasets would be provided to the IAEA by early 2003. It was agreed that REGATE would be a high priority case whilst predictions against HATAC were at participant's discretion.

The original list also included Russian designed light water reactor (WWER) fuel irradiated in the Kola-3 reactor and ramp tested in the MIR test reactor. Unfortunately, agreement had not been obtained for the release of the data from the ramp tests, though the base irradiation histories became available in 2005. The ramp test data were considered of importance particularly to participants with WWER codes, therefore they were retained in the list of cases with the hope that release would be achieved within the timescale of the programme. The MIR data was finally released in 2007 and placed in the IFPE for the use of participants if required. It was not possible to obtain real histories and data for RIA and LOCA cases 24 and 25 respectively. It was agreed that these were extremely useful for testing transient codes. Kamimura (NUPEC) and Sartori (NEA) agreed to investigate the possibility of obtaining these data or idealized cases.

Case 26 identified several simplified histories which would test code application to very high burnup, these are:

26(1) To define the locus of the centre-temperature/burnup threshold for 1% FGR.

26(2a) To calculate FGR for an irradiation history of 15 kW/m constant power up to 100 MW·d/kgU.

26(2b) To calculate FGR for an irradiation history of 20 kW/m at BOL falling linearly to 10 kW/m at 100 MW·d/kgU.

26(2c) To calculate FGR for an idealized history supplied by the vendor BNFL.

At the first RCM it was agreed to add a further case, 26(2d), to be supplied by the vendor FANP which would be an idealized high burnup history for which a range of FGR measurements were available.

It was noted that five participants were concerned with the operation of pressurised heavy water reactors (PHWR or CANDU) type reactors and this system was not represented in the FUMEX-II list of cases. Because CANDU fuel elements do not have a plenum, FGR and rod internal pressure was of concern for the advanced CANDU reactor design and operating regimes. It was agreed that a further two idealized cases were to be included in the list to remedy the omission. These cases are designated 27(3a) and 27(3b).

The cases agreed by the participants at the end of the first RCM are given in Table 4 where the six highlighted cases were considered to be priority cases for all participants to complete. Further priority cases were selected at the second RCM, the notes of this meeting are given in Annex II, and these are identified with an asterix.

The codes participating in the exercise have been developed for a wide variety of purposes, including predictions for fuel operation in boiling water reactors (BWR), PWR, WWER, CANDU and other reactor types. They are used as development tools as well as for routine licensing calculations, where code configuration is strictly controlled. One particular feature has been the development of the European Commission (JRC Karlsruhe) TRANSURANUS code, to cover WWER operation. This code has been provided to several countries operating WWER reactors and several participants were using and developing a WWER version in the FUMEX-II exercise.

The list of participants and their codes and affiliations are given in Table 5. Several participants used more than one code and often code variants and development versions were used. The Indian participation was split into two teams using different codes.

It is important to recognise that the code predictions presented here are attempts at modelling very testing cases, designed to stretch the capabilities of the codes. The cases cover high burnup fuel performance where it is known that many codes under-predict fission gas release and many codes have used the results to improve their performance. Therefore, some of the presented predictions are less satisfactory, but this should not be taken to indicate that some codes do not perform well. The codes have been designed for different applications and have differing assumptions and validation ranges; for example codes intended to predict CANDU fuel operation with thin wall collapsible cladding do not need the clad creep and gap conductivity modelling found in PWR codes. Therefore, when a case is based on CANDU technology or PWR technology, it is to be expected that the codes may not agree. However, it is the very differences in such behaviour that is useful in helping to understand the effects of such internal modelling.

2.3. ADDITIONAL INFORMATION

The discussions at the first RCM are recorded in Annex I. The information includes the original case list and the revised version agreed at the meeting.

The discussions held during the second and third RCMs were important for the exchange of ideas and discussion of the issues. The records of these meetings are given in Annex II and Annex III respectively. A summary description of the codes provided by each code owner is given in the Appendix. Participants' reports to the project are appended in the CD attached to this publication.

TABLE 4. LIST OF CASES AGREED AT 1ST RCM, HIGH PRIORITY CASES ARE IN BOLD

No.	Case identification	Measurements made for comparison
1.*	Halden IFA 534.14, rod 18	EOL FGR and pressure, grain size 22 μm, Bu ≈ 52 MW·d/kgUO_2
2.*	Halden IFA 534.14, rod 19	EOL FGR and pressure, grain size 8.5 μm, Bu ≈ 52 MW·d/kgUO_2
3.	**Halden IFA 597.3, rod 7**	**Cladding elongation, at Bu ≈ 60 MW·d/kgUO_2**
4.	**Halden IFA 597.3, rod 8**	**FCT, FGR at Bu ≈ 60 MW·d/kgUO_2**
5.	Halden IFA 507, TF3	Transient temperature during power increase
6.	Halden IFA 507, TF5	Transient temperature during power increase
7.	**REGATE**	**FGR and cladding diameter during and after a transient at Bu ≈ 47** MW·d/**kg**
8	HATAC	FGR and cladding diameter during and after a transient at Bu ≈ 49 MW·d/kg
9.*	Kola-3, rod 7 from FA222	FGR, pressure and creepdown at Bu ≈ 55 MW·d/kgUO_2
10.	Kola-3, rod 52 from FA222	FGR, pressure and creepdown at Bu ≈ 46 MW·d/kgUO_2
11.*	Kola-3, rod 86 from FA222	FGR, pressure and creepdown at Bu ≈ 44 MW·d/kgUO_2
12.	Kola-3, rod 120 from FA222	FGR, pressure and creepdown at Bu ≈ 50 MW·d/kgUO_2
13.	Risø-3 AN2	Radial distribution of fission products and FGR-EOL, Bu ≈ 37 MW·d/kgUO_2
14.	**Risø-3 AN3**	**FGR and pressure–EOL, FCT, Bu ≈ 37 MW·d/kgUO_2**
15.	**Risø-3 AN4**	**FGR and pressure–EOL, FCT, Bu ≈ 37 MW·d/kgUO_2**
16.	HBEP, rod BK363	FGR–EOL, Bu ≈ 67 MW·d/kgUO_2
17.*	HBEP, rod BK365	Fission products and Pu distribution, FGR–EOL, Bu ≈ 69 MW·d/kgUO_2
18.	HBEP, rod BK370	Fission products and Pu distribution, FGR–EOL, Bu ≈ 51 MW·d/kgUO_2
19.	TRIBULATION, rod BN1/3	Pressure, FGR, cladding creepdown, Bu ≈ 52 MW·d/kgUO_2
20.	TRIBULATION, rod BN1/4	Pressure, FGR, cladding creepdown, Bu ≈ 51 MW·d/kgUO_2
21.	TRIBULATION, rod BN3/15	Pressure, FGR, cladding creepdown, Bu ≈ 51 MW·d/kgUO_2
22.	EDF/CEA/FRA, rod H09	Fission products and Pu distribution, FGR–EOL, Bu ≈ 46 MW·d/kgUO_2
23.	Kola-3 + MIR test	Temperature during ramp, FGR-EOL, Bu ≈ 55 MW·d/kgUO_2
24.	Kola-3 + MIR test	Pressure–EOL, Bu ≈ 55 MW·d/kgUO_2
25.	RIA	to be specified (real data or simplified case)
26.	LOCA	to be specified (real data or simplified case)
27.	**Simplified cases**	**(1) Temperature vs Bu for onset of FGR** **(2a) FGR for constant 15 kW/m to 100 MW·d/kgU** **(2b) FGR for 20 kW/m at BOL decreasing linearly to 10 kW/m at 100 MW·d/kgU** **(2c) FGR for idealized history supplied by BNFL** **(2d) FGR for idealized history supplied by FANP** (3a) FGR for CANDU idealized history (3b) FGR for CANDU idealized history

* These cases were added to the priority list at the 2nd RCM

Note: Abbreviations used in the Table 4 include; FCT for 'fuel centre temperature', Bu for 'burnup', BOL for 'beginning of life' and EOL for 'end of life'.

TABLE 5. LIST OF CODES AND ORGANISATIONS PARTICIPATING IN THE FUMEX-II EXERCISE

Code	Country	Institute
BACO	Argentina	CNEA
FEMAXI-PLUTON FRAPCON 3.2 MACROS-2	Belgium	Nuclear Research Center SCK CEN
PIN w99	Bulgaria	INRE
TRANSURANUS (WWER)	Bulgaria	Institute for Nuclear Research and Nuclear Energy
ELESTRES	Canada	AECL
METEOR	China	China Institute of Atomic Energy
FEMAXI–V PIN/PIN2FRAS	Czech Republic	Nuclear Research Institute, Rez
TRANSURANUS	EC	JRC Institute for Transuranium Elements
ENIGMA IMAGINE	Finland	VTT
FANP Development code (COPERNIC-3)	Germany/France	FRAMATOME ANP GmbH
FAIR FUDA PROFESS	India	BARC
FEMAXI JNES	Japan	NUPEC
INFRA	Republic of Korea	Korea Atomic Energy Research Institute
TRANSURANUS DCHAIN5V	Romania	Institute for Nuclear Research
START-3	Russian Federation	A.A. Bochvar Res. Institute of Inorganic Materials
PSI version TRANSURANUS	Switzerland	PSI
ENIGMA-B 7.7	UK	BNFL

3. THE INTERNATIONAL FUEL PERFORMANCE EXPERIMENTAL DATABASE

The aim of the International Fuel Performance Experimental Database (IFPE Database) is to provide, in the public domain, a comprehensive and well-qualified database on zircaloy-clad UO_2 fuel and recently MOX fuel for model development and code validation. The data encompass both normal and off-normal operation and include prototypic commercial irradiations as well as experiments performed in material testing reactors (MTR). To date, the database contains over 1200 individual cases, providing data on fuel centreline temperatures, dimensional changes and FGR either from in-pile pressure measurements or PIE techniques, including puncturing, EPMA and X ray fluorescence (XRF) measurements. This work in assembling and disseminating the database is carried out in close cooperation and coordination between OECD/NEA and the IAEA and the IFE/OECD/Halden Reactor Project.

The data sets are dedicated to fuel behaviour under thermal reactor irradiation, and every effort has been made to obtain data representative of BWR, PWR, WWER, CAGR and PHWR conditions. In each case, the data set contains information on the pre-characterisation of the fuel, cladding and fuel rod geometry, the irradiation history presented in as much detail as the source documents allow, and finally any in-pile or PIE measurements that were made. Special emphasis is given to data relevant for current issues such as behaviour at high burnup. The database contains, besides the compilation and evaluation of the experimental data, also the detailed primary documents from which the data were derived. The compilations contain for user convenience a synthesis with the data required for model development and validation. The IFPE contains all cases investigated both in the FUMEX-I and FUMEX-II exercises. Through the FUMEX exercises, feedback from modellers could be used to improve the content by removing some inconsistencies or errors. The IFPE database is now widely used in about 100 institutions in more than 30 countries. Feedback from users has been essential to ensure that the database improves with its use.

This database is restricted to thermal reactor fuel performance; principally with standard product Zircaloy clad UO_2 fuel, although the addition of advanced products with fuel and clad variants is not ruled out. Emphasis has been placed on including well-qualified data that illustrate specific aspects of fuel performance. Of particular interest to fuel modellers are data on: fuel temperatures, FGR, fuel swelling, clad deformation (e.g. creep-down, ridging) and mechanical interactions. Data on these issues are of great value if measured in-pile by dedicated instrumentation and in this respect, the IFPE database is fortunate in having access to several diverse experiments.

In addition to direct in-pile measurement, every effort is made to include PIE information on clad diameters, oxide thickness, hydrogen content, fuel grain size, porosity, EPMA and XRF measurements on caesium, xenon, other fission product and actinides.

4. OUTLINE DESCRIPTION OF CASES

4.1. CASES AGREED AT THE FIRST RCM

At the commencement of FUMEX-II there were no datasets addressing LOCA, RIA or MOX fuel available for use by the participants. With these exceptions, the other requirements of the participants detailed in the questionnaire responses shown in Table 3 were met by the following experiments as contained within the IFPE Database:

4.1.1. IFA-534.14 (cases 1 and 2)

These were two PWR rods with different grain size previously irradiated to 52–55 MW·d/kgUO_2 in the Goesgen reactor, re-instrumented with pressure transducers, and re-irradiated in the Halden reactor. The experiment provided on-line data on fission gas release as a function of burnup at high power. This experiment addresses items B, D of the priority list.

4.1.2. IFA-597.3 (priority cases 3 and 4)

Two sections of a BWR rod previously irradiated in Ringhals 1 at low powers to 60–62 MW·d/kgUO_2 were re-instrumented with centre-line thermocouples, a pressure transducer and a cladding elongation detector and re-irradiated in Halden. The data includes centre-line temperature, fission gas release and clad elongation at high burnup. This experiment addresses items B, D, E of the priority list.

4.1.3. IFA-507 (cases 5 and 6)

The experiment consisted of two rods equipped with centre-line thermocouples. The data obtained were in the form of fuel temperatures as a function of time during the period of increasing power. This case provided separate effects data for modellers on item C and was therefore selected for inclusion.

4.1.4. CEA/REGATE experiment (priority case 7)

There were two suitable rodlets to be included from this French irradiation program. The base - irradiation was in a power reactor up to 48 MW·d/kgUO_2 before re-fabrication and re-irradiation in the SILOE reactor where they experienced high power, up to 40 kW/m, for short periods. Experimental

data included fission gas release measurements, clad diameter/elongation at the end of life. These address items B, D and E.

4.1.5. CEA/HATAC experiment (case 8)

The experiment comprised the irradiation in the SILOE test reactor of two fuel segments taken from pre-irradiated 17 × 17 PWR fuel rods to measure the magnitude and kinetics for the release of both stable and radioactive fission gas during a succession of short transients. The sections were cut from rods irradiated in Fessenheim 1 at rod average burnup levels of 33.3 and 45.8 MW·d/kgUO_2. The base irradiation histories were typical of commercial irradiation conditions with a maximum linear heat rate not exceeding 22.5 kW/m and decreasing power towards end of life due to burn-out of the 3.1 wt% enriched fuel. Unfortunately this dataset was not made available during the duration of the CRP.

4.1.6. KOLA-3 rods (cases 9 to 12)

There is only a limited data base on WWER fuel rods. Therefore four rods were found valuable to participants interested in modelling WWER fuel behaviour. Rods identified as 7, 52, 86 and 120 from FA 222 provided data on fission gas release and rod diameter, thus satisfying the criteria A, B and D. The burnup range covered was from 40–55 MW·d/kgUO_2.

4.1.7. RISØ-3 rods AN2, AN3 and AN4 (case 13 and priority cases 14 and 15)

These are three PWR rods from the Risø-3 fission gas release programme. They were irradiated at low power approximately up to 40 MW·d/kgUO_2 before re-instrumentation with thermocouples and pressure transducers and re-irradiation in the Risø MTR. Data include on-line measurements on fuel temperatures, rod internal pressure and fission gas release. In addition, fission product radial distributions within pellets were determined during PIE. These cases address topics A, B and D.

4.1.8. High burnup effects programme (HBEP) (cases 16, 17 and 18)

From the 81 cases of the programme, BK363 and BK365 and BK370, irradiated to 51–69 MW·d/kgUO_2, provided high burnup data on fission gas release and fission product distributions measured by EPMA at the end of life. These cases fulfilled the requirements A, B and D at high burnup.

4.1.9. TRIBULATION (cases 19 to 21)

From this programme, rods BN1/3, BN1/4 and BN3/15 irradiated to ~50 MW·d/kgUO_2 fulfilled the high burnup requirements and conditions A, B and D. The data include fission gas release, rod internal pressure and cladding creep-down.

4.1.10. EDF/CEA/Framatome rod HO9 (case 22)

This PWR rod was irradiated up to 46 MW·d/kgUO_2 in a French power reactor. Data available include fission gas release and diameter measurements at end of life, fission product and plutonium distribution across pellets measured by EPMA. This case fulfils criteria A , B, D and E.

4.1.11. KOLA-3/MIR tests (cases 23 and 24)

Several rodlets, cut from full length rods of assembly 222, were tested in the MIR reactor at relatively high power. Data from two rods with burnups between 50 and 60 MW·d/kgUO_2 were selected as candidates. These rods have data on gas release and temperature during power ramps. They fulfil criteria B and D but permission to include the data was only obtained after completion of the CRP. These cases are included in the follow on exercise, FUMEX-III.

4.1.12. RIA and LOCA transients (cases 25 and 26)

From the questionnaire there was strong support for cases which tested the predictions of transient codes. Unfortunately it was found that very little data were available for these situations. For the case of RIA, permission was sought to include a case from CABRI REP–Na programme. For LOCA, permission will be sought to use the CEA FLASH 5 experimental data. In the event, only the NRU LOCA tests MT-4 and MT-6A were obtained in time for the CRP.

4.2. HIGH PRIORITY CASES

The number of cases supplied to participants was rather large, and it was unreasonable for them to compare predictions for all of them. However, one of the objectives of the programme was to evaluate the relative merits of the codes and their included models. To do this it was necessary to draw up a series of high priority cases for which all participants were expected to provide predictions. The original selection of these cases is shown in bold type in Table 4. At the 2nd RCM in Halden, additional high priority cases were identified as useful in helping to allow the modellers to discriminate which would be a good approach to modelling high burnup. In particular it was suggested that cases 1, 2 and 17 (IFA-534.14 rods 18 and 19, HBEP rod 365 respectively) were well suited and it was agreed that these should be priority cases for the next period of the CRP. For the WWER modellers, cases 9 and 11 (Kola-3 FA222 rods 7 and 86 respectively) were identified as priorities.

4.3. SIMPLIFIED CASES

In addition, all the simplified cases in case 27 were considered as high priority as these presented the best way of comparing the performance of the various models embedded in the codes**.**

- 27(1) to define the locus of the centre temperature/burnup threshold for 1% FGR; as well as an inter-code comparison, this case was useful in comparing predictions with the well-known Vitanza Criterion [10] derived from in-pile experimental measurements.
- 27(2a) to calculate FGR for an irradiation history of 15 kW/m constant power up to 100 MW·d/kgU.
- 27(2b) to calculate FGR for an irradiation history of 20 kW/m at BOL falling linearly to 10 kW/m at 100 MW·d/kgU.
- 27(2c) to calculate FGR for an idealized history supplied by BNFL.
- 27(2d) to calculate FGR for an idealized high burnup history, prepared by FANP for which a range of FGR measurements were available.
- 27(3a) and 3(b) to calculate FGR for idealized CANDU histories.

For each of these cases the modellers were provided with details of how the case should be constructed; for example, for case 27 (2d) the following guidelines were set:

- The reactor was a 15 x 15 design, modern PWR.
- The fuel rod had 22 bar helium fill gas.
- Fuel was in the form of standard UO_2 pellets, 4% enriched, 10 μm grain size (mean liner intercept, mli), low densification.
- The cladding was low corrosion Zr-4 cladding with standard creepdown.
- The irradiation history provided comprised 49 steps with 12 axial zones to a burnup of 100 MW·d/kgU.

The FGR measured on several rods exposed to the generic power history provided for case 27(2d) is given in Table 6:

TABLE 6. FGR MEASURED ON SEVERAL RODS FOR THE GENERIC POWER HISTORY

End of cycle	2	3	4	5
Full power days	673.3	1007.3	1349.0	1689.8
FGR (%)	6–8	6–8	9–13	18–20

With few exceptions, all high priority cases were tackled by participants so that a good code-to-code comparison could be made. In addition, participants were encouraged to consider other cases at their discretion. A summary of all cases attempted is given in Table 7. Tables 8, 9 and 10 provide details of the main input parameters for the priority cases.

TABLE 7. CASES CALCULATED BY THE PARTICIPANTS. THE ORIGINAL PRIORITY CASES IN BOLD

Organisation	Case number																												
	1	2	**3**	**4**	5	6	**7**	8	9	10	11	12	13	**14**	**15**	16	17	18	19	20	21	22	23	24	25	26	**1**	**27** **2**	**3**
CIAE	x	x		**X**										**X**	**X**	x	x	x										**X**	
INRNE (E)	x	x	**X**	**X**			**X**		x	x	x	x		**X**	**X**	x	x	x									**X**	**X**	
NUPEC	x	x	**X**	**X**			**X**	x					x	**X**	**X**	x	x	x	x	x	x						**X**	**X**	
VTT	x	x	**X**	**X**			**X**																				**X**	**X**	
Bochvar Inst.	x	x	**X**	**X**			**X**							**X**	**X**	x	x	x									**X**	**X**	**X**
KAERI	x	x	**X**	**X**			**X**						x	**X**	**X**	x	x	x	x	x	x	x					**X**	**X**	
CNEA	x	x	**X**	**X**	x	x	**X**		x	x	x	x	x	**X**	**X**	x	x	x	x	x	x	x					**X**	**X**	**X**
PSI	x	x	**X**	**X**			**X**							**X**	**X**		x										**X**	**X**	
INR			**X**	**X**										**X**	**X**	x	x	x											**X**
BNFL	x	x		**X**			**X**							**X**	**X**												**X**	**X**	
BARC (S)	x	x	**X**	**X**			**X**		x	x	x			**X**	**X**	x	x	x									**X**	**X**	**X**
BARC (D)	x	x	**X**	**X**			**X**							**X**	**X**		x										**X**		**X**
AECL	x	x		**X**			**X**		x	x	x	x		**X**	**X**	x	x	x									**X**	**X**	**X**
SCK CEN	x	x	**X**	**X**			**X**							**X**	**X**												**X**	**X**	
FANP	x	x	**X**	**X**			**X**							**X**	**X**	x	x										**X**	**X**	
INRNE (S)	x	x	**X**	**X**			**X**		x	x	x	x					x												
NRI	x	x							x		x					x	x	x									**X**	**X**	
ITU	x	x	**X**	**X**			**X**							**X**	**X**		x										**X**	**X**	**X**

Cases 1, 2 and 17 (IFA-534.14 rods 18 & 19, HBEP rod 365 respectively) were agreed to be additional priority cases for the second period of the CRP. For the WWER modellers, cases 9 and 11 (Kola-3 FA222 rods 7 and 86 respectively) were identified as priorities.

TABLE 8. MAIN CHARACTERISTICS OF EXPERIMENTAL FUEL RODS OF THE PRIORITY CASES

Case		1	2	3	4	7	14	15	17
Fuel rod		Rod 18	Rod 19	Rod 7	Rod 8	REGATE	AN 3	AN 4	BK365
Fuel stack length	mm	411	411	362.5	353.9	436.0	286.0	292.0	1017
Length of hollow section	mm	0.0	0.0	0.0	34.0	0.0	41.5	41.0	1017
Length of cylindrical plenum	mm	100.0	100.0	117.9	117.9	48.15	29.45	34.0	72.5
Mean diam. Gap	μm	170.0	170.0	211	211	168	205	205	168.6
Fuel pellet									
Dishing				One end	One end	Both ends	Both ends	Both ends	Both ends
Outer diameter	mm	9.12	9.12	10.439	10.439	8.192	9.053	9.053	8.188
Inner diameter	mm	0.0	0.0	0.0	2.5	0.0	2.5	2.5	2.475
Surface roughness	μm	1.0*	1.0*	1.38	1.38	1.0*	1.0	1.0	1.5*
Initial porosity	%	3.9	3.3	4.28	4.28	5.246	6.26	6.26	7.5
Open porosity	%	0.1	0.1	0.1	0.1	0.566	0.07	0.07	3.9
Porosity at end of densification	%	3.5*	2.4*	3.06	3.06	3.9*	3.93	3.93	6.7
Grain diameter	μm	22.1	8.5	7.83	7.83	13.53–16.65	6.00	6.00	13.5
Initial content of ^{235}U	wt%	3.84	3.79	3.347	3.347	4.487	2.95	2.95	6.97
Cladding									
Cladding material		Zry-4	Zry-4	Zry-2	Zry-2	Zry-4	Zry-4	Zry-4	Zry-4
Outer diameter	mm	10.75	10.75	12.250	12.250	9.50	10.810	10.810	9.515
Inner diameter	mm	9.29	9.29	10.650	10.650	9.36	9.258	9.258	8.3565
Surface roughness	μm	1.0*	1.0*	1.3	1.3	1.0*	1.0	1.0	0.955

* Best estimate data – values not provided

TABLE 9. SPECIFIC INPUT PARAMETERS USED FOR THE SIMULATION OF THE PRE-IRRADIATION

Case		1	2	3	4	7	14	15	17
Fuel rod		Rod 18	Rod 19	Rod 7	Rod 8	REGATE	AN 3	AN 4	BK365
Number of axial slices		3	3	3	4	8	6	6	10
Effective plenum volume	cm^3	5.1	5.1	4.62	4.58	1.69	1.69	2.10	4.0
Total free volume	cm^3	6.1	6.1	6.00	6.00	3.01	2.90	3.34	11.9
Fill gas		He	He	He	He	He	He	He	He
Initial pressure (at 20 °C)	MPa	2.15	2.15	0.10	0.10	2.50	2.31	2.31	2.88
Irradiation conditions									
Reactor type		PWR	PWR	HBWR	HBWR	PWR	PWR	PWR	PWR
Fast neutron flux (per linear heat rate)	$n \cdot cm^{-2} \cdot s^{-1}$ (per kW/m)	$5 \cdot 10^{12}$	$5 \cdot 10^{12}$	$2.3 \cdot 10^{12}$	$2.3 \cdot 10^{12}$	$3.8–4.8 \cdot 10^{12}$*	$3.4 \cdot 10^{12}$	$3.4 \cdot 10^{12}$	$2.716 \cdot 10^{12}$
Coolant inlet temperature	°C	308	308	286	286	300	287.7	287.7	255
Coolant mass flux	$kg \cdot m^{-2} \cdot s^{-1}$	3127	3127	1400**	1400**	3865	n/a**	n/a**	n/a**
Coolant pressure	MPa	15.5	15.5	7.00	7.00	15.5	15.52	15.52	13.73

* Prescribed time dependence

** Coolant mass flux not generally available so given as an approximate value, however, in the IFPE data, the cladding outer temperature was prescribed for each axial node.

TABLE 10. SPECIFIC INPUT PARAMETERS APPLIED FOR THE COMPUTATION OF THE RAMP TESTS WITH RE-FABRICATED RODS

Case		1	2	3	4	7	14	15
Fuel rod		Rod 18	Rod 19	Rod 7	Rod 8	REGATE	AN 3	AN 4
Number of axial slices		3	3	3	4	8	6	6
Effective plenum volume	cm^3	5.1	5.1	4.62	4.58	1.69	5.77	5.74
Total free volume	cm^3	6.1	6.1	6.00	6.00	3.01	7.00	7.90
Fill gas		He	He	He	He	He	He	Xe
Initial pressure (at 20 °C)	MPa	2.15	2.15	0.50	0.50	not modified	1.57	0.10
Irradiation conditions								
Reactor type		HWR	HWR	HWR	HWR	PWR	PWR	PWR
Fast neutron flux (per linear heat rate)	$n \cdot cm^{-2} \cdot s^{-1}$ (per kW/m)	$1.6 \cdot 10^{11}$	$1.6 \cdot 10^{11}$	$1.6 \cdot 10^{11}$	$1.6 \cdot 10^{11}$	$4.5 \cdot 10^{12}$	$4.0 \cdot 10^{11}$	$4.0 \cdot 10^{11}$
Coolant inlet temperature	°C	232	232	232	232	n/a	n/a	n/a
Coolant mass flux	$kg \cdot m^{-2} \cdot s^{-1}$	0*	0*	0*	0*	n/a**	n/a**	n/a**
Coolant pressure	MPa	3.2	3.2	3.2	3.2	13.0	15.3	15.3

* Natural convection

** Coolant mass flux not available or only available as an approximate value; however, the cladding outer temperature was prescribed for each axial node

5. CODE COMPARISONS

5.1. CODE INFORMATION

Following on from FUMEX-1, one objective of the present CRP was to see how code development had progressed in the intervening period and in particular, how the development to address higher burnup behaviour had been accomplished.

In order to compare the various approaches, at the 2nd RCM, two tables were constructed. The first, Table 11, gives an overall impression of each code, the mechanisms considered, the range of application and the code usage. This table has been simplified to give an overall picture of the structure of the codes. Several participants provided comments to their entries to this table which have been removed. They noted that the model descriptor headings did not necessarily quite fit what was in their particular code and the descriptions of the codes in the final reports by the participants appended to this report should be consulted for fuller details.

The second more detailed table itemizes the features of individual models within each code. This was completed by each participant and is reproduced here as Table 12. In the discussions that follow, this table is used as a framework to introduce and compare the various approaches used in high burnup modelling.

In several cases, the highest burnup for which a code was developed was dependent on its potential application. For example, the Argentine BACO and the Canadian ELESTRES codes are only required for low burnup application, hence many of the features specific to high burnup modelling, e.g. ‘rim’ formation are absent. There were four versions of the TRANSURANUS code used by ITU, Bulgaria, Romania and PSI Switzerland; these will be considered identical unless stated otherwise. The TRANSURANUS users group work together to develop the code, with the reference version held by ITU, so whilst the main code remains unchanged, various development models are tested by the various groups.

TABLE 11. QUESTIONNAIRE ON CODE STRUCTURE AND MODELS (SIMPLIFIED RESPONSES)

Code	Organisation	Based on	Mechanics																
			Code structure			fuel				Clad				Contact			Failure		
			Axial symmetry	**Finite element**	**Finite difference**	**Plain strain**	**Plain stress**	**Cracked pellet**	**Solid**	**Plain strain**	**Shell**	**Solid**	**Corrosion**	**Ridging**	**Stick**	**Sliding (non zero contact force)**	**cracking**	**Stress corrosion**	**Damage accumulation**	**Failure model**
BACO	CNEA		X		X	X	X	X		X					X	X	X			
COPERNIC3	FANP																			
ENIGMA	VTT																			
ENIGMA-B 7.7	BNFL		X		X	X		X		X	X			X	X		X			
DCHAIN 5V	INR																			
ELESTRES	AECL		X	X	X	X	X	X	X	X	X		X	X	X	X	X	X	X	X
FAIR	BARC		X	X				X			X				X				X	
FEMAXI-JNES	NUPEC	FEMAXI-4	X	X				X	X			X	X	X	X	X		X	X	
FEMAXI-V	INR			X		X	X	X			X					X				
FEMAXI-V mod 1	SCK CEN	FEMAXI-V	X	X		X	X	X			X				X	X				
FRAPCON 3.2	SCK CEN																			
IMAGE	VTT																			
INFRA	KAERI		X	X	X	X		X		X			X	X	X	X				
MACROS-II	SCK CEN	PLUTON-II	X		X	X	X	X		X	X			X	X	X			X	X
METEOR	CIAE																			
PIN2K	NRI				X	X	X	X			X									
PIN w99	INRNE		X		X	X					X									
PROFESS	BARC		X		X					X	X		X		X					
START-3	Bochvar Inst.		X		X	X		X		X					X			X	X	X
TRANSURANUS	ITU	URANUS	X	X	X	X		X		X	X		X		X	X		X	X	X
TRANSURANUS	INRNE																			
TRANSURANUS	INR																			
TRANSURANUS-PSI	PSI																			

TABLE 11. QUESTIONNAIRE ON CODE STRUCTURE AND MODELS (SIMPLIFIED RESPONSES) (cont.)

Code	Investigator	Burnup dependence						Fission gas release models							Code usage				Code application		
		Thermal conductivity	**Rim effect**	**Failure mechanism**	**Densification and swelling**	**Mechanical properties (fuel)**	**Melting point (fuel)**	**Diffusion**	**Grain sweeping**	**Percolation**	**Integrated swelling model**	**He adsorption & release**	**Grain growth**	**High Burnup structure**	**Empirical**	**R&D**	**Development**	**Licensing**	**Normal operating conditions QA**	**Accident conditions**	**Interim storage**
BACO	CNEA	X		X				X	X	X					X	X			X			
COPERNIC3	FANP																					
ENIGMA	VTT																					
ENIGMA-B 7.7	BNFL	X	X					X			X	X				X	X	X				
DCHAIN 5V	INR							X	X				X			X						
ELESTRES	AECL	X		X	X	X		X	X	X	X		X			X	X	X	X	X		
FAIR	BARC	X	X					X								X						
FEMAXI-JNES	NUPEC	X	X		X			X	X		X							X				
FEMAXI-V	INR	X	X	X	X			X	X	X	X					X						
FEMAXI-V mod 1	SCK CEN	X	X		X			X	X							X	X					
FRAPCON 3.2	SCK CEN																					
IMAGE	VTT																					
INFRA	KAERI	X	X		X	X	X	X		X				X		X	X		X	X		
MACROS-II	SCK CEN	X	X	X	X			X	X	X						X	X					
METEOR	CIAE																					
PIN2K	NRI	X	X					X	X	X						X						
PINw99	INRNE	X	X					X	X							X				X		
PROFESS	BARC	X	X		X			X	X		X		X	X	X	X	X			X		
START-3	Bochvar Inst.	X	X	X	X	X	X	X		X	X		X	X		X	X	X		X		
TRANSURANUS	ITU	X	X	X	X	X		X	X		X		X	X		X	X	X	X	X	X	X
TRANSURANUS	INRNE																					
TRANSURANUS	INR																					
TRANSURANUS-PSI	PSI							X	X													

TABLE 12. DETAILED MODELLING OF HIGH BURNUP

Code	Country/affiliation	High burnup fuel pellet rim								
		Porosity limited	Interlinkage small	FGR from rim	Burnup degradation of λ limited/ reduced	Matrix swelling limited/reduced	Full porosity contribution to swelling	Temperature limit for rim formation	Influence of stress and/or grain size on rim formation	Separate treatment of transition zone
BACO	Argentina/CNEA	-	no	no	-	-	-	no	-	-
ELESTRE	Canada/AECL	no extra rim porosity	-	no	-		no	no		
ENIGMA	Finland/VTT	-	-	no	-		-	-		
ENIGMA-B	UK/BNFL	no limit	no interlinkage modelled	no	no	no	yes	no limit	no	no
FAIR	India	yes	no	yes?	yes		no	yes		
COPERNIC development	France, Germany, US FANP	yes	yes	yes	yes	yes	yes	yes	no, mere dependence on local BU	no
FEMAXI	Belgium/SCK.CEN	no	no	no	yes		yes	-		
FEMAXI	Czech Republic/NRI	no	no	yes	yes	no?	no?	no	no	no
FEMAXI-JNES	Japan/JNES	no	no	yes	yes	no	no	yes	no	no
INFRA	Korea/KAERI	no limit	yes	no	no (mechanistic model)	no	yes	no limit but depending on Temp	no	no
MACROS	Belgium/SCK.CEN	no limit	not applicable	no	mechanistic concept		yes	no limit		yes
METEOR	China/CIAE	no	yes	yes	yes		no	yes	no	no
PINw99	Bulgaria/Czech Rep.	no limit	no	no	no/no		no	no/yes		
PIN2001	Czech Rep/NRI Rez	limit	no	yes	no	no	yes	no	no	no
PROFESS	India / BARC	no limit	-	yes	no	no	yes	no	no	no
START-3	RF/VNIINM	no limit	not always	yes	no, hardly ever goes to zero	yes, in line with Xe depletion	yes	yes, T-dependent functional	yes & yes	no, model applicable throughout
TRANSURANUS	Bulgaria-ITU	15% limit	-	yes,saturation	no		yes	no limit		
TRANSURANUS-DCHAIN-5	Romania/INR	15% limit	no	yes,saturation	no		yes	no limit		
TRANSURANUS-PSI	Switzerland/PSI	15% limit	-	yes,saturation	no		yes	no limit		

TABLE 12. DETAILED MODELLING OF HIGH BURNUP (cont.)

Code	High BU Fission Gas Release								
	Diffusion coefficients for FGR			**Xe concentration limit**			**Main contribution to high BU FGR**		
	BU enhancement of thermal diffusion coefficient	BU enhancement of athermal diffusion coefficient	"Phase transition" of diffusion coefficients	Rim	Transition zone	Thermal interior zone	From rim	From transition zone	From pellet interior
BACO	no	no	-	no	yes	yes	-	-	yes
ELESTRE	yes	yes		-	no	no			
ENIGMA	no	yes		no	no	no			
ENIGMA-B	no	no	no	no	n/a	no	zero	zero	1
FAIR	no	no		no	no	no			
COPERNIC development	no	no	no	yes	yes	yes	no	yes	yes
FEMAXI	no	no		-					
FEMAXI	no	no	no	no	?	?	no	yes	yes
FEMAXI-JNES	no	no	no	yes	yes	yes	no	no	yes
INFRA	no	no	no	yes	no	no			yes
MACROS	mechanistic yes	no		yes-mechanistic	yes-mechanistic	yes-mechanistic			
METEOR	Yes	no	no	no	no	no			
PINw99	no/yes?	no		no	no	no			
PIN2001	no	no	no	yes	no	no			
PROFESS	yes	no	no	no	no	no	yes	no	yes
START-3	no	no	no	no	no	no	yes, possible	no, hardly ever	yes, possible
TRANSURANUS	no	no		yes	no	no			
TRANSURANUS-DCHAIN-5	no	no		-	no	no			
TRANSURANUS-PSI	no	no		yes	no	no			

TABLE 12. DETAILED MODELLING OF HIGH BURNUP (CONT.)

Code	Re-solution				Radial power	Other mechanisms	Local Bu for start of rim restructuring (MW·d/kgU)
	intragranular	intergranular	inter/intra dep. on Bu	inter/intra dep. on Temperature	Pu build up		
BACO	not applicable	not applicable	not applicable	not applicable	no	empirical model	no rim
ELESTRE							-
ENIGMA							-
ENIGMA-B	irradiation induced only	irradiation induced only	no/no	no/yes	yes	no	40 pellet average
FAIR							45 pellet average
COPERNIC development	yes	yes	no	yes	yes		68
FEMAXI							calculated ca. 60
FEMAXI	yes	yes		yes			48.8
FEMAXI-JNES	yes	yes	yes	yes	yes	bonding	yes 48.8
INFRA							not Bu dependent (mechanistic model)
MACROS							calculated 45-60
METEOR	yes	yes	yes	yes	yes		
PINw99							yes ?
PIN2001	yes					microcracking	55
PROFESS	no	yes	no	yes	no	empirical model	28.8 pellet average
START-3	yes	no	no, intra/mechanistic	no, intra/mechanistic	yes	yes, there are	no, another concept
TRANSURANUS							60
TRANSURANUS-DCHAIN-5							60
TRANSURANUS-PSI							60

5.2. CODE MODELS

The code developers have all taken their individual approaches to modelling the various processes involved and it is important to take care when comparing the descriptions and definitions that different modellers use. Care has been taken in this report to try to accurately and explicitly represent the meaning of the modellers and the terminology they use. It is particularly important to be careful with different units used and similar terms meaning different things to different teams. As an example, the term 'burnup' has many meanings, ranging from assembly average, rod average, pellet average to local burnup. It is also measured as MW·d/kgU, MW·d/kgUO_2 or MW·d/kgHM, depending on the weight of the uranium, uranium oxide or heavy metal (which includes plutonium) used as the basis for the burnup calculation.

Where more detailed descriptions of the code structure and models used have been reported by the participants, a summary can be found in the Appendix and further details can be found in the reports appended to this publication.

5.2.1. Radial power distribution

Prior to calculating temperature, fission gas release, dimensional changes etc., it is important to correctly distribute the power in the radial direction. With the standard Bessel function treatment, power is depressed towards the pellet centre, and this depression decreases as the fissile elements burn out. However, at high burnup, resonance capture of thermal neutron by ^{238}U builds up a concentration of fissile plutonium preferentially at the pellet rim, thus perturbing the power and burnup distribution in the radial direction. For any fuel performance codes designed for high burnup application it is necessary to treat this phenomenon. One of the first models to do this was the BNFL RADAR model, and some codes use this. An alternative model which has been well publicised is the ITU TUBRNP model as used in the TRANSURANUS codes. However it is clear that code developers have devised their own routines such as PLUTON in FEMAXI-JNES, GETERA in START-3 and CIRTHE in the FANP COPERNIC3 code.

5.2.2. Fuel temperatures

It became clear at an early stage in the programme that all codes now contained models whereby the thermal conductivity of the fuel degraded with burnup. The usual form for UO_2 thermal conductivity, K, as a function of burnup, Bu, and temperature, T, is:

$$K = 1 / (A_0 + A_1.Bu + B.T) + \text{electronic term}$$

where A_0, A_1 and B are constants.

This form or a variant is used by most codes. Evaluation of the constants is based on experimental data e.g. centre thermocouple measurement of temperature in operating fuel rods notably in the research reactors at Risø and the Halden Project (codes ENIGMA, PINw99, COPERNIC3) or by taking values from thermal diffusivity measurements by laser flash on irradiated fuel sections, notably from the EPRI NFIR programme (INFRA code) or from simulated fuel, SIMFUEL, data (FAIR code). At high burnup, the fuel clad gap is closed thus eliminating the stochastic uncertainties inherent in gap conductance models. Predictions of fuel temperature are therefore dependent primarily on obtaining a good correlation between fuel conductivity, burnup and temperature. Thus, contrary to the findings of the FUMEX CRP, most codes provided quite satisfactory predictions of fuel temperature, and this must be taken as a major success for the previous CRP. Thus, from the outset, attention became focussed on formation of the high burnup structure (HBS) at the pellet rim and its influence on fuel performance, particularly fission gas release (FGR).

5.2.3. Rim structure formation

At high burnup PIE has shown that the fuel structure at the pellet periphery undergoes a restructuring whereby the original grains, ~10 μm or greater, convert to a much finer grain structure, typically of the order 0.1–0.3 μm diameter. At the same time, EPMA shows a decrease in xenon concentration in the matrix to constant levels ~2–3 wt%. More generally, this is known as high burnup structure (HBS) as this type of restructuring has been observed around plutonium rich particles in MOX fuel, but equally

it is known as ‘rim formation’ as a consequence of its location at the pellet periphery of standard UO_2 fuel.

Of the 19 codes for which contributions were received, some 15 codes considered the formation of a HBS at the pellet rim which, in different ways, had an effect on fuel behaviour. There is no treatment for restructuring in BACO and ELESTRES. The majority of codes initiated restructuring at a local burnup of 45–60 MW·d/kgU; whilst ENIGMA-B, FAIR and PROFESS invoked restructuring at a pellet average burnup of 40, 45 and 28.8 MW·d/kgU respectively. The codes FEMAXI-JNES, ENIGMA-B, PROFESS and PINw99 use empirical correlations. For example, in the PROFESS code, the model is based on measured rim data of Owaki et al [11] on fuels having burnup levels up to 60 MW·d/kgU. In this model the rim width is expressed in terms of rod average burnup by the following equation:

$$w = 1.37 \cdot 10^{-3} Bu - 0.0384$$

where,

w = rim width (cm)

Bu = pellet average burnup (MW·d/kgU)

The rim porosity, based on the reported porosity measurements, is expressed as a function of local burnup by the following equation:

$$P_{rim} = 1.78 \cdot 10^{-1} LBu - 6.77$$

where,

P_{rim} = porosity in the rim (%)

LBu = local fuel burnup (MW·d/kgU)

INFRA, METEOR, TRANSURANUS and START-3 have no implicit burnup criterion but invoke restructuring by other means and it is interesting to briefly review the basis of how these codes calculate HBS formation.

In the INFRA code, intra-granular bubbles are both nucleated and destroyed along fission fragment tracks. However, at a critical gas atom concentration taken as $5.1 \cdot 10^{26}$ atoms·m^{-3}, bubbles become stable. Under the influence of the stress field of these over-pressurized bubbles, the adjacent matrix restructures to form sub-grains. Rapid gas atom transport to, and within, this grain structure transfers fission gas to the bubbles causing further over-pressurization, enlargement of the volume covered by the sub-grain structure and depletes the matrix of gas atoms, thus fulfilling all the characteristics of the HBS. The formation criterion depends on gas atom concentration and therefore by default depends on burnup, grain size and temperature, Fig. 1.

In the CIAE METEOR code, it is considered that as the result of irradiation damage and the formation of fission products, a strain energy, E^*, builds up in the lattice as a function of irradiation. At temperatures below ~800–900 K, point defects are not very mobile, hence as a function of irradiation, their concentration and concomitant lattice strain energy increases with burnup.

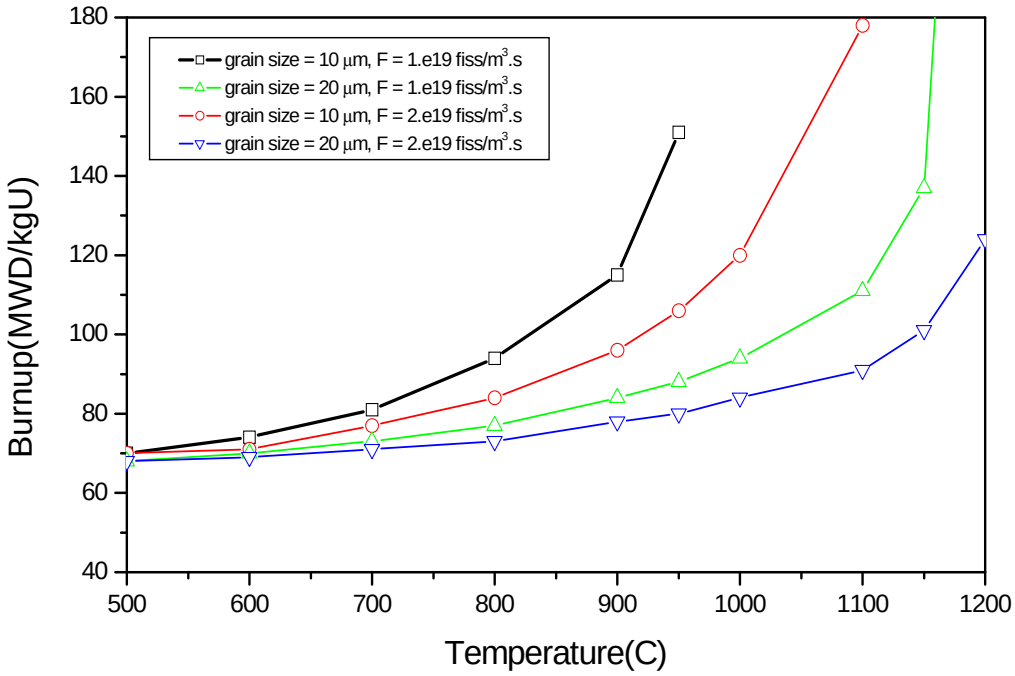

FIG. 1. HBS formation threshold as a function of temperature and burnup for the INFRA code.

Fuel restructuring begins when the lattice energy E^* exceeds a critical value Es, then the excess energy (E^* - Es) is converted into 'new' grain boundaries in a restructured zone; the surface area of these new grain boundaries is S so that:

$$E^* < Es, \qquad S = 0$$

$$E^* > Es \qquad S = \frac{3}{a_s}\left[1 - \frac{2\gamma}{2\gamma + \frac{a_s}{3}(E^* - Es)}\right]$$

where a_s is the sub-grain radius and γ is the surface energy.

As will be seen later, the value of S is used in the calculation of FGR.

In TRANSURANUS the formation and properties of the restructured zone is driven by the calculation of local burnup by the TUBRNP model. When the local burnup proceeds through an interval of 60–75 MW·d/kgHM, the HBS is formed in the corresponding fuel zones. For a local burnup above Bu_1 = 75 MW·d/kgHM, the model assumes a transfer of a fraction of the fission gas from the grains into the HBS, driven by a burnup dependent rate equation [12]. In agreement with the conclusions of the International Workshop on the High Burnup Structure in Nuclear Fuels held at ITU in June 2004 [13], the fission gas is first retained in the HBS. As soon as the local burnup exceeds an additional empirical threshold (present standard value: Bu_2 = 85 MW·d/kgHM), the HBS is assumed to be saturated, i.e. all additionally arriving fission gas is immediately released to the free volume.

The model in START-3 assumes that restructuring nucleates at grain boundaries and is caused by the accumulation of irradiation damage in the matrix. The volume fraction ε_s of HBS is calculated as an empirical function of the effective burnup $b_x(t)$ from the equation:

$$\varepsilon_s(t) = 1 - \exp\left[-k_d\left(\frac{b_x(t)}{b_0}\right)^3\right]$$

where b_0 is a reference burnup and k_d is a factor dependent on the original grain structure.

The effective burnup takes account of the irradiation history, notably the irradiation temperature such that the parameter increases at a slower rate during periods at elevated temperature. In this way, it is a measure of the irradiation damage present in the lattice. Restructuring commences at grain boundaries and progresses towards grain centres by way of dislocations. At any time prior to complete transformation, the thickness δ_s of the restructured layer is related to the volume fraction via the expression:

$$\varepsilon_s(t) = \frac{d_o^{\,3} - [d_o - \delta_s(t)]^3}{d_o^{\,3}}$$

As will be seen when discussing FGR from the rim region, the main property of the HBS is to provide a rapid transfer of gas atoms from the matrix into bubbles situated on the original grain boundary structure.

Most codes that considered rim formation increased the swelling rate of this region; only FAIR and the TRANSURANUS codes placed a maximum limit on this which, for TRANSURANUS is 15%. Some codes reduced the matrix swelling in proportion to the amount of fission gas entering the micron sized porosity. Some codes, including START-3, the FANP code and METEOR considered this porosity could interlink to release fission gas. There was a division of opinion whether or not there was significant FGR from restructured fuel in the rim region.

All codes that invoked rim structure formation reduced the local fuel thermal conductivity as a function of burnup. In some cases the degree of degradation was reduced when compared to the general formulation to account for annealing of irradiation damage and removal of fission gases into porosity.

5.2.4. Fission gas release

When considering FGR in general, the location across the pellet radius from which gas release occurred was discussed in terms of three regions:

- Rim, the thin 100–500 μm zone in high burnup fuel adjacent to the pellet periphery.
- Transition zone, un-restructured and non-interlinked grain boundaries where, at low burnup, negligible FGR occurs.
- Pellet interior, central ‘hot’ regions of the fuel where the temperatures are sufficiently high for fission gas atom mobility with accumulation at grain boundaries and release to the rod free volume via interlinked grain boundary bubbles and grain edge tunnels.

Only for FEMAXI and the FANP code could there be a significant contribution from the intermediate zone and only for PROFESS and START-3 could a significant component come from the rim region.

5.2.4.1. FGR from the pellet interior

For most codes, the greater part of the FGR occurred mainly from the central regions of the fuel even at high burnup. The dominant mechanism for release is one of single atom diffusion to grain boundaries with release via grain boundary saturation and venting. The formalism is based on the Booth model sometimes modified using the Speight model to account for trapping at intra-granular bubble, in which case the diffusion coefficient D is replaced by an effective one D_{eff} given by:

$$D_{eff} = \frac{b(F) \cdot D}{(b(F) + g(T))}$$

Where $g(T)$ and $b(F)$ correspond to the capture and escape probabilities from intra-granular bubbles.

Atoms escape from the bubbles when a fission fragment travelling near to or through the bubble completely destroys it, returning all the gas atoms to the matrix; this process is independent of temperature. In the BNFL ENIGMA-B code, the bubble is not completely destroyed, only losing a ‘chip’ of its volume whose size is temperature dependent.

The diffusion coefficient is invariably composed of two or three terms of the form:

$$D = D_1(T) + D_2(T,F) + D_3(F)$$

where T is temperature and F is fission rate.

In the ITU version of TRANSURANUS they use $D = D_1(T) + D_3(F)$ whereas in the new FGR model introduced by PSI into their version they use $D = D_1(T) + D_2(T,F)$, as does the VTT version of ENIGMA, whilst the BNFL version employs all three terms. In a minority of cases, ELESTRES, MACROS and METEOR and PIN, the diffusion coefficient is enhanced as a function of burnup in order to increase FGR at high burnup.

The majority of codes moderate accumulation of gas atoms at the grain boundary by using a non-zero concentration of gas atoms adjacent to the grain boundary. This is maintained by a flux of atoms from the grain boundary which is proportional to fission density and grain boundary gas concentration. The effect of this is to delay the burnup at which the grain boundaries become saturated with gas and the commencement of fission gas release from the fuel. An exception to this is the original model in TRANSURANUS which retains the original Booth diffusion model without re-solution.

Working in parallel with diffusion, particularly at high temperatures, many codes accumulate gas atoms on grain boundaries by grain boundary sweeping. Using a grain growth law, e.g. Ainscough [14], a change in grain radius from r_i to r_{i+1} during a timestep releases a fraction f to the grain boundaries in proportion to the volume of matrix swept out:

$$f = \frac{r_{i+1}^{\,3} - r_i^{\,3}}{r_i^{\,3}}$$

In addition, at very high temperatures, some codes e.g. the PSI FGR model in their TRANSURANUS has a contribution to gas release from columnar grain growth.

To increase release during ramp conditions, the code PIN2K used by Rez invokes an additional contribution to release by micro-cracking.

5.2.4.2. FGR from the intermediate region

No code has a special treatment for this region, it comes about because the temperatures are too low for appreciable migration of fission products, hence the release is low or confined to knockout and recoil from crack surfaces. This is covered by an athermal release term to fit data from low power commercial irradiations. A typical correlation as used in TRANSURANUS is:

$F_{athermal} = 6.1705 \cdot 10^{-5} \times$ Burnup (MW·d/kgU).

A unique feature of the COPERNIC3 code is that it proposes a limit to the concentration of fission gas that can be maintained in the matrix so that above this limit there is a spontaneous release from the fuel.

$$Xe_{loc}(Bu,T) = Xe_{\min}(T) + [Xe_{\max}(T) - Xe_{\min}(T)].\exp(-C_1 \Delta Bu)$$

where:

Bu is the local burnup.

$B_0(T)$ is the threshold burnup.

ΔBu $= (Bu - B_0)$.

T is the local temperature.

C_1 is a model parameter.

Xe_{max} is the maximum xenon concentration which can be reached for a certain temperature T at a burnup $B_0(T)$ (linear increase from zero to Xe_{max}).

Xe_{min} is the minimum xenon concentration reached for this temperature when ΔBu is large (local burnup much bigger than the limit burnup B_0).

Xe_{loc} is the limiting local xenon concentration between Xe_{max} and Xe_{min} for a local burnup above B_0 (exponential decrease from maximum concentration Xe_{max} to minimum Xe_{min}).

This limiting concentration is dependent on both burnup and temperature as illustrated for a MOX particle in Figure 2 which shows code calculations against data from Ref. [15].

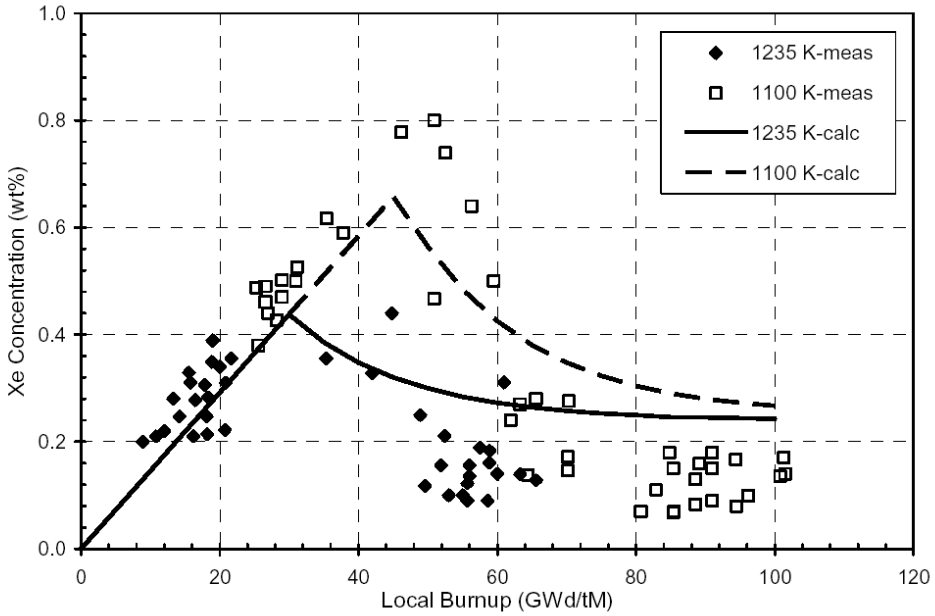

FIG. 2. Limiting xenon concentration as measured for Pu particles in MOX fuel and calculated in the COPERNIC3 code.

5.2.4.3. FGR from the rim region

There are three generic concepts for treating FGR from the rim region.

a) Empirical models

The first is an empirical correlation with burnup; for example, PINw99 uses a formulation based on Lösönen [16], whilst FEMAXI-JNES uses that of the HBEP, namely that the rim exists above a burnup (*Bu*) of 48.8 MW·d/kgU and the rim width, *w*, above this burnup is given by:

$$w\ (\mu m) = 2.19 \times (Bu - 48.8),$$

above a *Bu* of 62.2 MW·d/kgU the FGR from this region is given by

$$FGR = 0.99625 \times (Bu - 62.2).$$

b) Enhanced release mechanisms

The second concept is used in the codes START-3, INFRA and METEOR, and assumes that the newly formed grain boundaries in the rim region form a pathway for the rapid transport of gas atoms from the matrix to bubbles. For example, START-3 contains a model which considers the dynamic formation of re-crystallized grains as a function of burnup which accumulate fission gas atoms by athermal, fission induced diffusion. The new boundaries channel the gas atoms into inter-granular bubbles on the original grain boundary structure. At high burnup, these bubbles saturate the grain boundary resulting in release to the free volume through interlinkage. In which case, the local FGR can be quite high.

The models in the INFRA code and the Chinese version of the METEOR code are similar in concept to that in START-3 in so far as there is enhanced gas atom diffusion through the newly created grain

boundaries of the HBS to bubbles which interlink to release gas in the same way as for thermal release in the hotter regions of the pellet. The main difference between these codes is the way the HBS is assumed to form.

c) Threshold models

Finally, the third concept is based on EPMA observations of xenon depletion, TRANSURANUS and COPERNIC3 assume a limiting gas atom concentration above which release occurs. In the case of TRANSURANUS, at a local burnup above 75 MW·d/kgHM, the model assumes a transfer of a fraction of the fission gas from the grains into the HBS, driven by a burnup dependent rate equation. The fission gas is first retained in the HBS, but as soon as the local burnup exceeds an additional empirical threshold (presently 85 MW·d/kgHM), the HBS is assumed to be saturated, i.e. all additionally arriving fission gas is immediately released to the free volume.

In COPERNIC3 the assumption is that there is clear experimental evidence for only small FGR from the high burnup rim structure to the rod free volumes. The main contribution of the rim region to FGR enhancement is via pellet temperature increase, if any. The bulk of the gas produced in the pellet rim remains in closed spherical rim porosity (at least 80% according to measurements [17]). This is modelled as a small athermal contribution to FGR. It amounts to about 1.0–1.5 % pellet release for a pellet burnup between 80 and 90 MW·d/kgU. The intrinsic specific surface described in [18] is linked to the rim porosity P_{RIM}:

$$(S/V)_{rim} = \min(C_{1RIM}, C_{2RIM}.P_{RIM})$$

where C_{1RIM} and C_{2RIM} are modelling constants.

The low release from the rim region implies that other mechanisms have to be found to explain high burnup effects, and this is explained through the limiting xenon solubility described above for release from the intermediate region. This solubility limit applies to all regions and can even result in additional release from the rim. A schematic representation of the FGR model in COPERNIC3 is shown in Fig. 3.

5.2.5. Summary

It can be said that there is a consensus that FGR occurs in the central regions of the fuel predominantly by a diffusion process involving transport of gas from the grains to grain boundaries and by grain boundary saturation and grain edge interlinkage to form tunnels open to the free volume. Within this framework there are several different treatments:

- Some codes treat trapping and re-solution at intra-granular bubbles.
- With the notable exception of TRANSURANUS, most codes consider re-solution at grain boundaries.
- Some codes have burnup dependent diffusion coefficients.
- Codes invariably have multi term diffusion coefficients but they are not all alike.
- Many codes have a parallel transfer from the grain to grain boundaries by grain boundary sweeping.
- COPERNIC3 has a limiting solubility criterion for xenon above which there is total release.

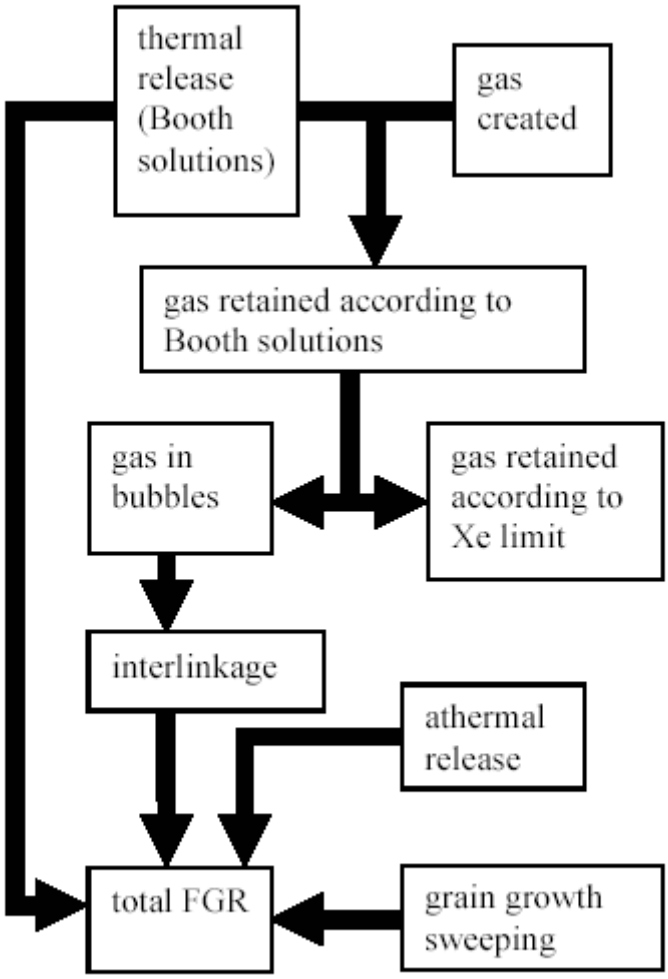

FIG. 3. Scheme of the FGR model in the FANP COPERNIC3 code.

Only COPERNIC3 has an independent release process for the intermediate region, i.e. the solubility limit.

Opinion is divided over release from the rim region. In some codes there is no release, in some there only a small release whilst in others the release can be significant. Of the codes predicting release from this region:

- Some have empirical correlation with burnup.
- Some view the new grain boundary structure as a means for rapidly transferring gas from the matrix into bubbles from which release proceeds by interlinkage.
- Some assume a limiting concentration above which there is total release.

6. CODE COMPARISON, SIMPLIFIED CASES

6.1. SPECIFICATION OF THE SIMPLIFIED LWR CASES

Following the lead taken in the original FUMEX CRP, a number of simplified cases were constructed in order to investigate mathematical stability and more easily compare model and code predictions without the vagaries of real power histories. In this section, each case is outlined together with the reason for its inclusion before presenting the results and comparing the predictions.

The first idealized case, 27(1) was to ask the codes to try to match the experimental finding, represented by the Vitanza criterion, of a burnup dependent threshold temperature at which more than 1% FGR can be expected. The second idealized case was to illustrate code predictions of FGR as a function of burnup up to 100 MW·d/kgU. There were four separate idealized cases for this task:

- 27 (2a) a constant power of 15 kW/m from BOL to 100 MW·d/kgU;
- 27 (2b) a linearly decreasing power from 20 kW/m at BOL to 10 kW/m at 100 MW·d/kgU;
- 27 (2c) more realistic power history supplied by G Rossiter of BNFL;
- 27 (2d) idealized 'real' history supplied by F Sontheimer of FANP.

The objective of this part of the exercise was to demonstrate that codes could predict a smooth development of FGR up to 100 MW·d/kgU without any instability or 'cliff-edge' behaviour. The results were requested to be reported in either ASCII or EXCEL format as FGR (%) versus Burnup (MW·d/kgU). For cases 27(1), 27(2a) and 27(2b) the predictions of the exercises are relatively insensitive to rod design, and therefore, unless stated otherwise, the specification given in Table 13 was to be used. This specification is typical for a BWR rod design as irradiated in the Halden reactor, therefore it was assumed that there was a low value to the fast flux and, in turn, negligible clad creep down:

The specifications for cases 27(2c) and 27(2d) were specified by BNFL (Table 14) and FANP (Table 15) respectively.

Power histories for these two cases are shown in Fig. 4 (case 27(2c)) and Fig. 5 (case 27(2d)). In the last case, the history provided by FANP was a 5 cycle history which was generic to a number of rods which had undergone PIE; hence a range of FGR data was available at the end of irradiation cycles 2-5.

TABLE 13. SPECIFICATION FOR CASES 27(1), 27(2A) AND 27(2B)

Standard fuel specifications for cases 27(1), 27(2a) and 27(2b)

PELLETS

Solid, flat ended UO_2,

Enrichment	13wt% ^{235}U,
Outside diameter	10.61 mm,
Length	12.7 mm,
Grain size	15 microns diameter,
Density	95% TD.

If densification is a necessary input to the code, assume the density increases to 95.5% after a standard densification test.

CLADDING

Standard Zr-2

Inside diameter	10.8 mm
Thickness	0.95 mm.

FUEL ROD

Use single axial zone with no axial form factor and a large plenum to avoid thermal feedback.

Fill gas	5 bar helium

CLAD WATERSIDE TEMPERATURE, *TCO* (°C),

Use Jens Lottes correlation for Halden conditions

$TCO = 240 + 0.4162 \times [\text{Power (kW/m)}]^{0.75}$

TABLE 14. SPECIFICATION FOR THE BNFL CASE 27(2C)

Fuel specification for BNFL idealized case 27(2c)	
FUEL PELLET DATA	
Composition	UO_2 (see Note A)
Method of manufacture	ADU
Inner diameter	Zero (solid pellets)
Outer diameter	8.2 mm
Length	9.8 mm
Geometry	Two dishes per pellet and no chamfers
Dimple (dish) diameter	5.24 mm
Dimple (dish) depth	0.3 mm
Total dimple (dish) volume per Pellet (fraction of hypothetical cylindrical pellet volume)	1.26%
^{235}U enrichment	8.0 wt%U (all remaining U can be considered to be ^{238}U)
Density (fraction of TD)	95%
Density (absolute)	10.431 $g \cdot cm^{-3}$ (using TD = 10.98 $g \cdot cm^{-3}$)
Stoichiometry (O/M)	2.00
Grain size (mean linear intercept)	50 μm (for grain diameter multiply by 1.5)
CLADDING DATA	
Composition	Standard Zircaloy-4 (see Note B)
Outer diameter	9.50 mm
Inner diameter	8.36 mm
Wall thickness	0.57 mm
ROD PARAMETERS	
Total length	3875 mm
Fuel stack length	3658 mm
Plenum length	162 mm
Plenum free volume	7.5 cm3 (excludes volume occupied by plenum spring)
Fill gas composition	100% He
Fill gas pressure	25 bar (abs) at 20 °C
Assembly geometry	17 x 17
IRRADIATION DATA	
Reactor: Hypothetical 2800 MW(th) Westinghouse 3-loop PWR	
Fast flux (> 1 MeV)	2.183×10^{16} $n \cdot m^{-2} \cdot s^{-1}$ per W/gU
Ratio of thermal heat to total heat for rods	0.975
Densification (for use only if cannot be calculated internally)	0.23 vol% (4.6% of initial porosity) over rod average burnup of 3 MW·d/kgU
Coolant inlet temperature	291 °C
Coolant outlet temperature	327°C
Coolant pressure	15.5 MPa (abs)
Coolant mass velocity	3300 $kg \cdot m^{-2} \cdot s^{-1}$

TABLE 14. SPECIFICATION FOR THE BNFL CASE 27(2C) (cont.)

Fuel specification for BNFL idealized case 27(2c)

IRRADIATION HISTORY

Cycle number	Effective full power days (EFPD)	EOC rod average burnup (MW·d/kgU)
1	469	26.25
2	478	50.70
3	472	70.86
4	473	88.71
5	470	103.6

Notes

A Fuel is intended to be representative of advanced fuels with improved fission gas retention. For modelling purposes, fuel is to be modelled as standard UO_2 with a large grain size.

B Cladding is intended to be representative of advanced cladding with improved corrosion resistance. For modelling purposes, cladding is to be modelled as standard Zircaloy-4 cladding with no corrosion, i.e. zero oxide

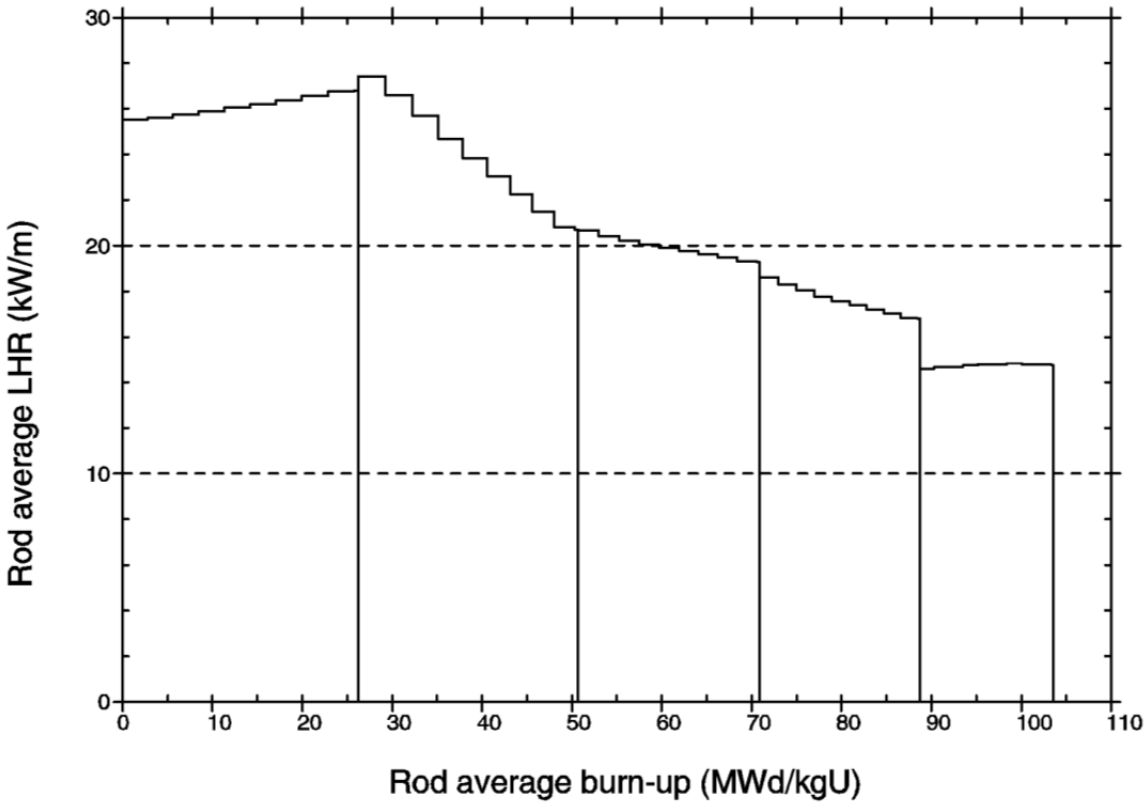

FIG. 4. Power history for BNFL case 27(2c).

TABLE 15. SPECIFICATION FOR THE FAN-P CASE 27(2D)

Specification for FAN-P idealized case 27(2d)	
FUEL	
Standard UO_2 pellets	
Diameter	9.12 mm
Pellet length	11.0 mm
porosity	4.5%
enriched ^{235}U	4%
grain size (mli)	10 μm
Standard swelling behaviour	
Low densification (stable fuel)	
Stoichiometric composition	
CLADDING	
Low corrosion Zr-4	
Standard creep-down properties	
Clad outer diameter (mm)	10.750
Clad inner diameter (mm)	9.290
Thickness (mm)	0.730
FUEL ROD	
15 x 15 design	14.3 mm pitch
Fuel stack length	3500 mm
Fuel-clad gap	170 μm
Total free volume	30 cm^3
Fill gas	22 bar helium
REACTOR	
Modern PWR	
Coolant pressure	155 bar
Inlet temperature	290°C
Mass flow	0.40 $kg \cdot s^{-1}$
Fast flux not given, suggested value	4.0×10^{16} $n \cdot m^{-2} \cdot s^{-1} \cdot (kW/m)^{-1}$
POST IRRADIATION DATA	

End of cycle	Full power days	Measured FGR (%)
2	673.7	6–8
3	1007.3	6–8
4	1349.0	9–13
5	1689.8	18–20

6.2. SPECIFICATION OF CANDU CASE 27(3A). THE EFFECT OF POWER ON FGR

The purpose of case 27(3a) was to investigate differences among codes for the effects of linear rating on fission gas release. The specification for code input is given as case 1 in Table 16. The requirement was to calculate several parameters as detailed below for a single zone fuel rod reaching a discharge burnup of 800 MW·h/kgU at constant powers between 10 and 60 kW/m at 5 kW/m intervals. It is worth noting the unit for burnup generally used for PWHR and CANDU plant (MW·h/tU) is based on a unit of time in hours compared with the use of days in defining LWR burnups.

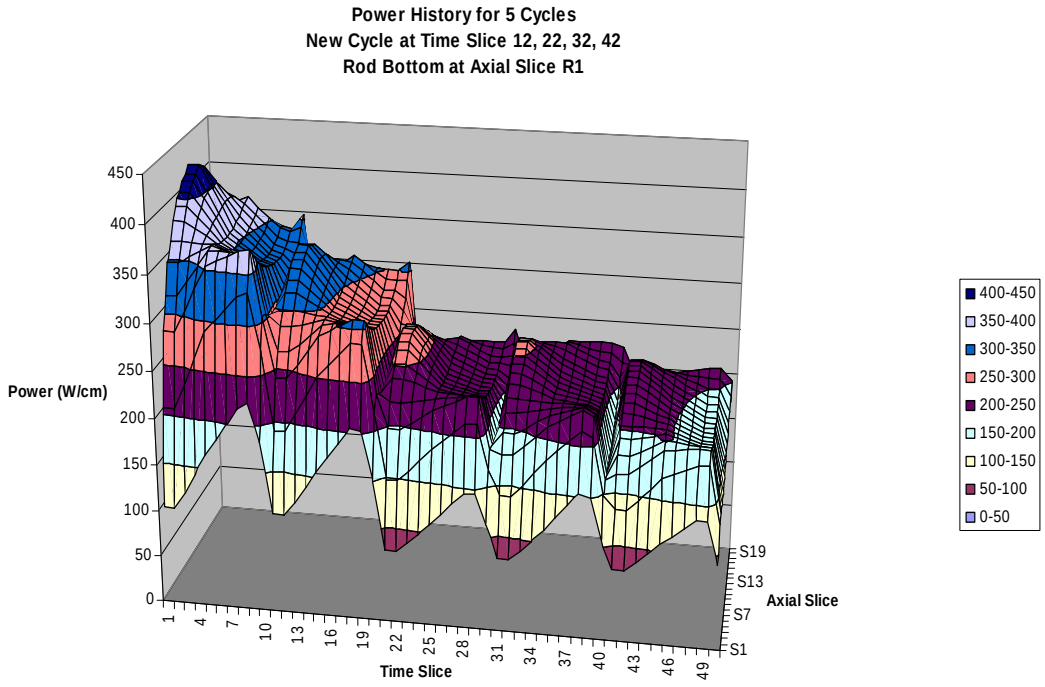

FIG. 5. Power history for FAN-P case 27(2d).

Plots were required for the following parameters as listed as well as end-of-life values, including end of life values at room temperature:

- Fission gas release (%) vs. linear rating, with burnup as a parameter.
- Fission gas release (%) vs. burnup, with element linear rating as a parameter.
- Total fission gas released (mm3, at STP) for each case.
- Internal gas pressure vs. burnup, with element linear rating as a parameter.
- Sheath temperature vs. burnup, with element rating as a parameter.
- Pellet surface temperature vs. linear rating and vs. burnup.
- Pellet centreline temperature vs. linear rating and vs. burnup.
- Gap conductance vs. burnup, with element linear rating as a parameter.
- Sheath inner diameter at midplane vs. burnup, with element linear rating as a parameter.
- Pellet outer diameter at midplane vs. burnup, with element linear rating as a parameter.
- Diametral gap between the pellet and the sheath at midplane as a function of burnup, with element linear rating as a parameter.
- Total sheath strains (thermal, elastic, plastic, and creep) at midplane and at ridge, vs. burnup, with element linear rating as a parameter.
- Oxide thickness at sheath outer surface at midplane as a function of burnup, with element linear rating as a parameter.

6.3. SPECIFICATION OF CANDU CASE 27(3B). TO CALCULATE FGR FOR IDEALIZED HISTORIES

The purpose of case 27(3b) was to compare code predictions of the effect of envelope power on fuel performance parameters and to investigate the sensitivity to coolant temperature and pressure

(compared with case 1) on fuel performance. Data for this case are given as case 2 in Table 16. The power history for this case is shown in Fig. 6. The output for this case was specified as follows, to include parameter values at room temperature and end of life:

- Fission gas release (%) vs. burnup.
- Total fission gas released (mm^3 at STP).
- Internal gas pressure vs. burnup.
- Sheath temperature vs. burnup.
- Pellet surface temperature vs. burnup.
- Pellet centreline temperature vs. burnup.
- Gap conductance vs. burnup.
- Sheath inner diameter at midplane vs. burnup.
- Pellet outer diameter at midplane vs. burnup.
- Diametral gap between the pellet and the sheath at midplane vs. burnup.
- Total sheath strains (thermal, elastic, plastic, and creep) at midplane and at ridge, vs. burnup.
- Oxide thickness at sheath outer surface at pellet midplane as a function of burnup.

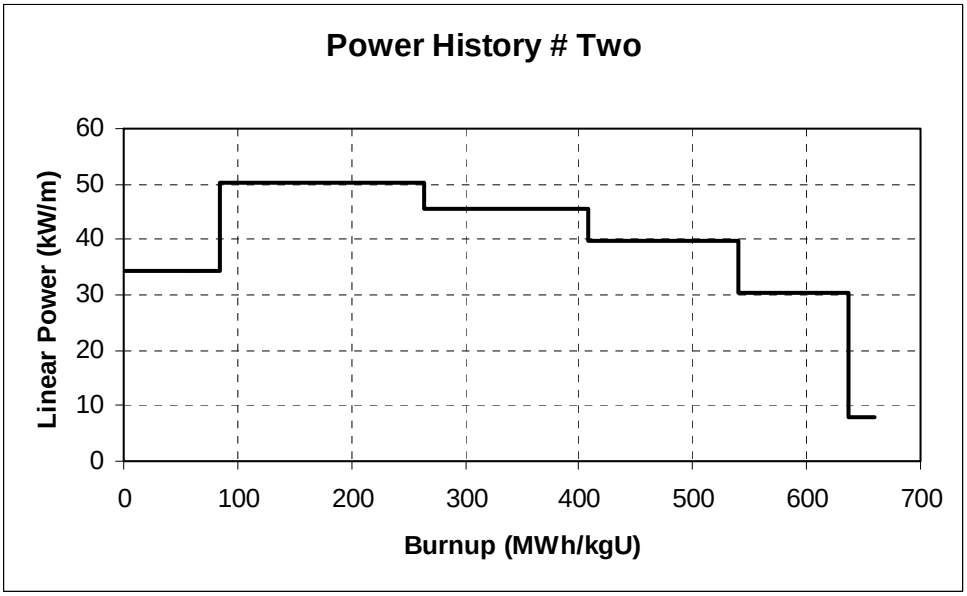

FIG. 6. Power history for CANDU case 27(3b).

TABLE 16. SPECIFICATION OF THE CANDU CASES 27(3A) AND 27(3B)

Variables	Unit	Case 27(3a)	Case 27(3b)
Number of pellets in a fuel element		31	31
Pellet outside diameter	mm	12.2	12.2
Pellet dish depth	mm	0.25	0.25
Pellet land width	mm	0	0
Pellet shoulder	mm	0.25	0.25
Pellet inside diameter	mm	0	0
Pellet chamfer: depth in radial direction	mm	0.25	0.25
Pellet chamfer: width in axial direction	mm	0.06	0.06
Pellet density	$Mg \cdot m^{-3}$	10.6	10.6
Pellet length to diameter ratio		1.27	1.27
Pellet grain size	mm	10	10
Enrichment	wt.% ^{235}U	2	2
Pellet stack length	mm	480.3	480.3
Number of fuel elements in a bundle		37	37
Pellet-sheath diametral gap	mm	0.08	0.08
Axial gap in the element	mm	2	2
Sheath outside diameter	mm	13.12	13.12
Sheath wall thickness	mm	0.42	0.42
Filling gas pressure	atm	1	1
Fraction of helium in filling gas	%	80	80
Fraction of argon in filling gas	%	20	20
Pellet surface roughness	mm	1	1
Sheath surface roughness	mm	0.5	0.5
Coolant temperature	K	561	576
Coolant pressure	MPa	10.7	12.5
Steam quality	%	0	0
Heat transfer coefficient between coolant and the sheath	$kW \cdot m^{-2} \cdot K^{-1}$	50	50

6.4. CASE 27(1): TO DEFINE THE LOCUS OF THE CENTRE TEMPERATURE/BURNUP THRESHOLD FOR 1% FGR.

Participants were asked to perform calculations of FGR for a series of cases with constant power, providing the locus of centreline temperature (°C) and burnup (MW·d/kgU) at which 1% FGR was predicted, with an accuracy of within the range ±0.01% over a temperature range 1500–800°C,

Although the power histories were artificial, the case reproduces the conditions of the Vitanza threshold [10] which was devised from experimental measurements of pressure, burnup and centreline temperature. It was requested that all results should be supplied in either ASCII or EXCEL format as TF(°C) versus rod average burnup (MW·d/kgU).

6.4.1. Results, comparison and discussion of case 27(1)

Figure 7 shows a summary of the code predictions for a 1% FGR threshold and includes the Vitanza threshold for comparison.

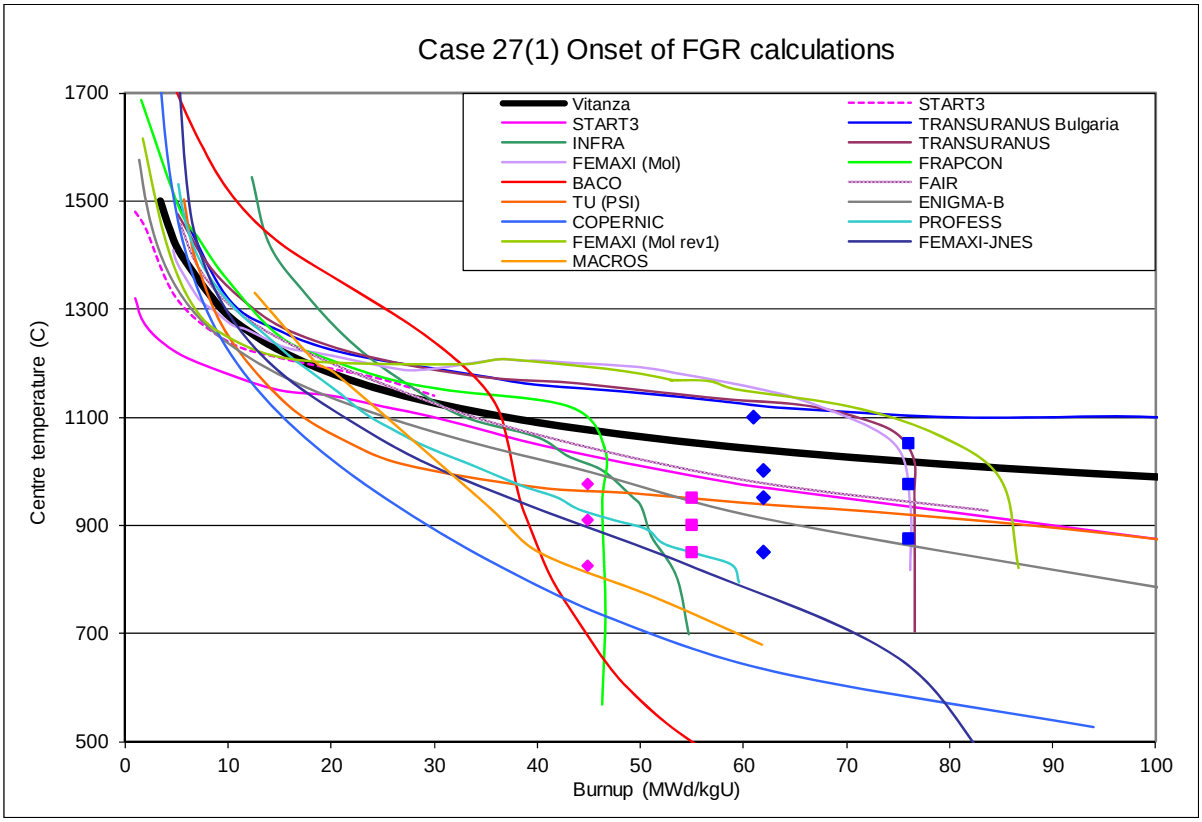

FIG. 7. Modelling the Vitanza Criterion. Calculations to show the bounding temperature-burnup relationship, above which more than 1% fission gas release is predicted. The points represent calculations with differing assumptions for the codes START3 (pink) and TRANSURANUS (Bulgaria) (blue) exploring the high burnup region where high gas release is independent of temperature.

The experimental database on which the threshold was based had a maximum burnup of around 35-40 MW·d/kgU and later data has suggested that at higher burnup the threshold is unduly conservative. There is considerable evidence that there is an enhancement of FGR at high burnup where the rim effect of enhanced porosity at the pellet surface has developed (e.g. Ref. [17]).

The code predictions do show a scatter, but it is believed that the predicted behaviour at low burnups does represent the actual data fairly well. The outlier codes are either development versions or PHWR codes. However, it is instructive to see just how the codes extrapolate to higher levels of burnup when thermal conductivity degradation and HBS become important features of fuel behaviour.

Figure 7 gives some indication of the difficulties encountered at high burnup. For many codes an FGR in excess of 1% is predicted, regardless of temperature above a burnup limit. This behaviour appears

as a vertical line in the plot, and the points shown represent variations of modellers' assumptions to see where this limit might be.

To illustrate the development of the codes, two examples have been given, though several other codes have used this case to explore the range of validation of their models as well. Two lines are drawn for differing runs of the START-3 code with different modelling choices and the points (pink for START 3) illustrate the effect on the high burnup predictions showing different burnups at which the 1% release threshold is no longer temperature dependent. The points in blue illustrate the same high burnup effect for the TRANSURANUS (Bulgaria) code.

Figure 8 is a simplified version of Fig. 7, highlighting the modelling trends and indicating where additional data would be useful in determining what effects are occurring at these high burnups.

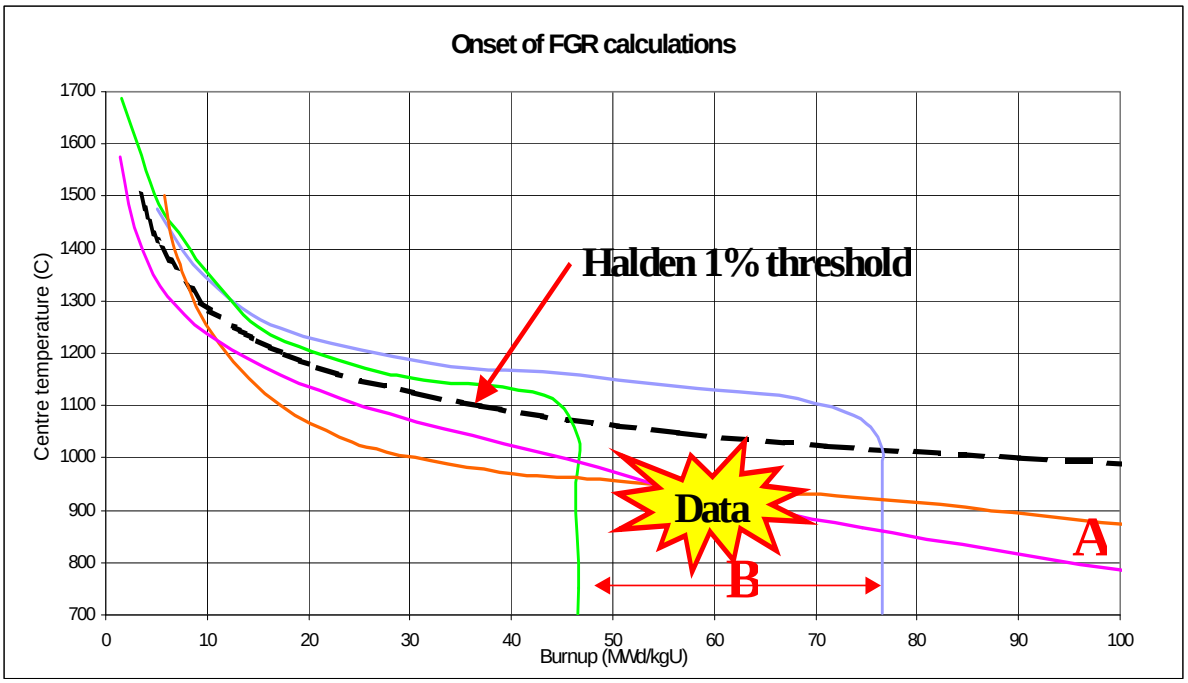

FIG. 8. Simplified diagram of the fission gas threshold calculations, indicating two distinct types of predictive behaviour at high burn up (marked A and B). The region where additional data would be most useful is highlighted.

The important feature of the experimental data that is informing the modelling is that there is enhanced fission gas release at high burnup compared with that expected using normal modelling assumptions. Three main approaches to deal with the high burnup effect have been used by the modelling teams:

- Contribution of FGR from the pellet rim–release from the restructured region.
  - Magnitude of the effect was variable.
- Burnup dependent diffusion parameters.
  - Diffusion coefficient.
  - Irradiation induced re-solution.
- Limiting saturation concentration of gas in the UO_2 matrix.

In the majority of cases, explicit consideration was also taken for the thermal effect of the rim porosity.

The two general trends A and B shown in the figure are a result of these assumptions; where release is assumed to come from a restructured region, the type A behaviour is found, and release is initiated at a burnup limit, with little temperature dependence. Where the modelling has burnup dependence of diffusion parameters, a more continuous extrapolation of the existing Vitanza curve is seen, this is type B behaviour.

6.5. CASE 27(2): TO CALCULATE FGR FOR GIVEN IRRADIATION HISTORIES UP TO 100 MW·d/kgU

The second idealized case was to illustrate code predictions of FGR as a function of burnup up to 100 MW·d/kgU. There were four separate idealized cases for this task:

- 27 (2a) a constant power of 15 kW/m from BOL to 100 MW·d/kgU;
- 27 (2b) a linearly decreasing power from 20 kW/m at BOL to 10 kW/m at 100 MW·d/kgU;
- 27 (2c) more realistic power history supplied by G Rossiter of BNFL;
- 27 (2d) idealized 'real' history supplied by F Sontheimer of FANP.

The objective of this part of the exercise was to demonstrate that codes could predict a smooth development of FGR up to 100 MW·d/kgU without any instability or 'cliff-edge' behaviour.

6.5.1. Results comparison and discussion the cases 27(2a) and 27(2b)

The calculated results for these simplified cases are shown in Figs 9 and 10 for case 27(2b) and Fig. 11 for case 27(2c). The codes give a very wide range of predictions for the histories, which are again designed to challenge high burnup predictive capability. The results for both cases are very similar. The codes generally predict low FGR below 1% for normal burnups, to 50 MW·d/kgU, but at higher burnups the predictions vary, in a similar manner as seen for case 27(1), those codes that model release from a rim or gas saturated region tend to give the highest FGR at extremely high burnups.

It is clear that there is no consistency in the predictions of fission gas release from these very simple power histories at high burnups.

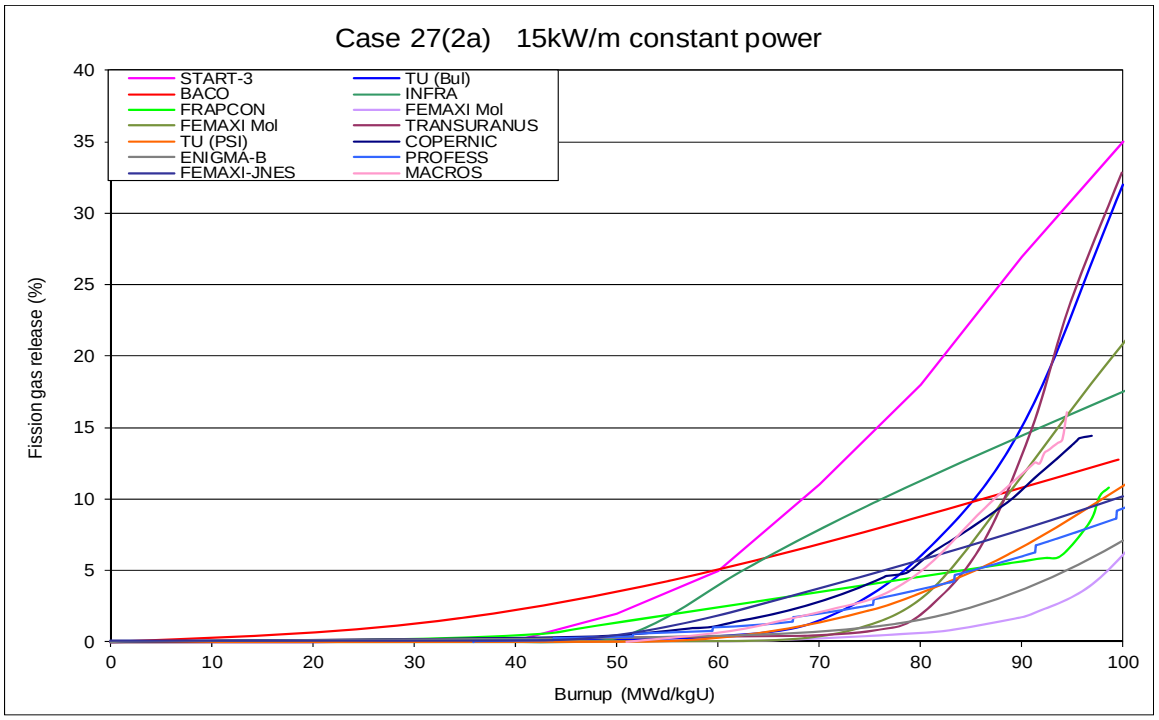

FIG. 9. Calculated values of fission gas release for an idealized irradiation at a constant power of 15 kW/m to a burnup of 100 MW·d/kgU.

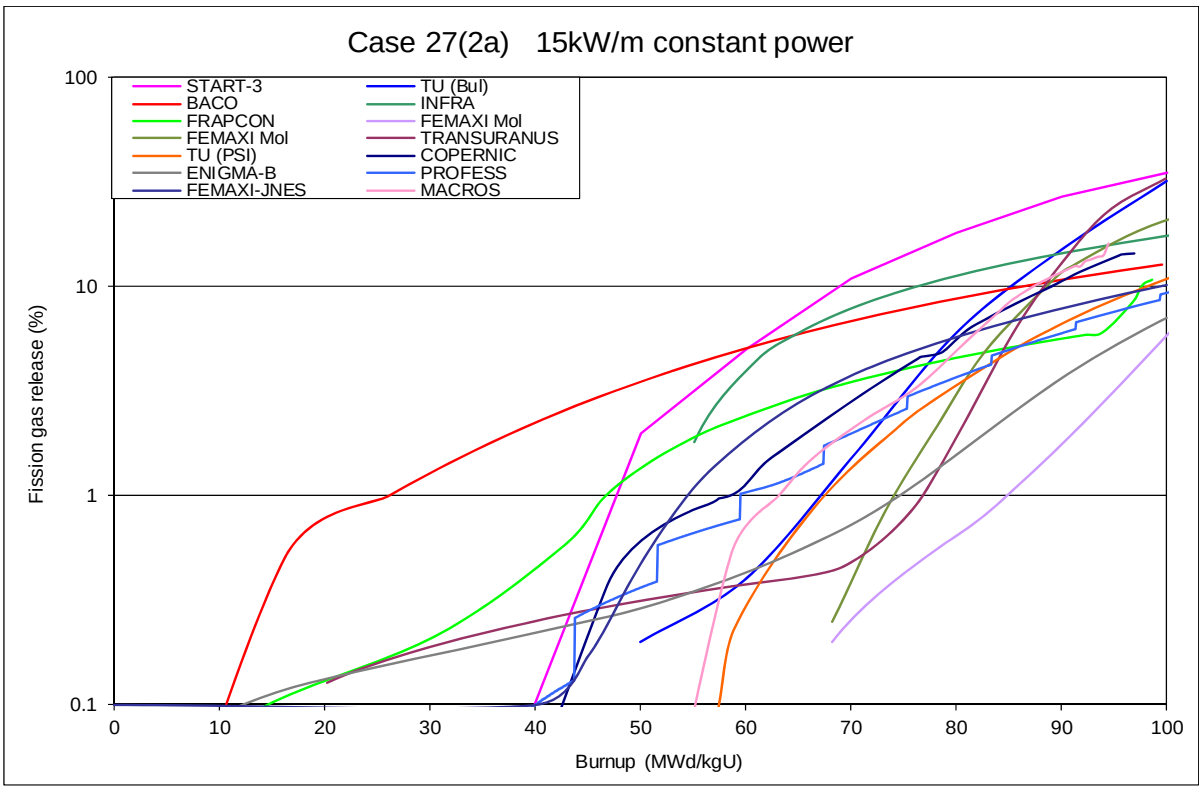

FIG. 10. The data of Fig 9 shown on a logarithmic scale to demonstrate that most codes predict below 1% FGR at burnups below 50 MW·d/kgU.

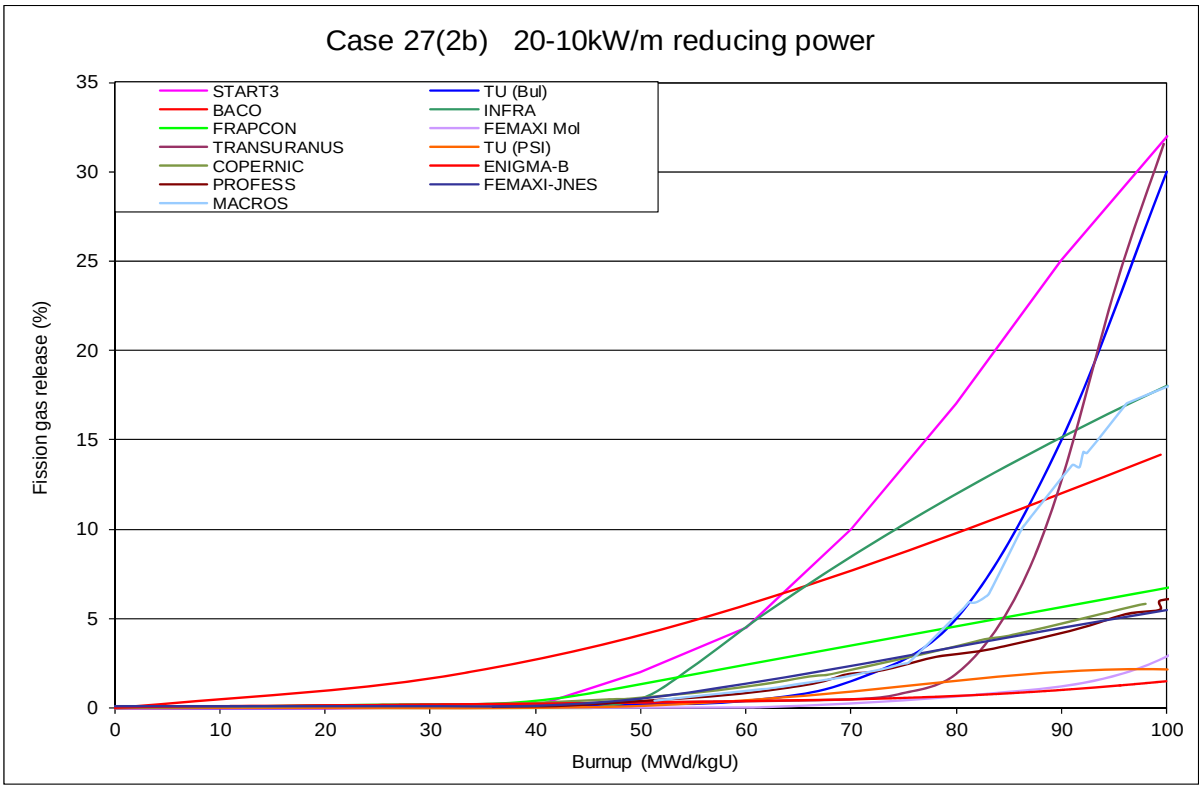

FIG. 11. Case 27(2b) Fission gas release calculated for an idealized irradiation history where the power reduces linearly from 20 kW/m to 10 kW/m to a burnup of 100 MW·d/kgU.

6.5.2. Results comparison and discussion of the idealized power histories, 27(2c) and 27(2d)

These cases were provided by fuel vendors, to illustrate possible fuel irradiations that are proposed for advanced fuel cycles. Figure 5 shows the power profile for a notional history provided by BNFL, the actual case was a 12 axial zone history with a final rod average burnup of 103 MW·d/kgU. The predictions of the codes are shown in Fig. 12, and again show low levels of FGR predicted at normal burnup, up to around 60 MW·d/kgU However, despite a drop in power as burnup proceeds, the FGR is expected to continuously increase, significantly so by several of the codes.

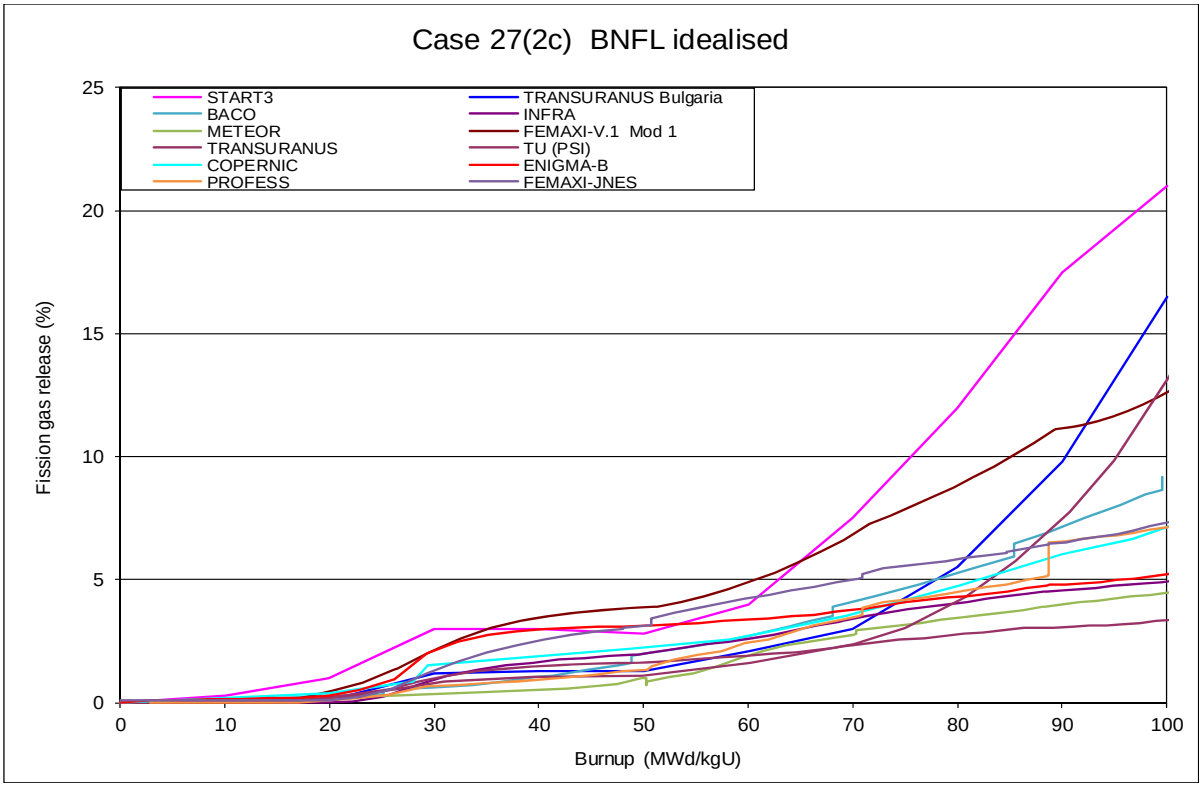

FIG. 12. Case 27(2c) Code predictions for the BNFL idealized high burnup irradiation.

The history provided by FANP (now Areva) in Figure 6 was more onerous than the BNFL history at low burnups, but did not extend to the same extreme burnup. The power history was representative of test irradiations of FANP fuel, and the case was also provided with details of the expected range of FGR up to 70 MW·d/kgU. It was good to see that the codes tended to give a good representation of the release, showing excellent agreement up to 60 MW·d/kgU, and still giving good agreement at 70 MW·d/kgU (Fig. 13). Due to the power history in this case, it seemed to be less sensitive to details of the high burnup modelling, the majority of the FGR was well described by normal models and significant release had already occurred at low burnups.

Around half the codes, COPERNIC3, TRANSURANSUS, INFRA, MACROS and START-3, showed an increasing release from a burnup of around 50 MW·d/tU, following the apparent trend in the data, whilst the other codes did not. However, the overall predictions are within the normal validation range of most of the codes.

6.6. CANDU CASES 27(3A) AND 27(3B)

CANDU fuel is different from light water reactor (LWR) fuel in many respects. Natural UO_2 is used as fuel and the length of the fuel bundle is relatively short (about 0.5m). The cladding used for the fuel elements is a thin wall, collapsible cladding which collapses on to the fuel pellet during reactor operation leaving no pellet-clad gap. There is no plenum in the fuel element and the fuel bundle is placed horizontally in the core. The normal discharge burnup of fuel is 7 MW·d/kgU.

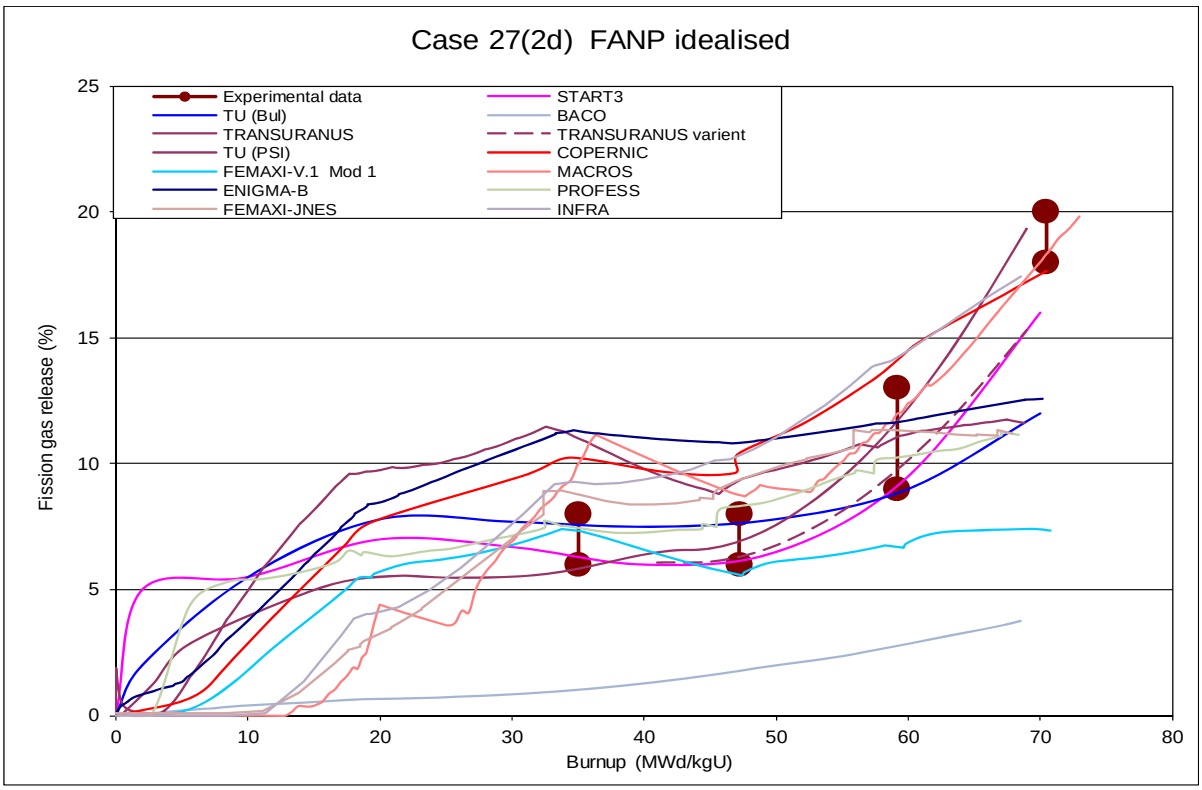

FIG. 13. Code predictions for the FANP idealized high burnup irradiation. Expected fission gas release values are shown for the end of the 2nd, 3rd 4th and 5th cycles. Two curves for TRANSURANUS are shown to illustrate the effect of code model changes.

In order to widen the scope of the CRP to include CANDU type reactors, two idealized cases were supplied by AECL. The simplified CANDU cases 27(3a) and 27(3b) were provided specifically for FUMEX-II. Only 6 codes provided calculations for these CANDU cases.

Results were requested for 10 different performance parameters, including mechanical properties. The performance of the codes with regard to fuel temperature and fission gas release predictions is discussed here as comparative data is available. Detailed results of the code predictions, including many mechanical interaction plots, can be found in the reports of the participants appended to this document. The summary here is restricted to fission gas release and fuel temperatures.

It should be noted that some of these predictions are made by codes that are not qualified for CANDU conditions and that the idealized cases extend the burnup beyond the validation range of the specialised CANDU codes.

6.6.1. Case 27(3a)

The simplified CANDU case 27(3a) involved calculation of performance parameters for constant power operation for 10, 20, 30, 40, 50, and 60 kW/m up to a burnup of 33.4 MW·d/kgU (800 MWh/kgU). The results of fuel centre temperature calculations by the codes for case 27(3a) are summarized in Fig. 14 for fuel centre temperatures calculated by codes at 0.0 and 33.4 MW·d/kgU at a power rating 40 kW/m. Detailed calculations for the codes are collected in Fig. 15. It is observed from the above figures that four codes, PROFESS, FAIR and ELESTRES and START3 show increases in fuel centre temperature with burnup as expected. The other two codes however, show an opposite trend. The calculated fuel centre temperatures at 0 MW·d/kgU for power rating of 40 kW/m are in the range 1200–1350°C.

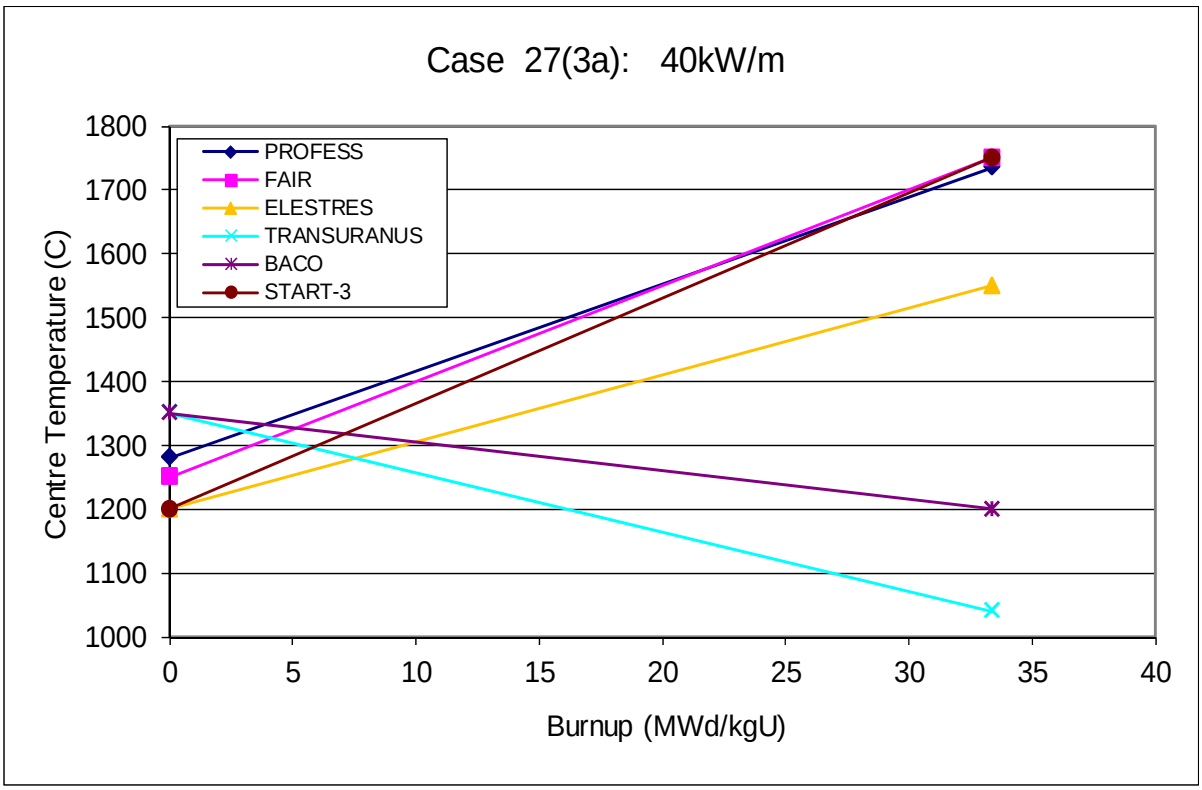

FIG. 14. Summary of the calculated centre temperatures at 0 and 34.4 MW·d/tU burnup at a power of 40 kW/m.

It should be noted that both the codes that show the drop in temperatures are operating well outside their validation range. This can be seen in the discontinuities in their detailed outputs shown in Fig. 15.

The predictions of fission gas release from fuel for case 27(3a) are shown in Fig. 16. Most codes predict a release of about 40% at 60 kW/m at 33.4 MW·d/kgU burnup. Some of the codes predicted clad lift-off at power rating beyond 45 kW/m.

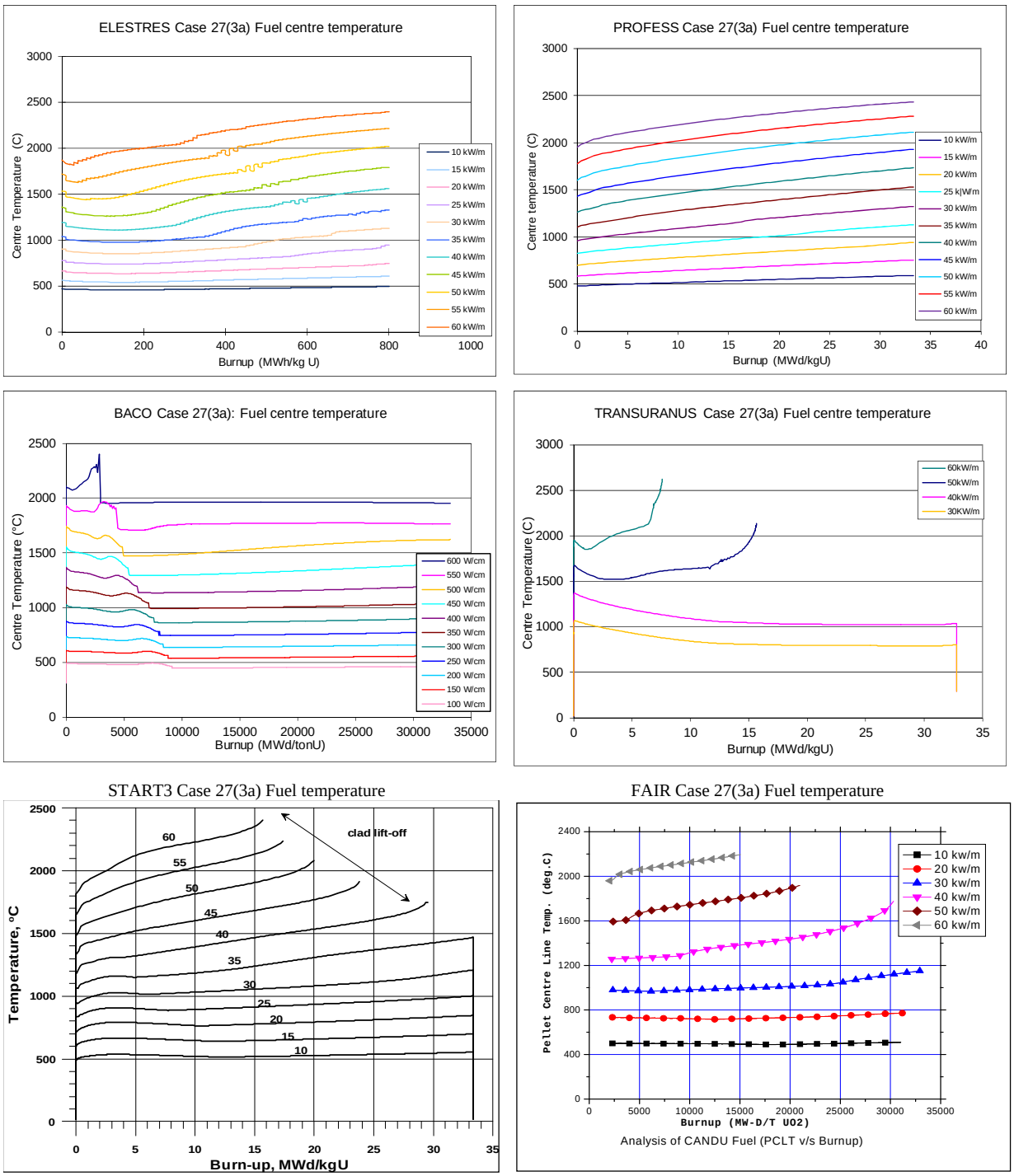

FIG. 15. Calculated fuel centre temperatures for the idealized CANDU case 27(3a) as a function of constant power.

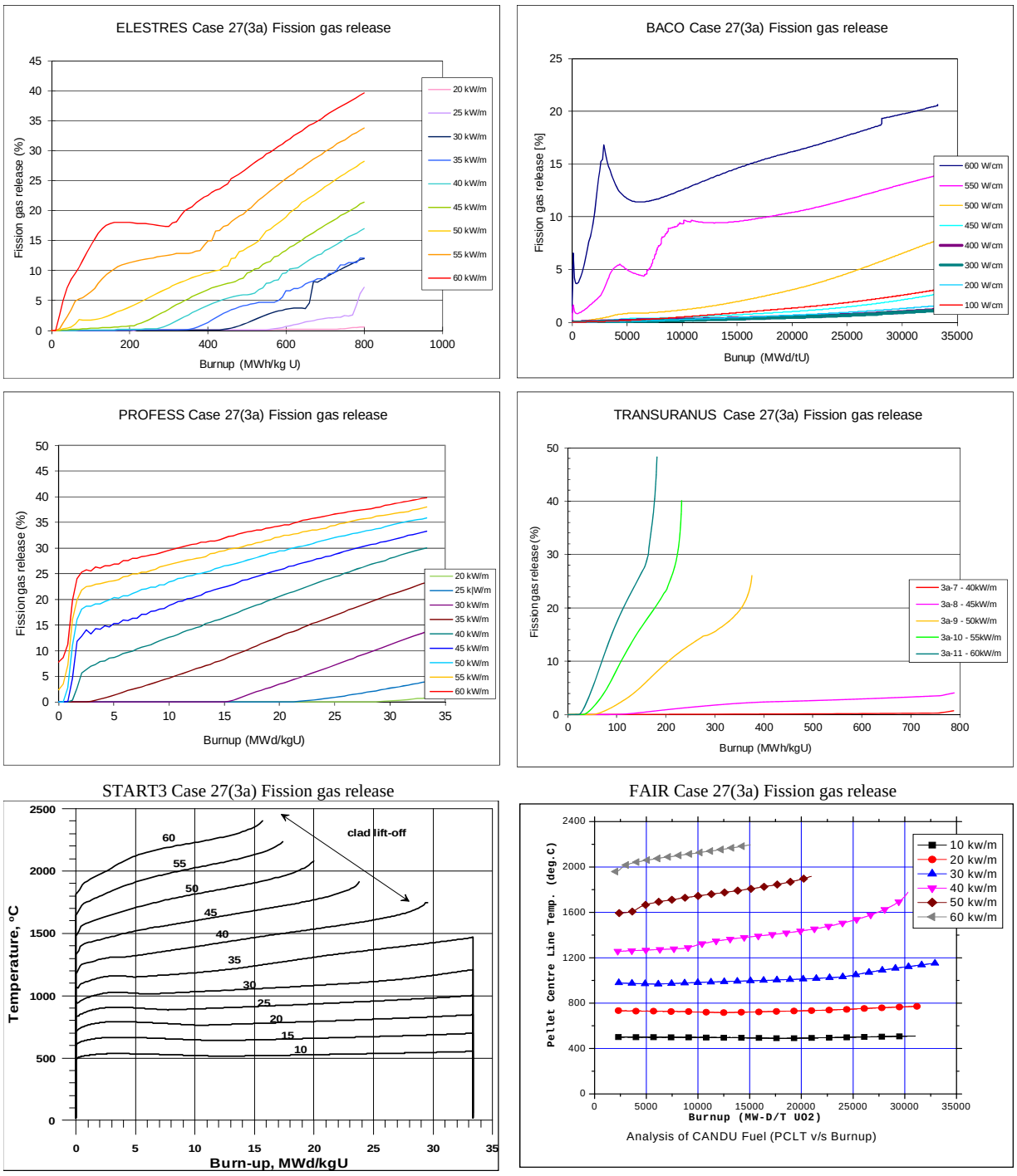

FIG. 16. Calculated fission gas releases for the idealized CANDU case 27(3a) as a function of constant power.

6.6.2. Case 27(3b)

CANDU case 27(3b) involved calculating the fuel pin behaviour for an idealized, extended power history representing the bounding CANDU power envelope up to a fuel burnup of 27.5 MW·d/kgU. A comparison of fission gas release (%) calculated by the six codes at fuel burnup 5, 10, 15 and 27.5 MW·d/kgU are compared in Fig. 17. A large scatter is found in the calculated FGR at all burnups.

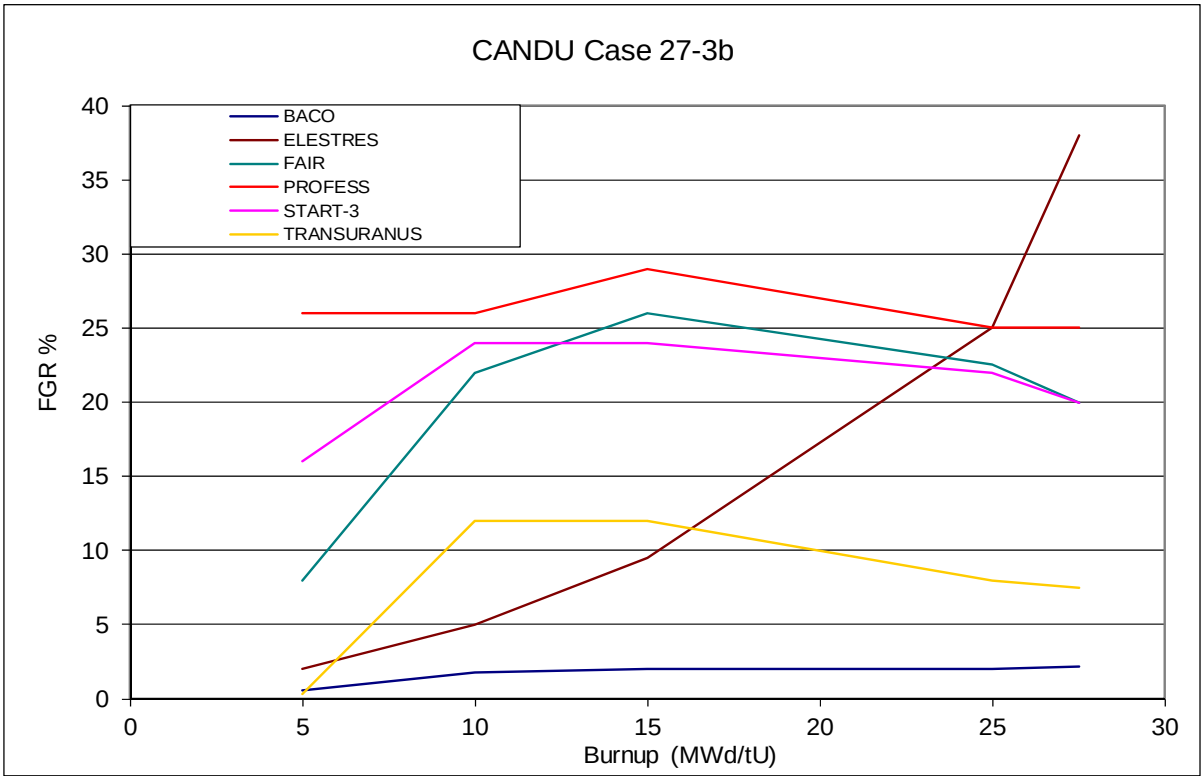

FIG. 17. Summary of fission gas release predictions for the idealized CANDU case 27(3b)

Detailed results of the modelling for fuel temperature, fission gas release and internal gas pressure are given in Figs 18 and 19. The wide variations seen reflect the difficult conditions of the idealized, bounding case.

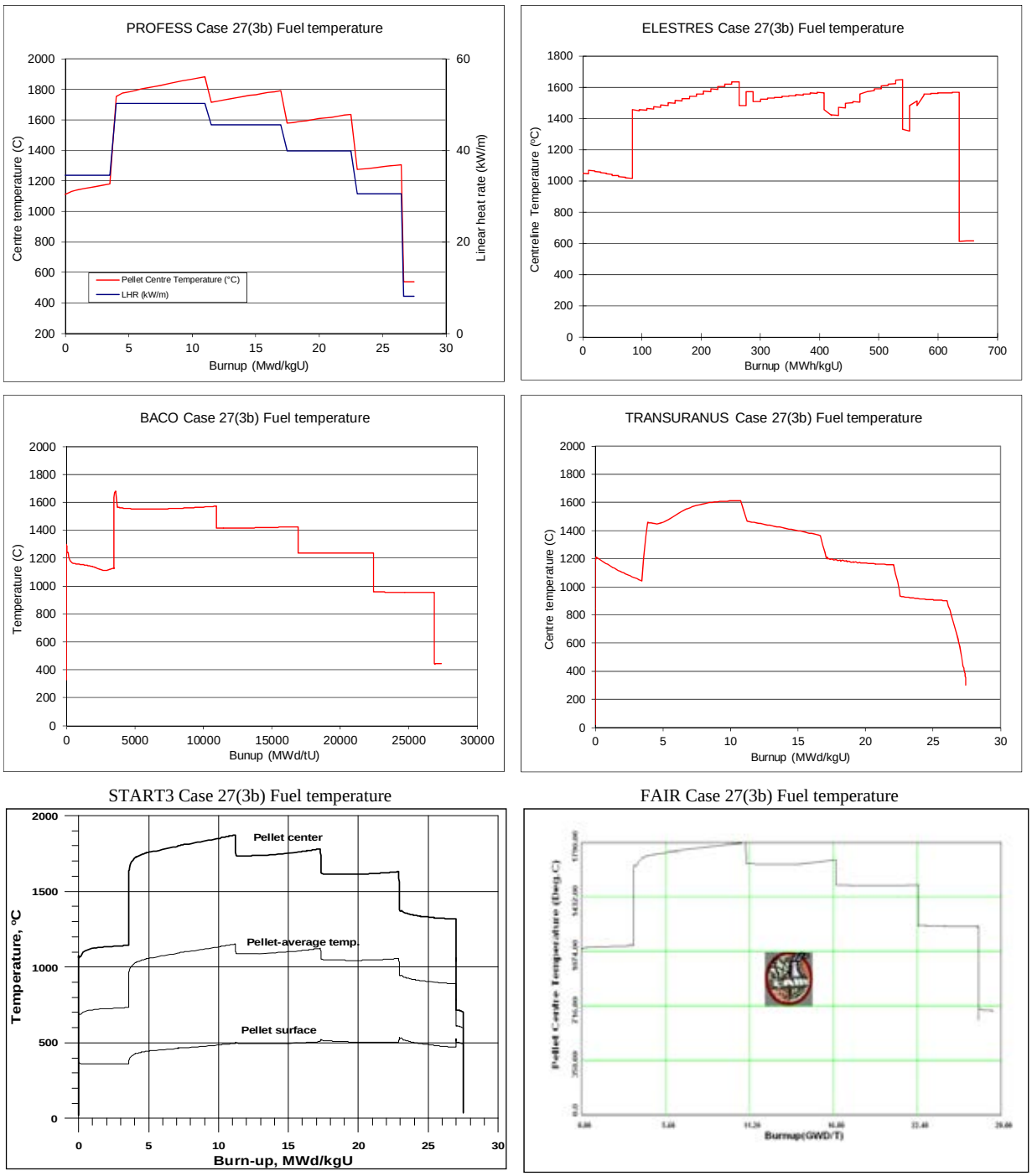

FIG. 18. CANDU idealized case 27(3b) Detailed modelling results for fuel temperature for bounding history of an advanced CANDU fuel cycle

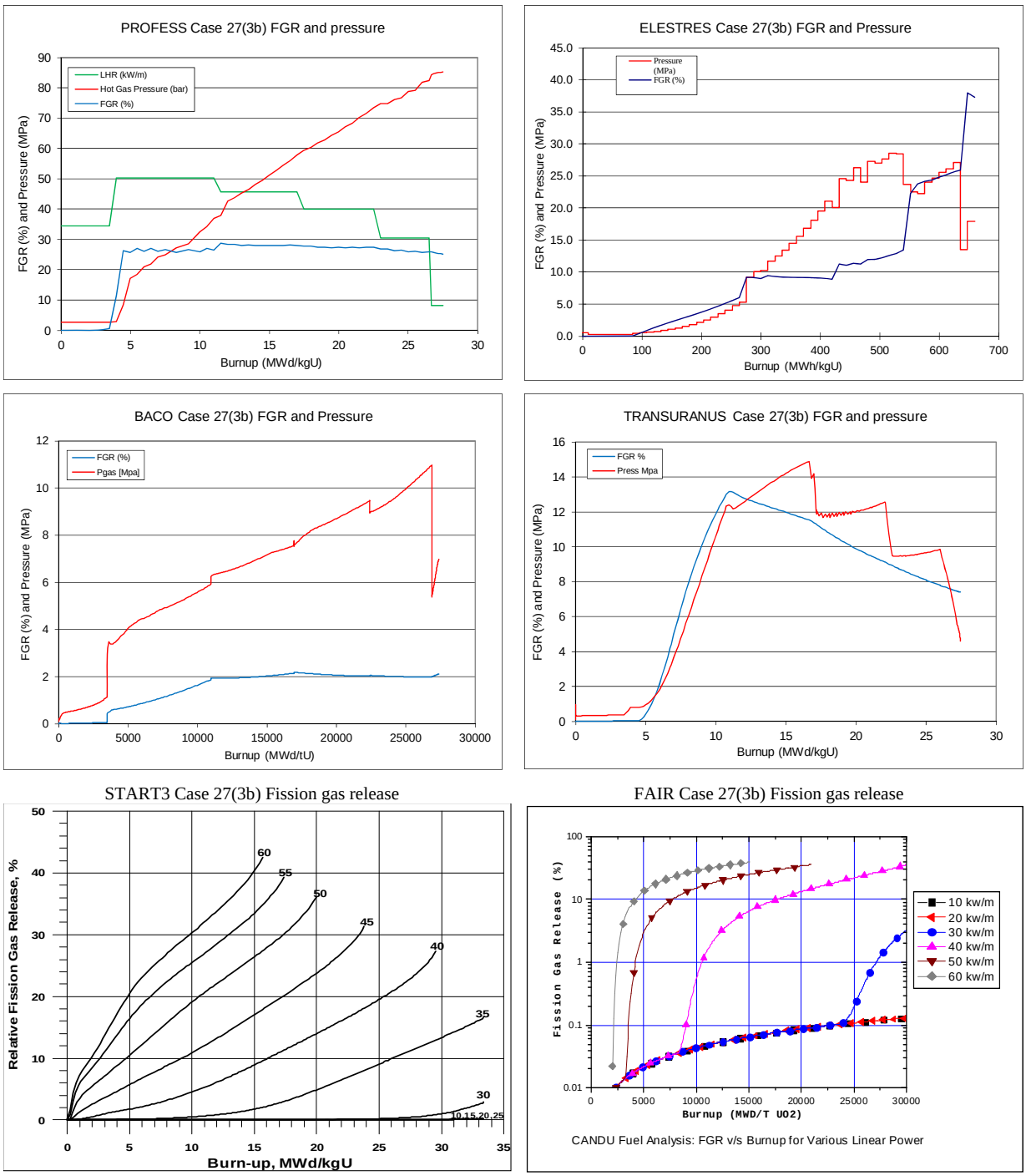

FIG. 19. CANDU idealized case 27(3b) Detailed modelling results for fission gas release and pressure for bounding history of an advanced CANDU fuel cycle.

It is clear from these results that there is no agreement on the predictions for the advanced CANDU power histories at high burnups. The extrapolation from the existing CANDU database is very large and the LWR codes are not validated against the high linear heat ratings of the CANDU fuel.

.

7. CODE COMPARISON WITH REAL CASES

The following real cases were chosen from the IFPE Database as they addressed key issues identified by the participants as requiring attention in their codes. Participants were requested to perform all of the high priority cases so that a meaningful inter code comparison could be made as well as a number of other optional cases to be chosen according to their preference. This section presents case by case results and discussion for the high priority cases and only briefly considers additional optional cases where predictions are available.

The high priority cases chosen were (Table 17).

TABLE 17. HIGH PRIORITY CASES

No.	Case identification	Measurements made for comparison
1.	Halden IFA 534.14, rod 18	EOL FGR and pressure, grain size 22 μm, Bu ≈ 52 MW·d/kgUO_2
2.	Halden IFA 534.14, rod 19	EOL FGR and pressure, grain size 8.5 μm, Bu ≈ 52 MW·d/kgUO_2
3.	Halden IFA 597.3, rod 7	Cladding elongation, at Bu ≈ 60 MW·d/kgUO_2
4.	Halden IFA 597.3, rod 8	FCT, FGR at Bu ≈ 60 MW·d/kgUO_2
7.	REGATE	FGR and cladding diameter during and after a transient at Bu ≈ 47 MW·d/kgUO_2
9.	Kola rod 3	WWER priority: FGR, pressure, creepdown at Bu ≈ 55 MW·d/kgUO_2
11.	Kola rod 86	WWER priority: FGR, pressure, creepdown at Bu ≈ 44 MW·d/kgUO_2
14.	Risø-3 AN3	FGR and pressure-EOL, FCT, Bu ≈ 37 MW·d/kgUO_2
15.	Risø-3 AN4	FGR and pressure-EOL, FCT, Bu ≈ 37 MW·d/kgUO_2
16.	HBEP, rod BK363	FGR-EOL, Bu ≈ 67 MW·d/kgUO_2
17.	HBEP, rod BK365	Fission products and Pu distribution, FGR–EOL, Bu ≈ 69 MW·d/kgUO_2
18.	HBEP, rod BK370	Fission products and Pu distribution, FGR–EOL, Bu ≈ 51 MW·d/kgUO_2

7.1. CASES 1 AND 2: IFA-534.14, RODS 18 & 19

7.1.1. Experimental history and details

These cases taken together give data for the effect of grain size on FGR and the kinetics of release at high burnup.

Two refabricated rods from IFA 534.14 were modelled. Rod 18 (case 1) had a grain size of 22 microns whilst rod 19 (case 2) had a grain size of 8.5 μm.

The base irradiation history in Goesgen was given in three axial zones with a flat axial power profile. The irradiation powers were low up to a discharge burnup of 52 MW·d/kgUO_2. During re-fabrication at Kjeller, it was found that the rods had 100–150 μm of HBS at the pellet rim. The Halden re-irradiation commenced at a power of ~30 kW/m falling to ~20 kW/m over ~3 MW·d/kgUO_2. The full power history of case 1 is shown in Fig. 20 and that of case 2 was similar.

FGR was measurements were made in both rods, rod 18 (large grain) and rod 19 (small grain) which achieved values of 8.89 and 4.68% respectively. Predictions for both rods were required of:

- FGR versus burnup;
- Rod internal pressure versus burnup.

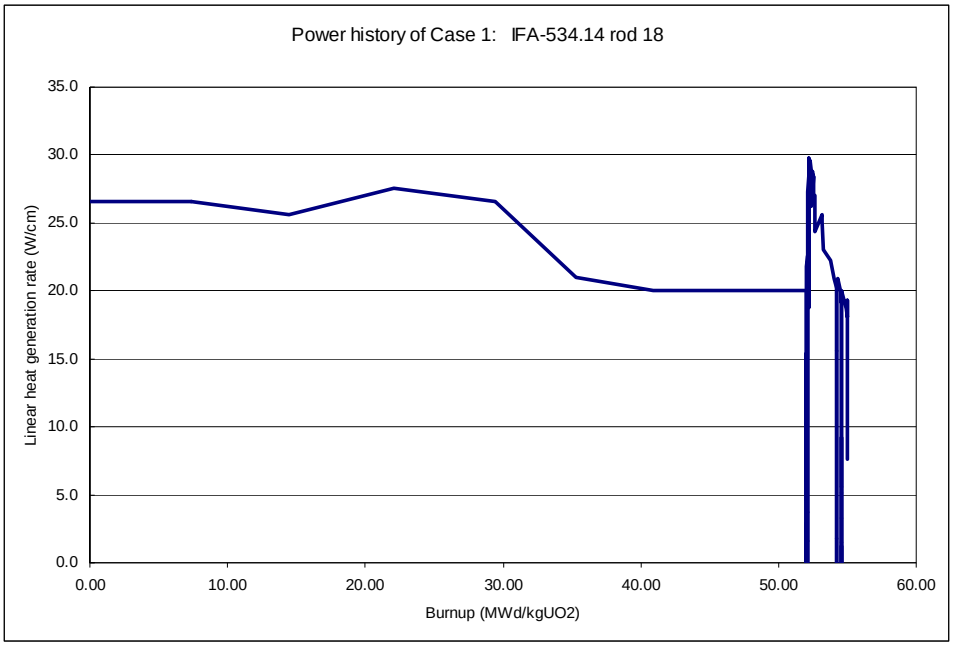

FIG. 20. Base and ramp irradiation of the refabricated Goesgen rod, IFA 534.14 rod 18.

7.1.2. Fission gas release calculations

Figures 21 and 22 show the predicted FGR from the rods 18 and 19 respectively. The code predictions generally give values for both the base irradiation FGR and the FGR during the Halden irradiation.

There is no experimental measurement of the release from the base irradiation, the experimental result is only for the FGR during the Halden irradiation and is therefore best compared with the incremental FGR calculated from the code predictions, which is plotted as 'transient' release.

The majority of the codes give under-predictions of the releases in these cases, and there is quite a wide spread in the predictions for the base release, which will give difficulties in calculating the transient release measured during the test. A further difficulty is in the modelling of re-fabricated rods which often requires special handling the data input to the codes.

Figure 23 shows the transient releases only, and it is easier to see the generalised under-prediction of the codes.

The effect of grain size on the code results is best seen by comparing the ratio of the FGR predictions for the two rods (Fig. 24). It is expected that the release from the large grain size rod 18 should be smaller than rod 19 and the experimental ratio (rod 19/rod 18) was found to be 1.85, roughly proportional to the grain size ratio. This result is in good agreement with the predictions of a simple Booth release model, where the release from a spherical grain is inversely proportional to its radius.

It is good to see that most codes gave a ratio close to the experimental value, not only for the transient release, but also for the base irradiation predictions as well, indicating that the modelling of this effect is appropriate.

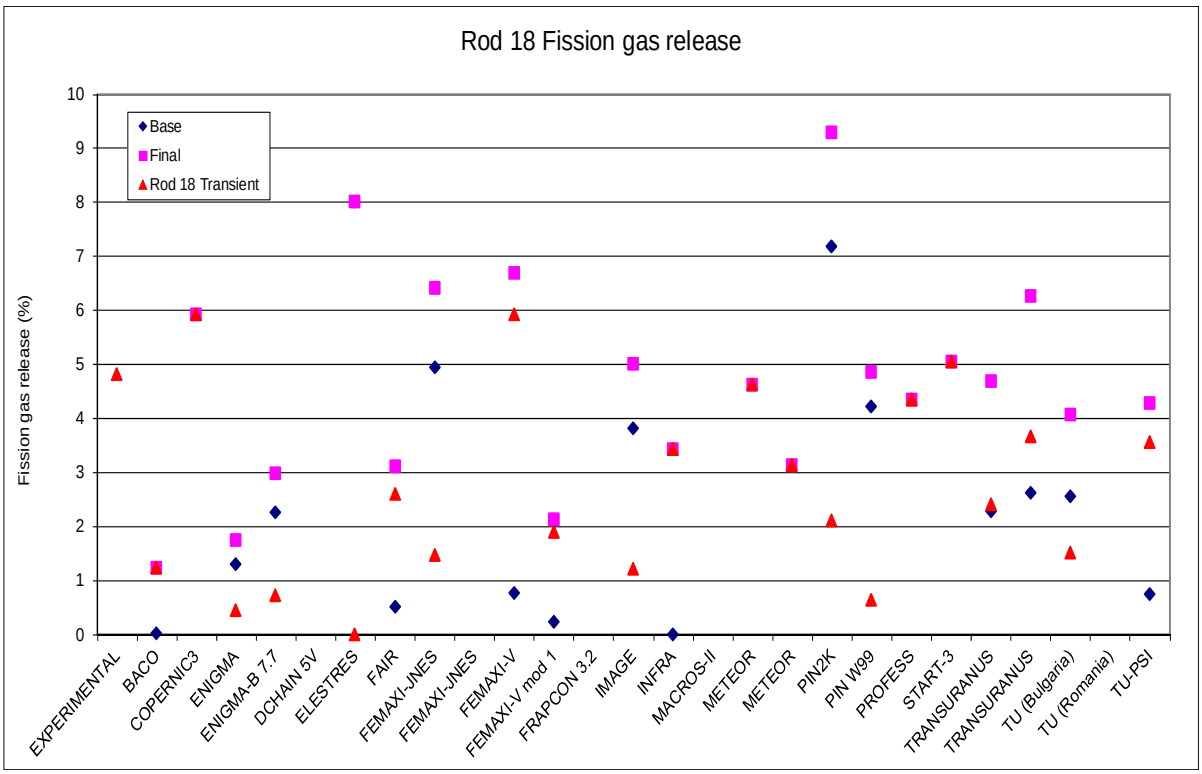

FIG. 21. Case 1: Predicted FGR from IFA 534.14 rod 18. The code predictions of FGR are shown, both at the end of the base irradiation and at the end of the test irradiation in Halden. The experimental measurement is for the release during the Halden irradiation only.

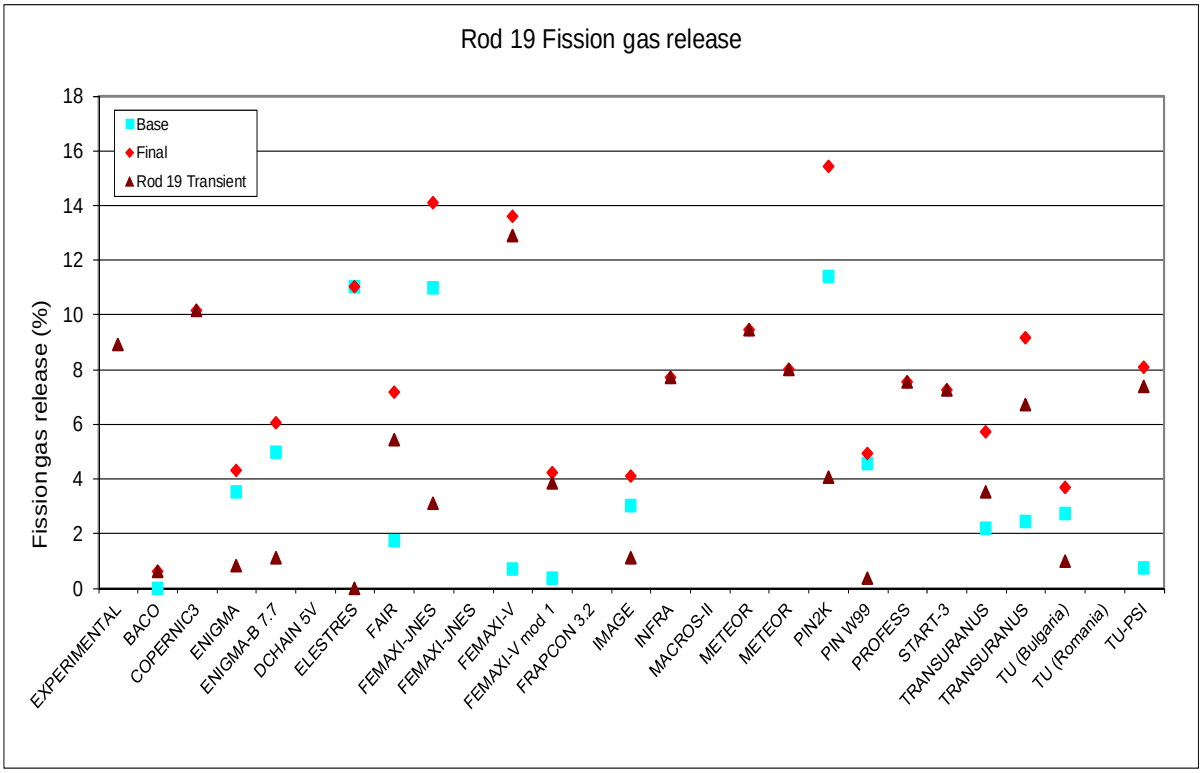

FIG. 22. Case 2: Predicted FGR from IFA 534.14 rod 19. The code predictions of FGR are shown, both at the end of the base irradiation and at the end of the test irradiation in Halden. The experimental measurement is for the release during the Halden irradiation only.

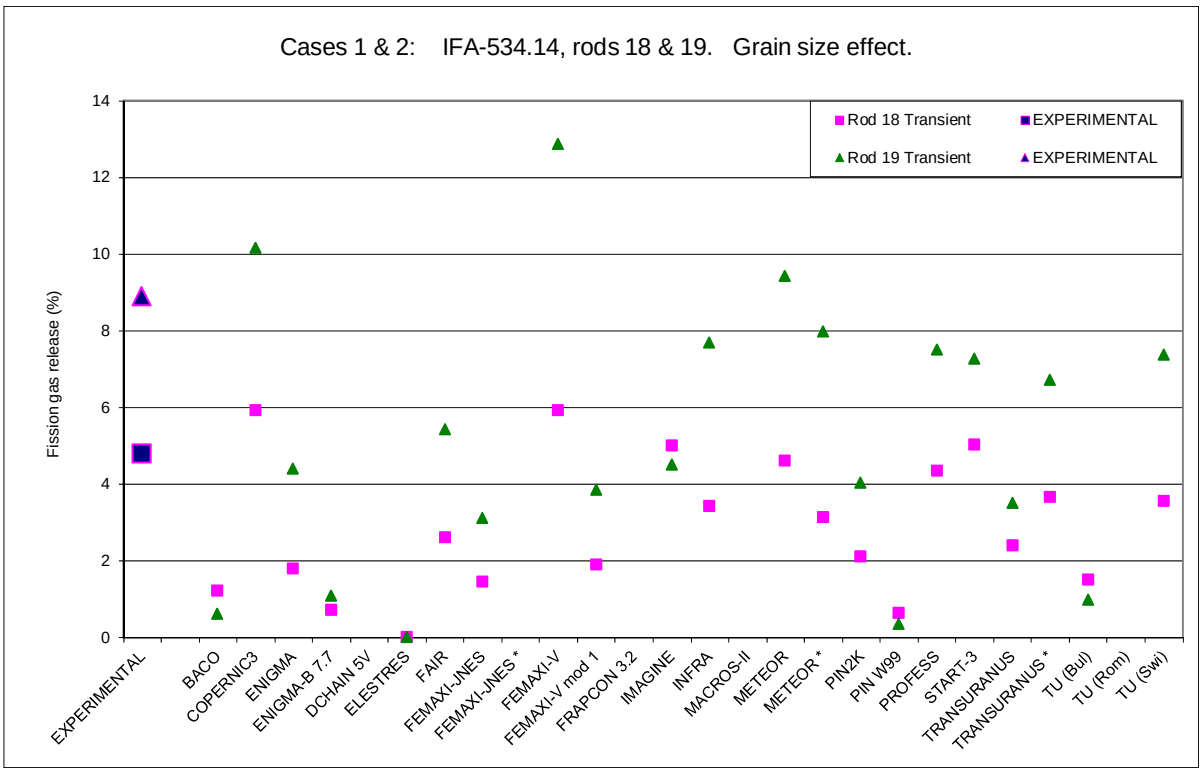

FIG. 23. Predicted and measured FGR from rods 18 and 19 for the release during the re-irradiation in the Halden reactor.

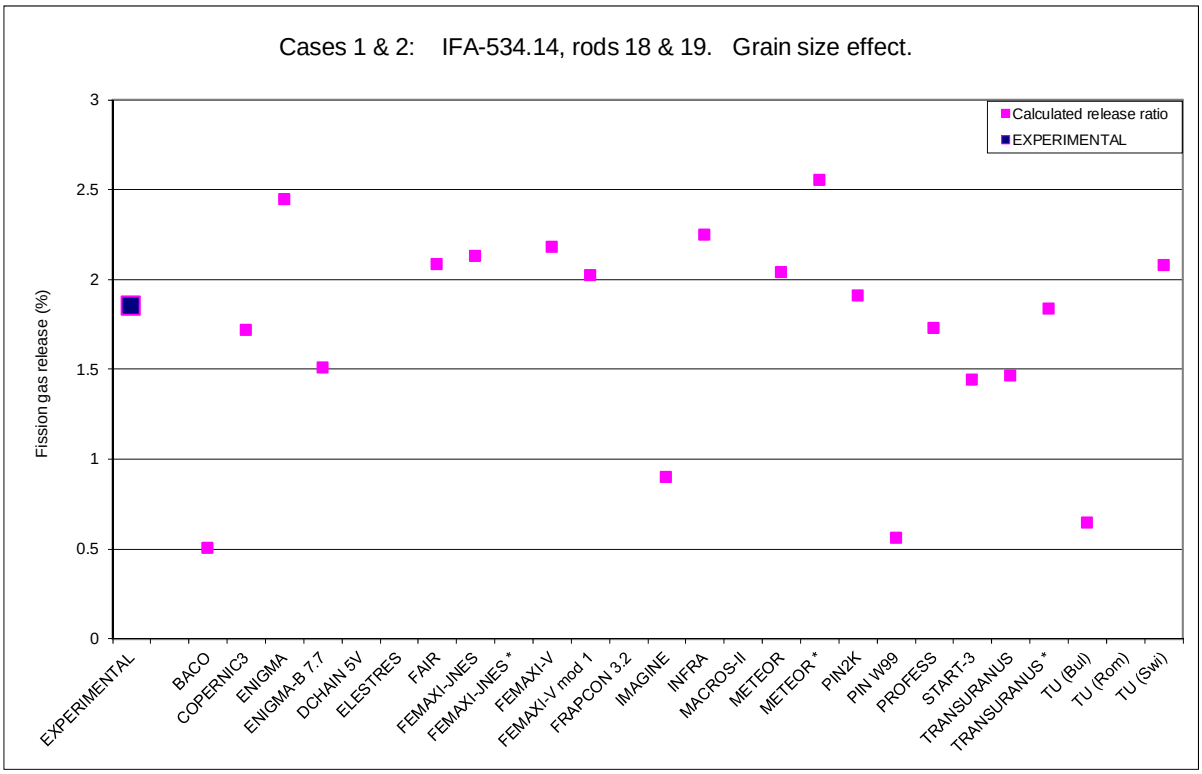

FIG. 24. Cases 1 and 2, Halden IFA 534.14, rods 18 and 19. Grain size effect comparison. The code predictions of the ratio of fission gas release from the rods are shown.

The predictions of internal gas pressure are given in the participants' reports appended to this publication.

7.2. CASES 3 AND 4: IFA-597.3, RODS 7 AND 8

7.2.1. Experimental history and details

This experiment also utilised re-fabricated rods. The mother rod was irradiated at a low average power, typically ~16 kW/m, for several years in the Ringhals BWR to a discharge burnup of 59 MW·d/kgUO_2. During PIE an FGR of 2.5–3% was measured, and a restructured zone to a depth of >200 μm was found near the pellet periphery.

The history for the base irradiation and the Halden re-irradiation was supplied for four axial zones: top, middle, bottom and at the thermocouple location for the re-fabricated fuel sections. Two rods were cut from the same mother rod and therefore have identical dimensions, specification and irradiation history. Both rod 7 and 8 were fitted with a centerline thermocouple. In addition, rod 7 had a cladding elongation detector, whilst rod 8 was fitted with an internal pressure sensor. Thus data are available for the kinetics of PCMI and FGR during the Halden irradiation.

The FGR measured after gas extraction was ~15% but unfortunately, the pressure sensor only recorded accurately the first 8–9%, as at this point the sensor reached the maximum of its range. The elongation detector operated correctly for the whole of the Halden irradiation and showed an initial large extension which gradually reduced throughout the 2.5 MW·d/kgUO_2 re-irradiation.

After irradiation extensive PIE was performed, so extra information is available for comparison with code predictions although as these were not requested, they will not be considered here.

Predictions were required for:

- Centerline temperature versus power during initial and final ramp.
- FGR versus burnup.
- Clad elongation versus burnup.

The irradiation histories of the rods are shown in Figures 25 and 26 and the experimental fission gas measurements are shown in Fig. 27. The pressure detector reached the end of its range at around 60 MW·d/kgUO_2, and the measurement is unreliable after this point. The PIE measurement at the end of the experiment gave an FGR of 15.8%. Clad elongation measurements are shown in Fig. 28.

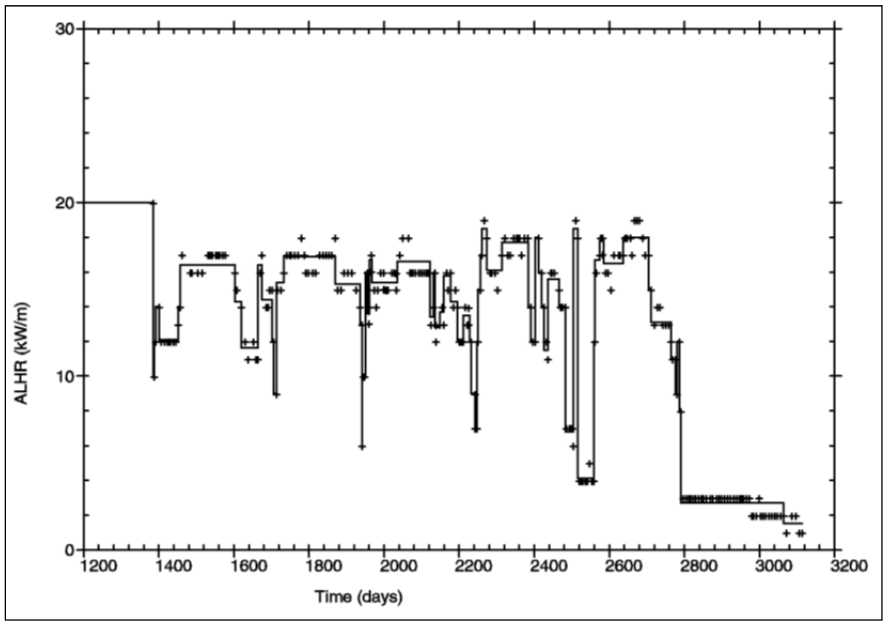

FIG. 25. Base irradiation history of IFA 597.3, carried out at Ringhals BWR.

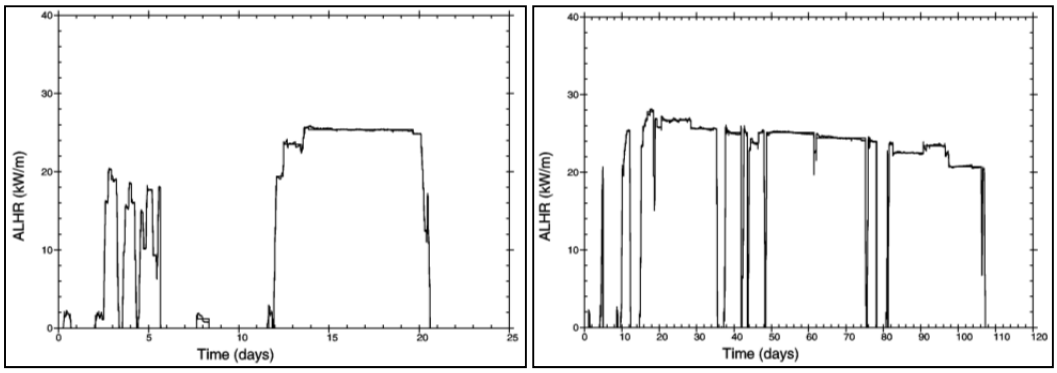

FIG. 26. Halden irradiation periods for IFA597.3 rod 8 (rod 7 similar to second period).

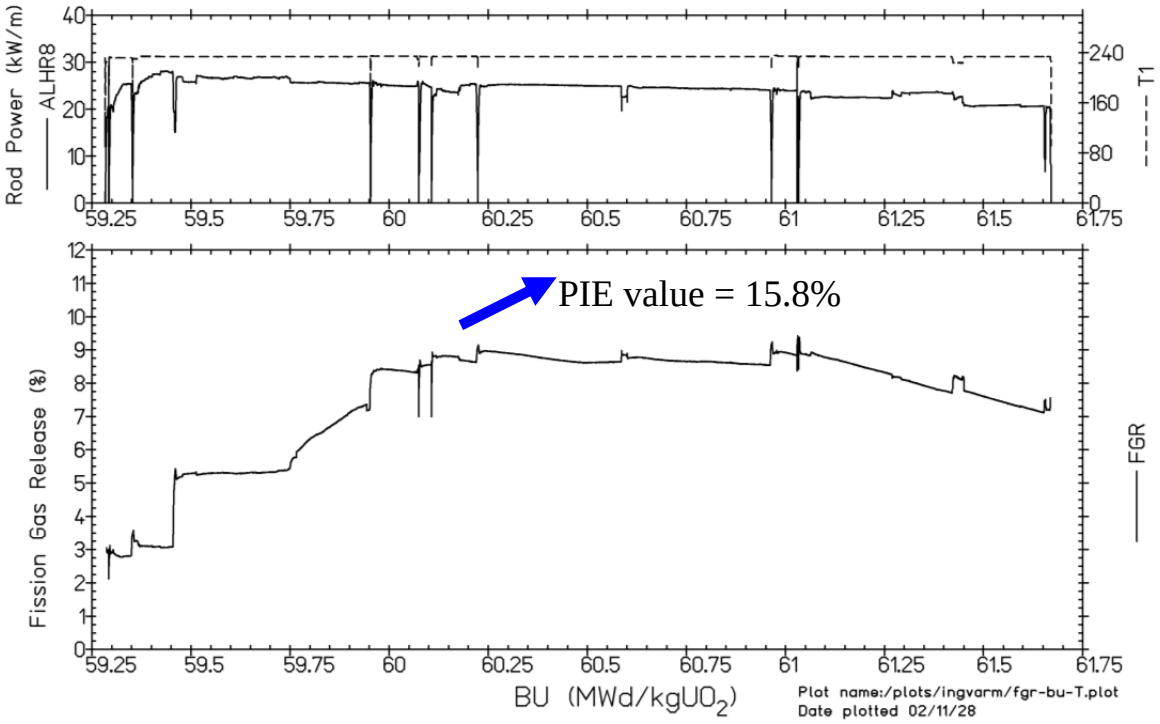

FIG. 27. Fission gas release measurement. The pressure detector reached the end of its travel at around 60 MW·d/kgUO_2 and the measurement is unreliable after this point. The PIE measurement at the end of the experiment gave an FGR of 15.8%.

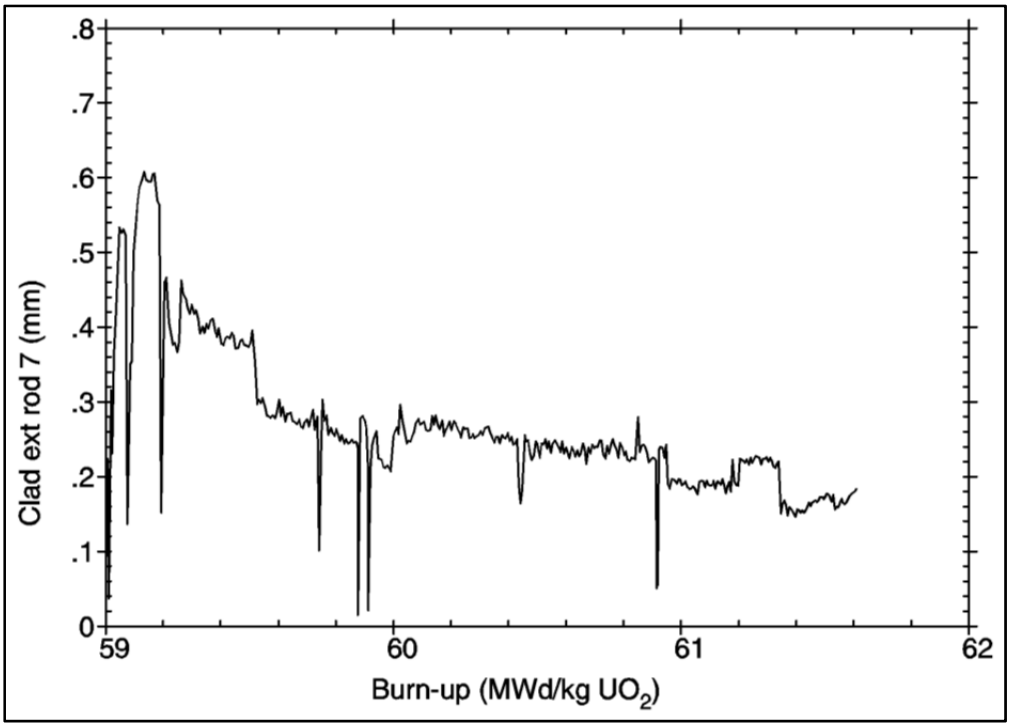

FIG. 28. Axial extension measurements for IFA597.3 rod 7.

The main characteristics of this irradiation that make it suitable as a case study were:

- Flat axial power profile.
- 4 axial zones.
- Top, middle, bottom and at the thermocouple position.
- Low average power.
- Long irradiation time.
- 59 MW·d/kgUO_2.
- 2.5–3.3% FGR at the end of the base irradiation.
- >200 μm HBS at pellet rim.

7.2.2. Centreline temperatures

Due to the re-fabrication of the rods, the first ramp to power gave a good opportunity to calculate temperatures with zero gap and no fission gas contamination. The final ramp tests the codes ability to follow the various changes in thermal conductivity and gap conditions that have occurred during the Halden irradiation. The code predictions are shown separately in Fig. 29 with the Halden measurements of centre temperature for the two ramps for comparison.

The results show that nearly all of the codes model the temperatures well, with some modelling the experimental data extremely well. This result shows that the modelling of fuel temperature is well advanced and reflects the experience in the previous FUMEX CRP.

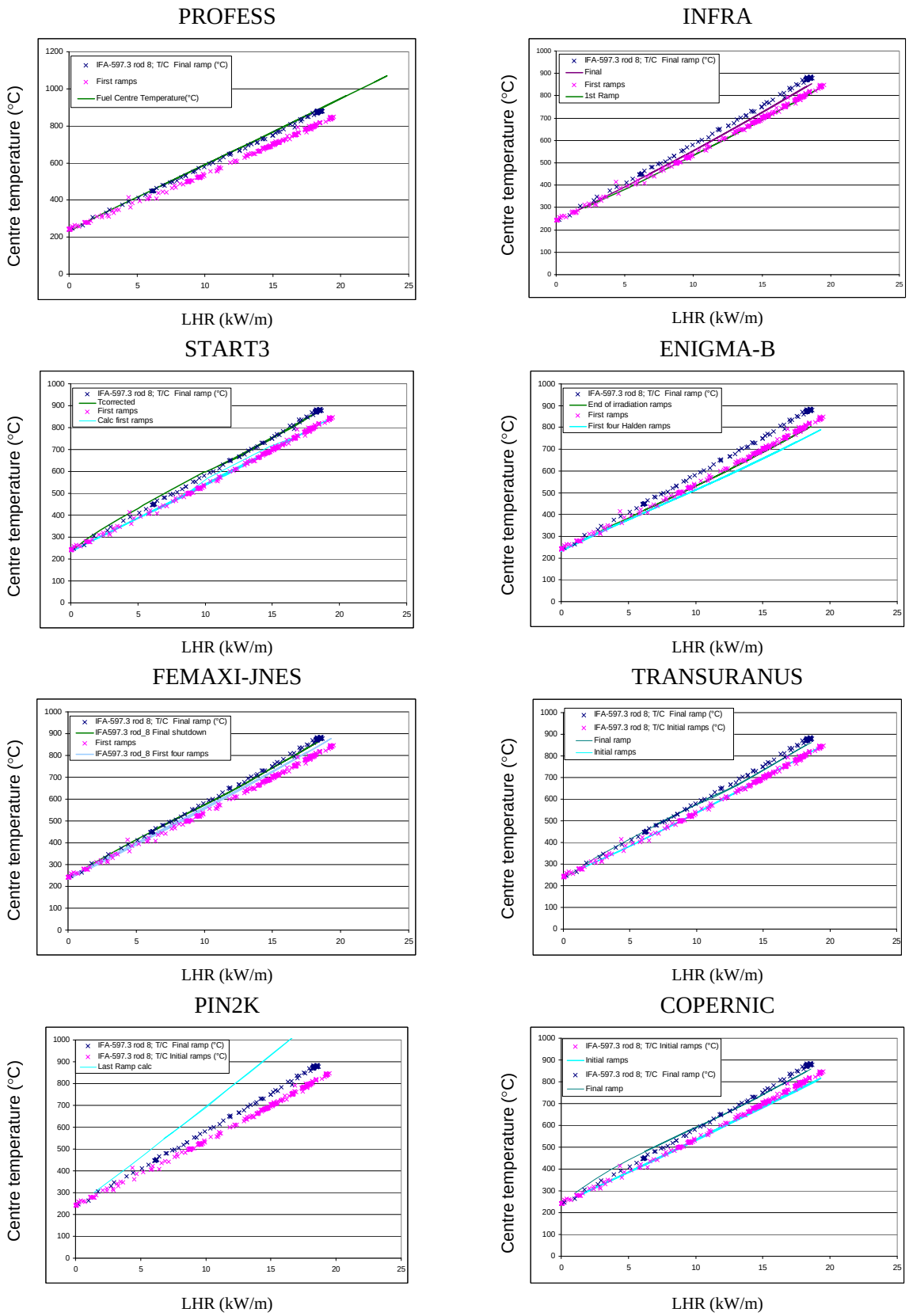

FIG. 29. Code calculations of fuel centre temperature for power ramps at the start and end of the irradiation of the re-fabricated IFA534 Rod 8 as a function of linear heat rate (kW/m).

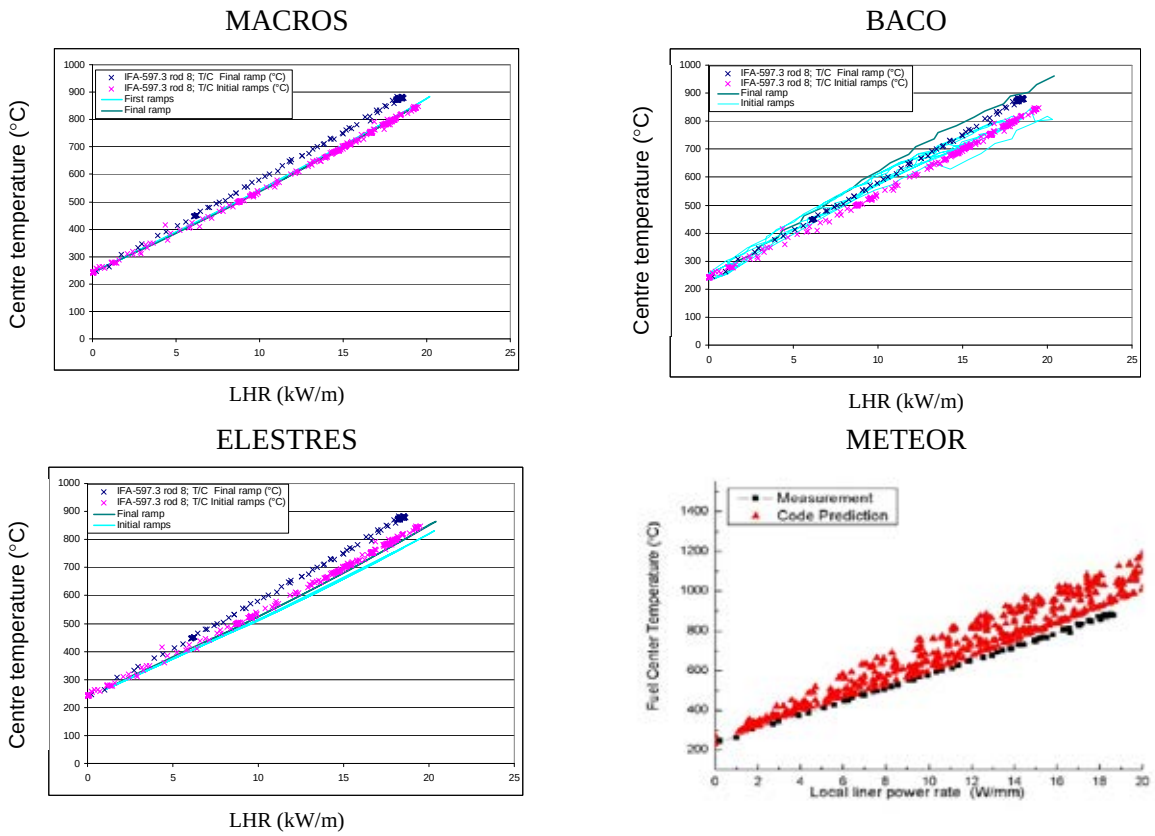

FIG. 29. Code calculations of fuel centre temperature for power ramps at the start and end of the irradiation of the re-fabricated IFA534 Rod 8 as a function of linear heat rate (kW/m). (cont.)

7.2.3. Fission gas release predictions

The code predictions for the fission gas release measurements are shown for each code in Fig. 30. The experimental data shows the fission gas release as calculated by the pressure gauge for the first half of the irradiation period with the final PIE measurement available for the end of the period. The release from the base irradiation is accounted for by the initial value of the pressure gauge value (around 3% for rod 8).

Several codes had difficulties in matching the burnup of the base irradiation and the results have not been adjusted to allow for this effect, so that some results are offset on the X-axes of the plots.

Many of the codes were able to model the final gas release measurement, and others were able to match the kinetics revealed by the pressure transducer, but not many were able to do both.

The results are summarized in Fig. 31.

PROFESS

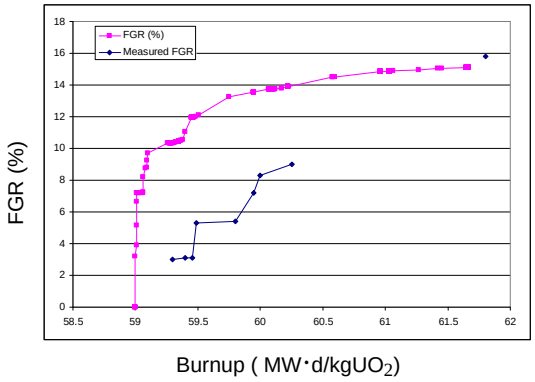

INFRA

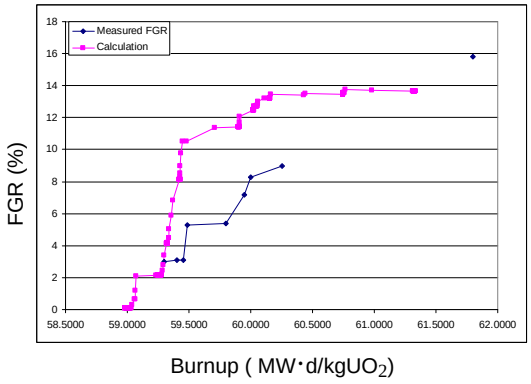

START3

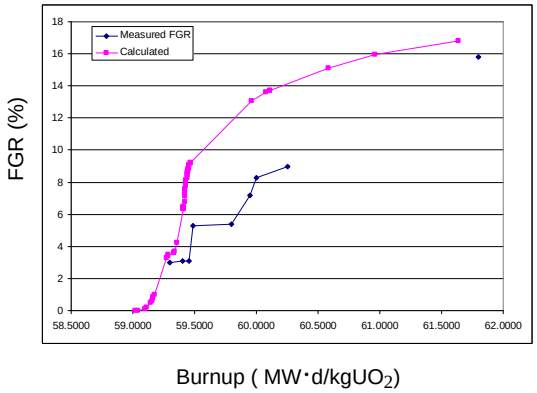

ENIGMA-B

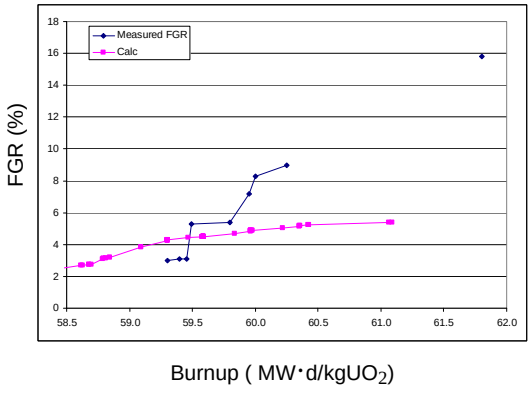

FEMAXI-JNES

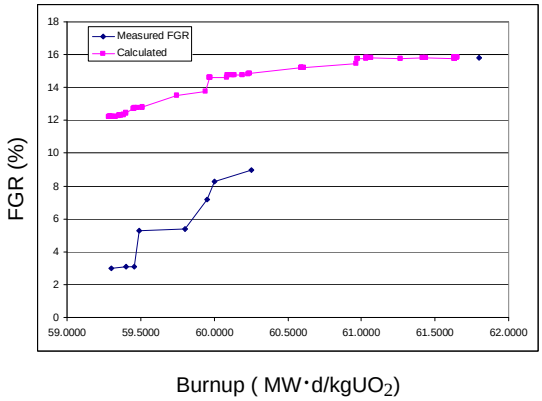

TRANSURANUS

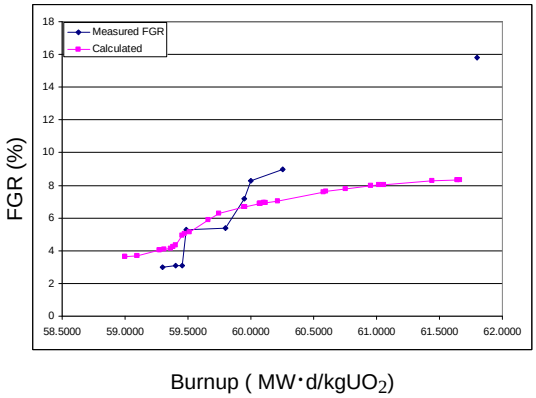

PIN2K

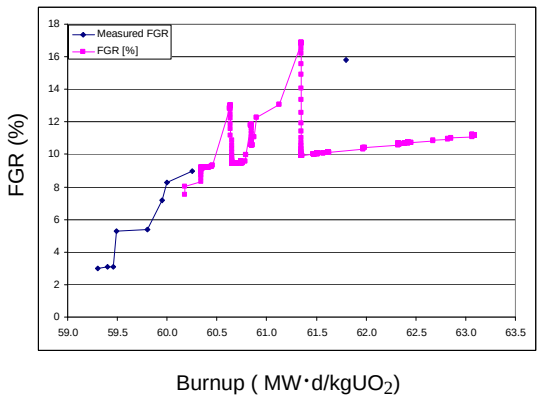

COPERNIC3

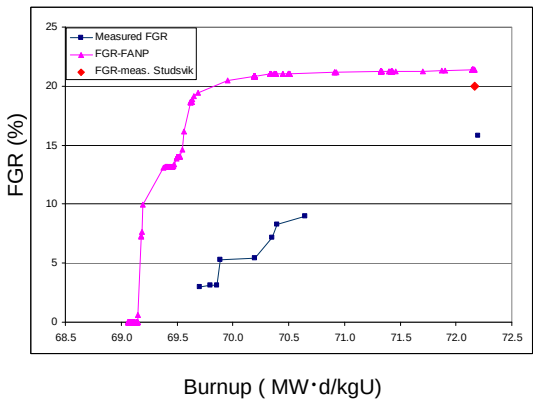

FIG. 30. Calculations of the FGR during the final irradiation period of IFA597.3 rod 8.

DCHAIN5V

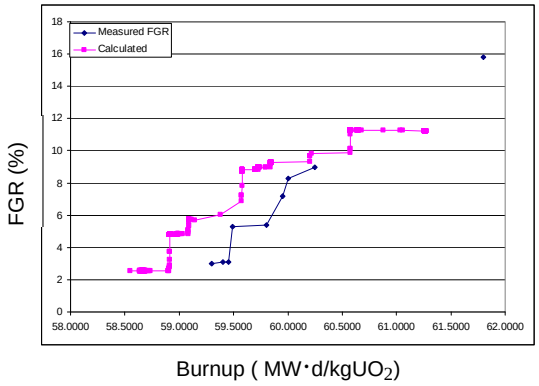

MACROS

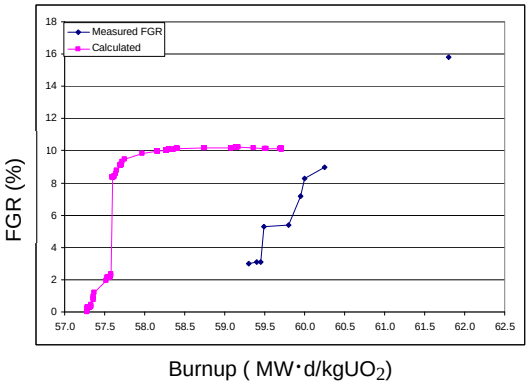

BACO

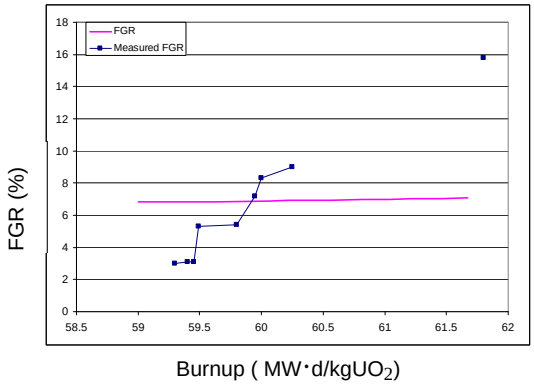

FEMAXI (Czech)

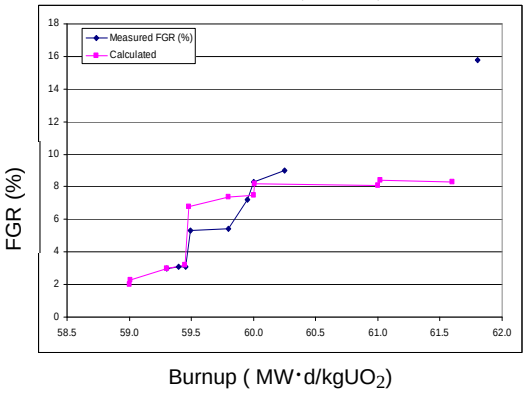

TRANSURANUS (Switzerland)

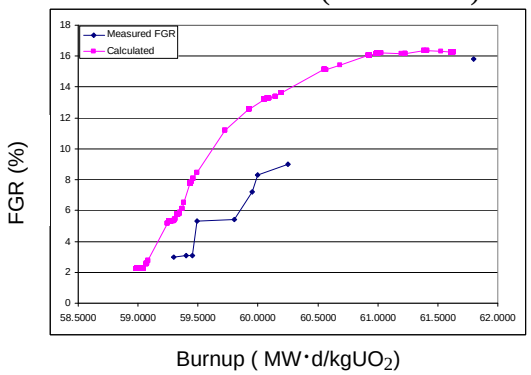

METEOR

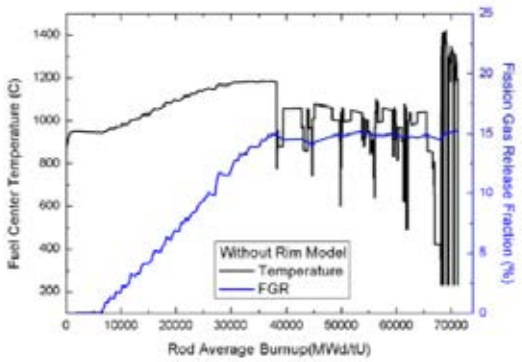

ENIGMA and IMAGINE (Finland)

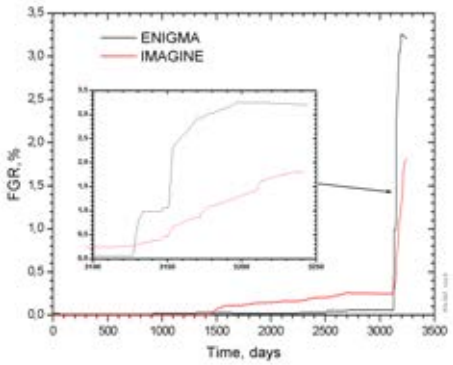

FIG. 30. Calculations of the FGR during the final irradiation period of IFA597.3 rod 8. (cont.)

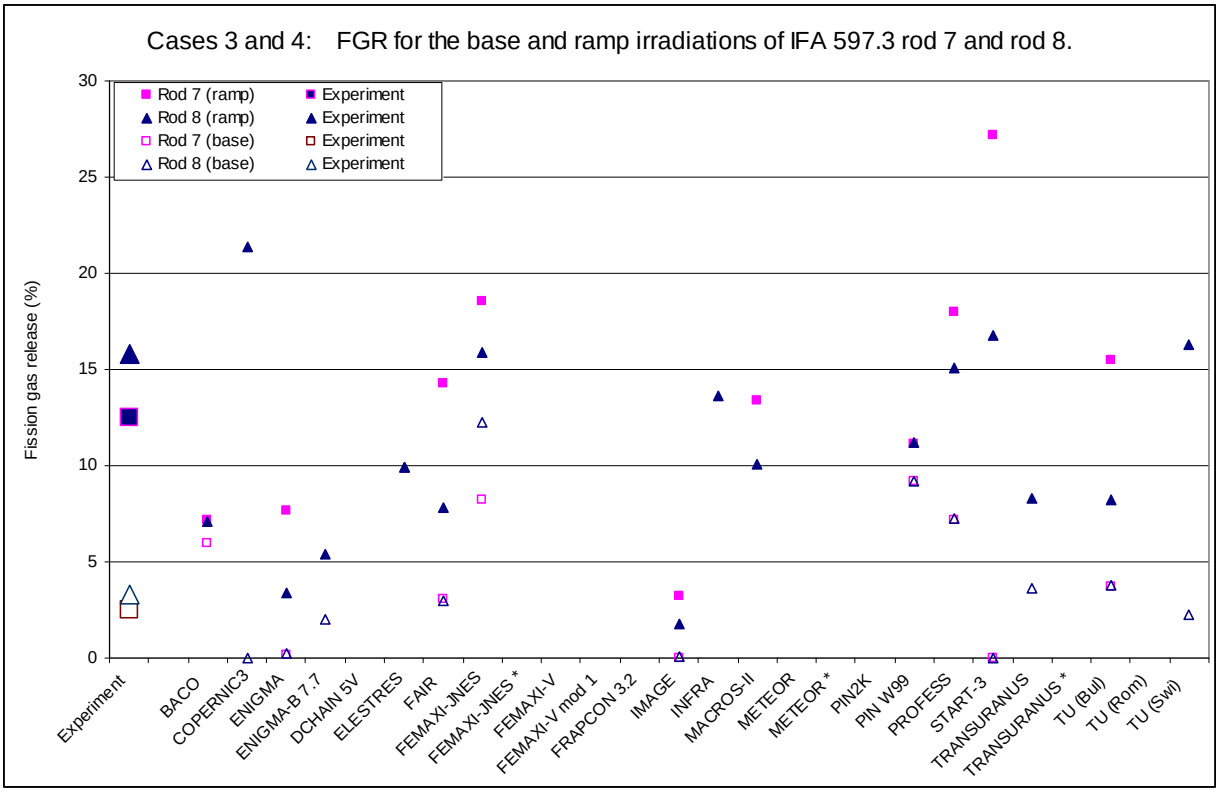

FIG. 31. FGR calculations for cases 3 and 4 showing the predicted and measured values at the end of the base irradiation and after the ramp.

7.2.4. Clad elongation

Not all codes were able to attempt this case, though for some the results are very good, with the predictions matching the trend and absolute values well. There were many problems for the codes in calculating the burnup for this case and most of them have adjusted their calculated burnup from the base irradiation to match the Halden experimental value that was provided. The results are shown in Fig. 32. Several of the codes used this case to adjust their models and several provided different predictions for differing versions of their code. These variations are not generally shown in the figures, but can be found in the detailed reports of the participants appended to this publication.

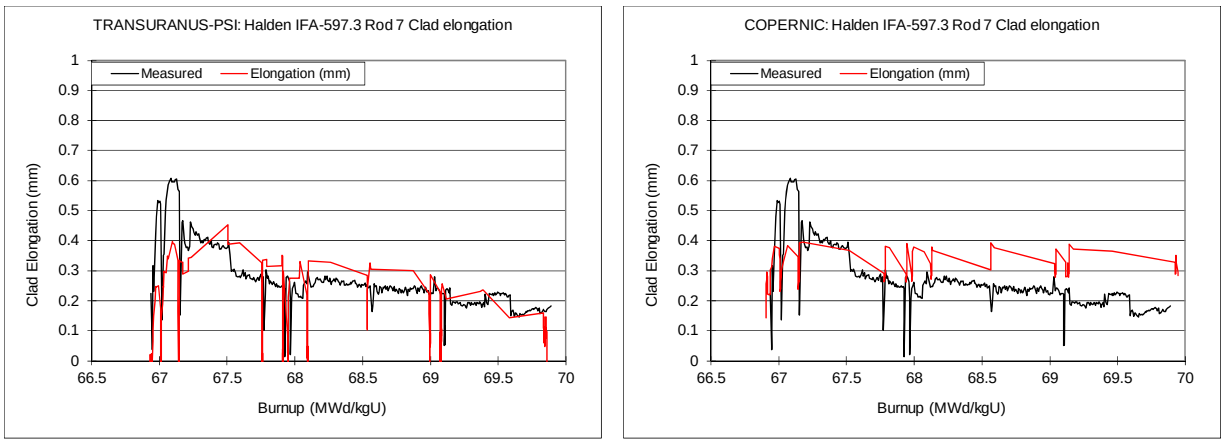

FIG. 32. Clad elongation calculations for Rod 7 (case 3).

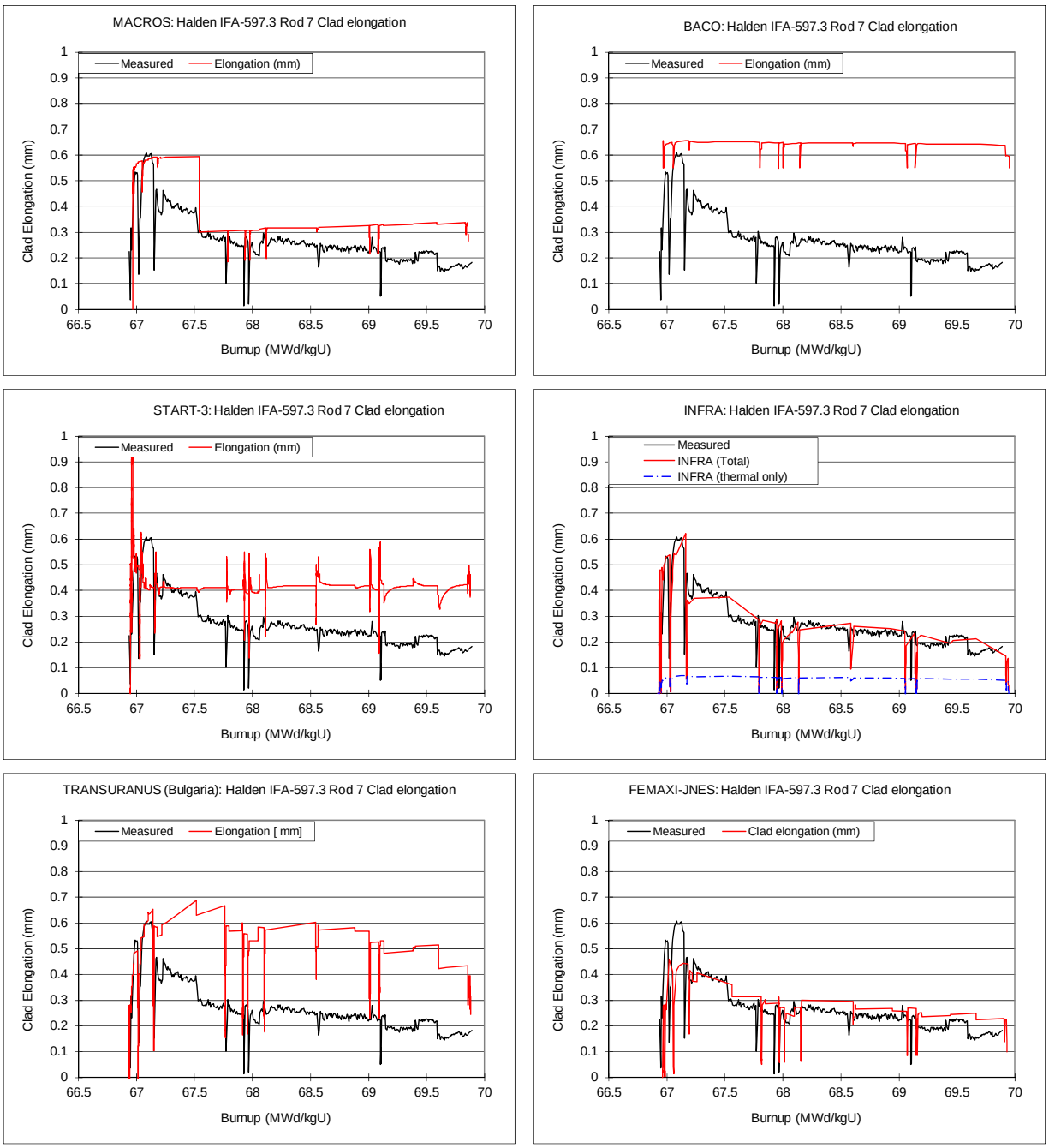

FIG. 32. Clad elongation calculations for Rod 7 (case 3). (cont.)

7.3. CASE 7: REGATE

7.3.1. Power history

All the previous cases came from Halden and therefore, to widen the database to eliminate any bias, this case was included to provide data on FGR and clad diameter change on a short fuel segment irradiated in a commercial PWR and ramped in the SILOE test reactor.

The original segment was irradiated in the Gravlines 5 PWR up to 47.415 MW·d/kgHM. Non-destructive PIE was conducted on discharge with measurements made on clad diameter and a FGR of 1.5% estimated by non-destructive ^{85}Kr gamma measurement.

The segment was not subject to any re-fabrication and was power ramped in the Aquilon device in SILOE. The re-irradiation consisted of a pre-condition power step of 19.5 kW/m (peak) for 48 hours

prior to ramping at 1.0 kW/m/min up to 38.5 kW/m (peak) which was held for 1.5 hours. The rod average power history is shown in Figure 33.

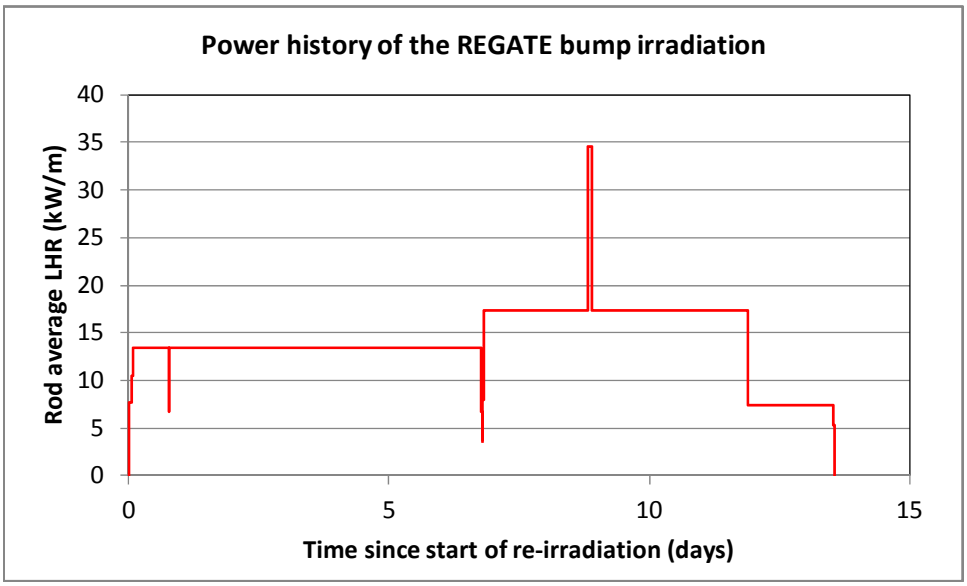

FIG. 33. Rod average power history for the REGATE bump irradiation in the SILOE reactor.

Subsequent PIE measured oxide thickness and clad diameter. FGR was measured at 9.3% by ^{85}Kr and 10.2% after puncturing and gas extraction. Detailed ceramography was carried out at the location of maximum power and EPMA radial distributions of: Cs, Nd, O, Pu, U and retained Xe were measured at the same location.

The following predictions were required:

- FGR versus time.
- Axial diameter trace.

7.3.2. Fission gas release predictions

The fission gas release predictions are summarized in Fig. 34. The experimental results for the base and transient irradiations periods are shown. Figure 35 separates out the transient release predictions.

Figure 36 shows the kinetic predictions of four of the codes, which are typical. In general there was no detailed study of the release during the transient, the release was very rapid for all the codes that attempted this task.

It is clear that most codes predict both base and transient release quite well. An example of an exception to the general trend are the FAIR and ELESTRES codes, which are both CANDU codes, and this example shows the problems that such codes have with difficult PWR histories.

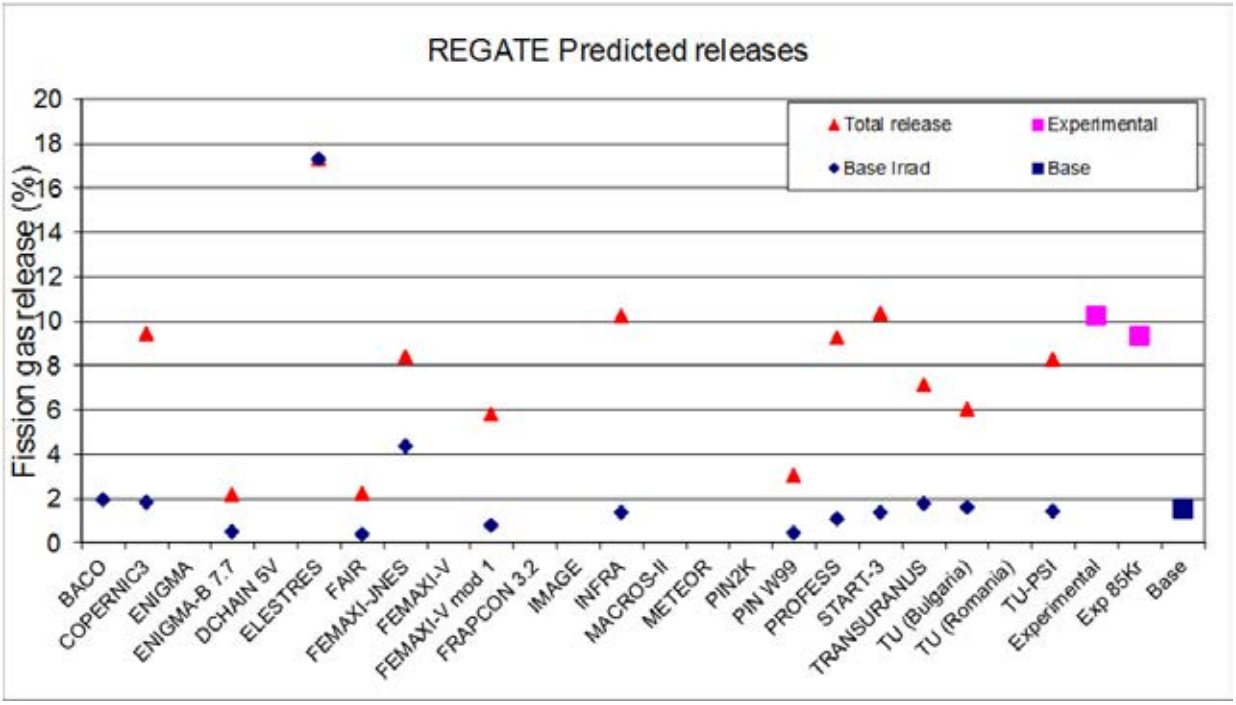

FIG. 34. Results of code calculations for the REGATE experiment, case 7.

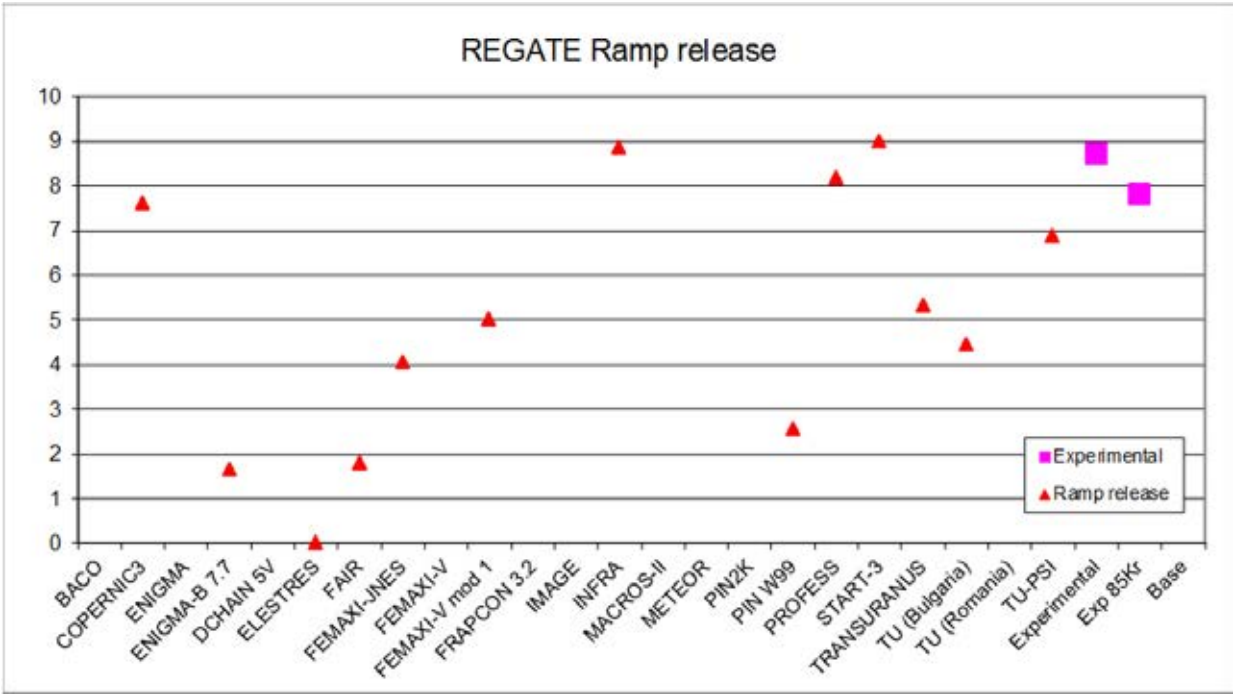

FIG. 35. Predicted releases during the ramp for the REGATE experiment, case 7.

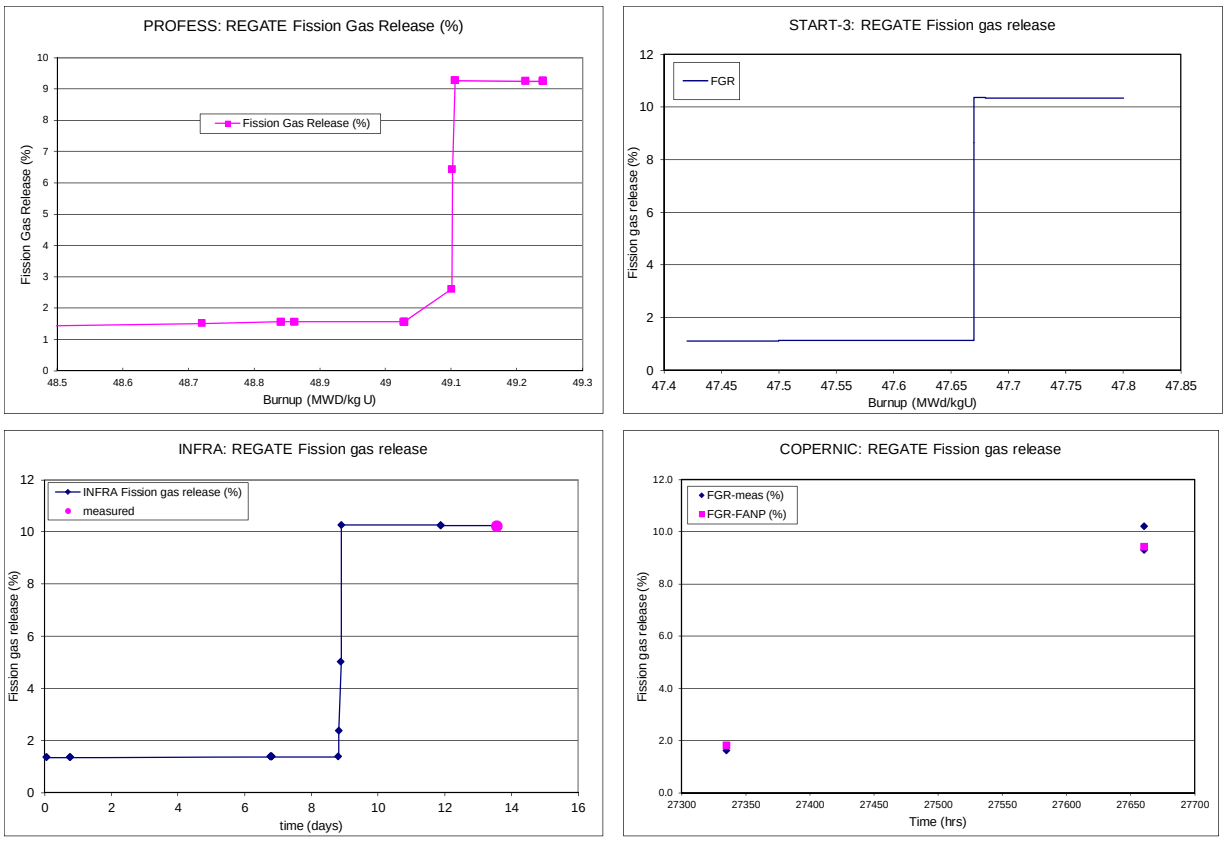

FIG. 36. Fission gas release prediction the REGATE experiment, case 7. Four code predictions are shown as a function of time or burnup, showing predictions of a simple step release with little time dependence.

7.3.3. Predictions of diametral strain

The priority case 3, IFA 597 rod 7, was intended to test codes handling of the mechanical treatment of fuel pellets and PCMI. The results from the 7 codes that were able to attempt an axial variation of clad diameter are shown in Fig. 37. Additionally, other codes were able to estimate the maximum diameter, e.g. the ELESTRES code calculated a value of 9.51 mm, which is close to the peak measurement. The codes had to calculate the pre-test irradiation, and there were variations in the calculated burnup which caused some difficulties.

Most of the codes that attempted this calculation were reasonably successful.

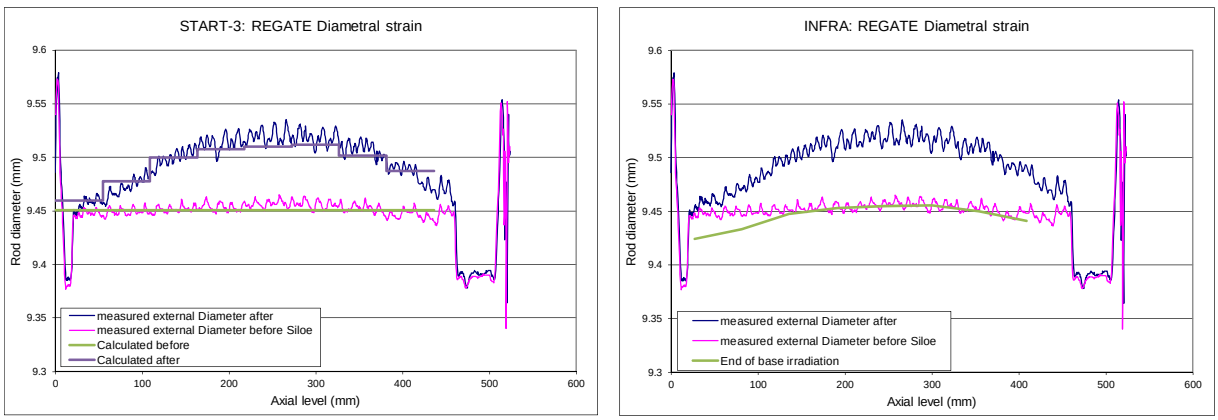

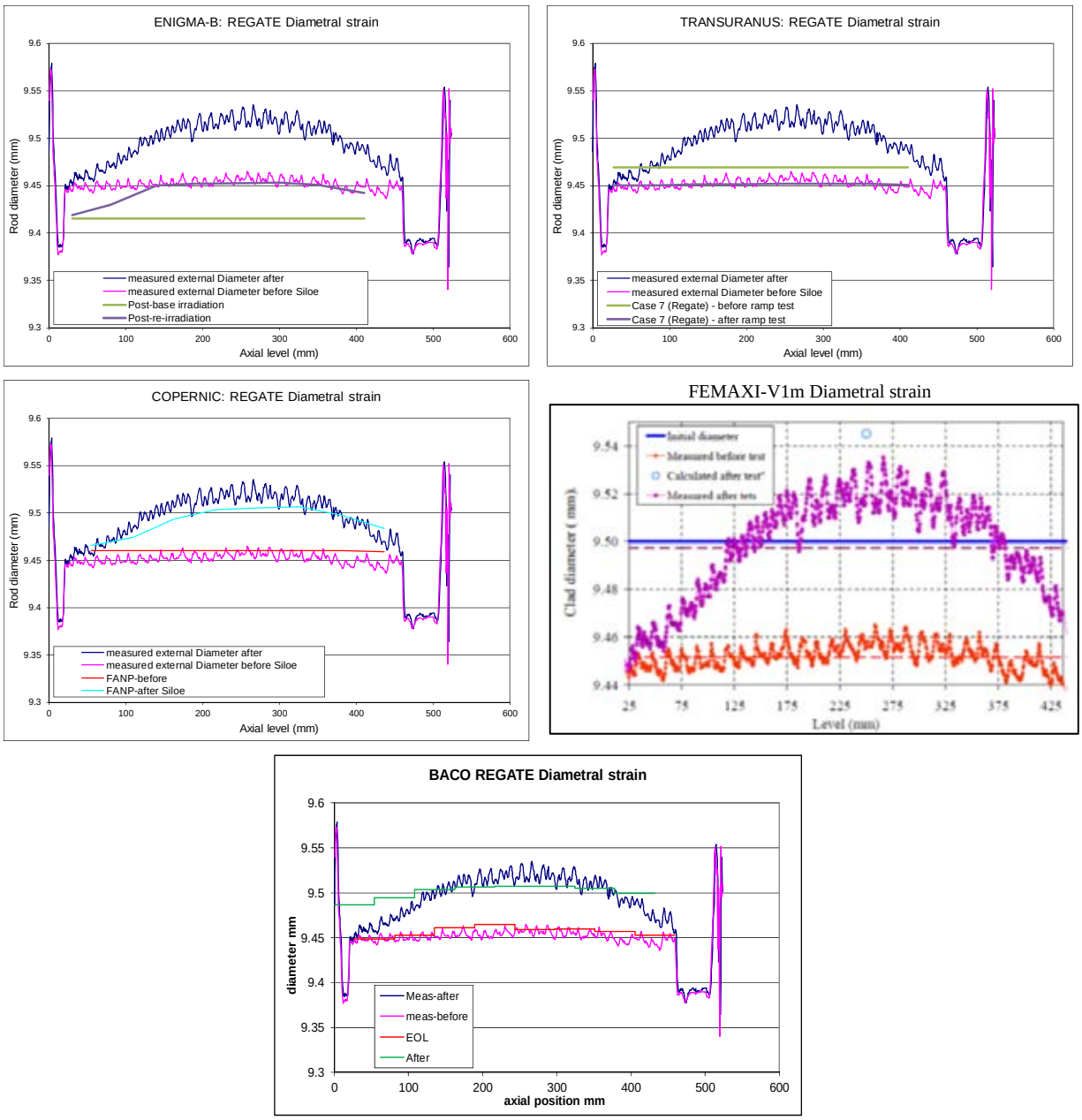

FIG. 37. Predictions of the codes able to calculate the axial variation of rod diameter following the test ramp.

7.4. CASES 14 AND 15: RISØ-3 RODS AN3 AND AN4

7.4.1. Power histories

These cases are very similar to the Halden IFA-597.3; the sections were cut from commercially irradiated PWR mother rods of near identical specification and irradiation history to 35.6 MW·d/kgUO_2. During re-fabrication with pressure transducers and centre-line thermocouples, AN3 was back filled with helium whilst AN4 was back filled with xenon. Both were subjected to the same bump test history in Risø of ~72 hours at 40 kW/m, hence the data they produced demonstrated the difference in centre-line temperature, the kinetics and magnitude of FGR between closed gap rods with and without full fission gas contamination.

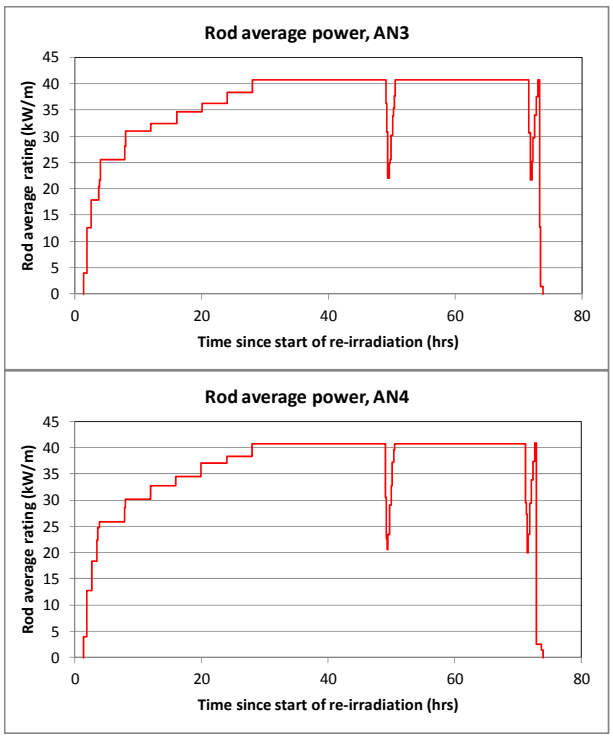

FIG. 38. Power histories for the AN3 and AN4 power ramps.

Although a substantial amount of PIE was performed on these rods, the only predictions requested for both AN3 and AN4 as follows:

- Centre-line temperature versus power during first rise to power.
- FGR versus time.
- Rod internal pressure versus time.

Code predictions for the gas pressure measurements can be found in the participants' reports which are appended to this publication.

7.4.2. Centreline temperatures

Modelling of the temperatures measured during the Risø bump tests is shown in Fig. 39. The majority of the codes follow the measured fuel centre temperature during the ramp quite well and show the expected higher temperature for the xenon filled rod. The codes generally have many input options and some of the results show some of these, showing how the choice of input parameters to a code can alter the predictions significantly, and with different input data can match the measurements much more closely. In general, the codes having most difficulty in predicting the temperatures well were the CANDU codes, which are not well suited to LWR conditions.

One feature of the Risø temperature ramps that was not modelled by any code was the temperature overshoot on each step during the rise to power.

The overall result is that the temperatures are well predicted by all the codes, and the modelling of fuel centre temperature is generally satisfactory.

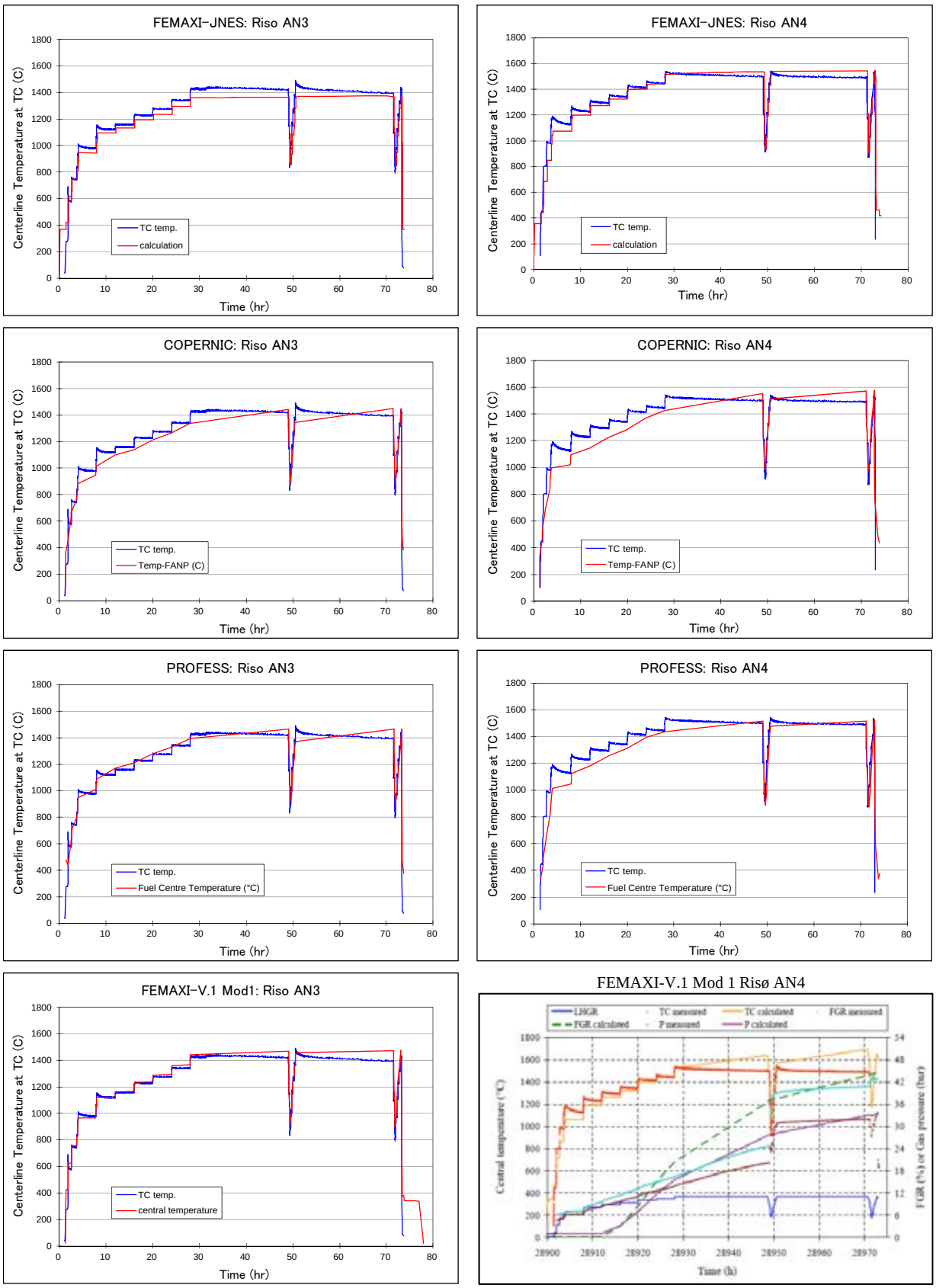

FIG. 39. Fuel centre temperatures calculated for the bump ramps at Risø AN3 and AN4.

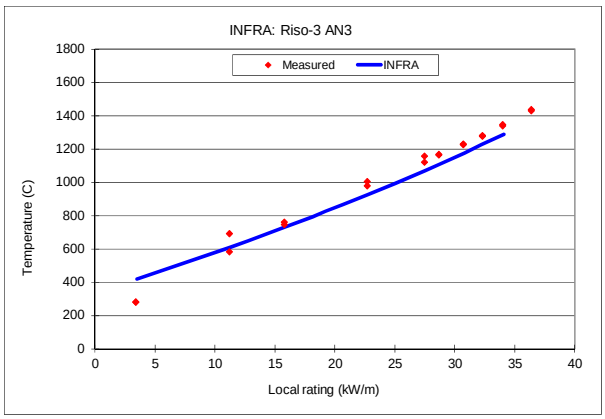

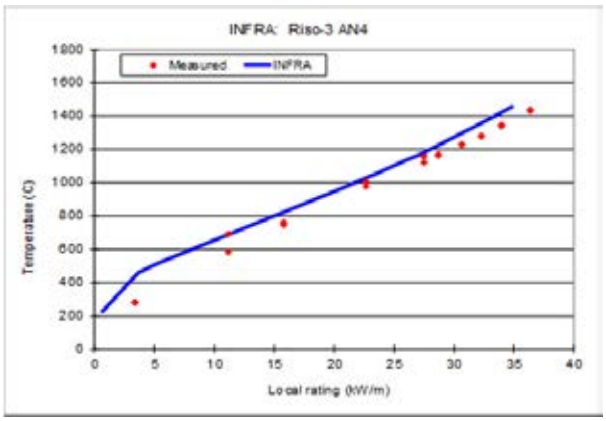

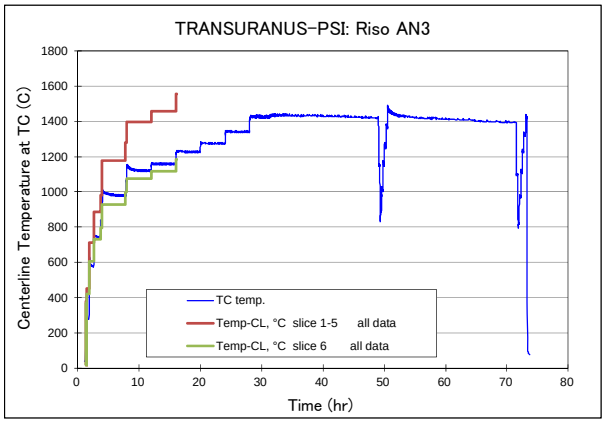

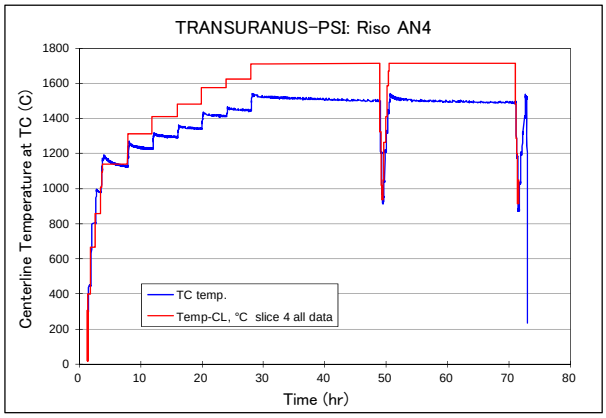

TRANSURANUS: Risø AN3

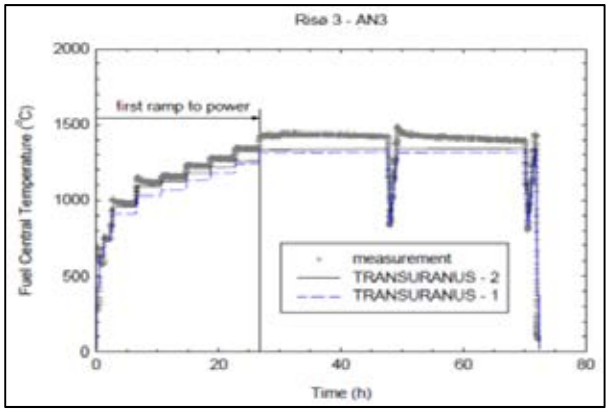

TRANSURANUS Risø AN4

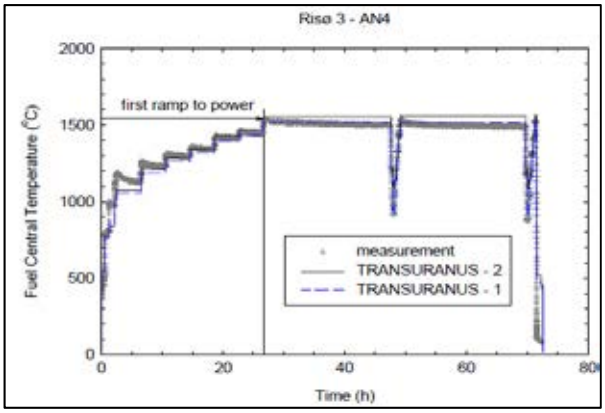

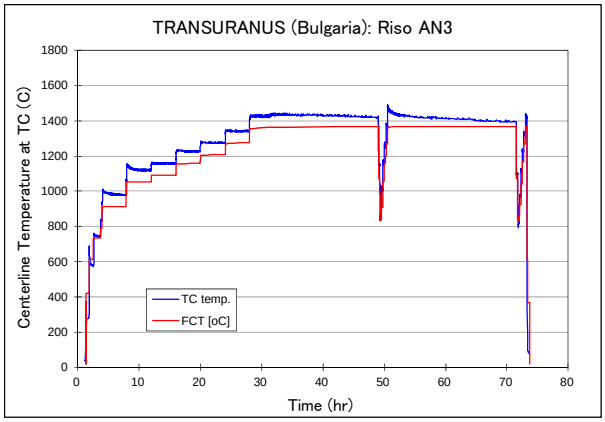

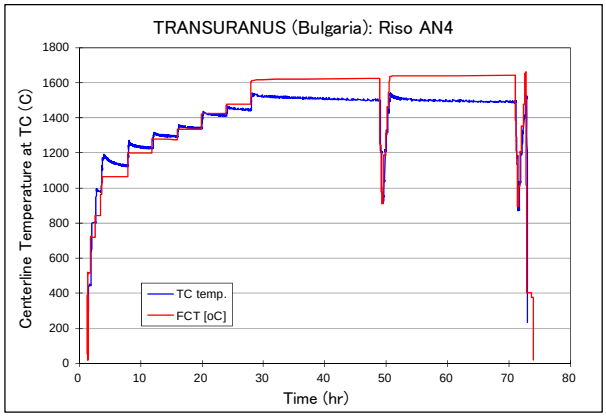

FIG. 39. Fuel centre temperatures calculated for the bump ramps at Risø AN3 and AN4. (cont.)

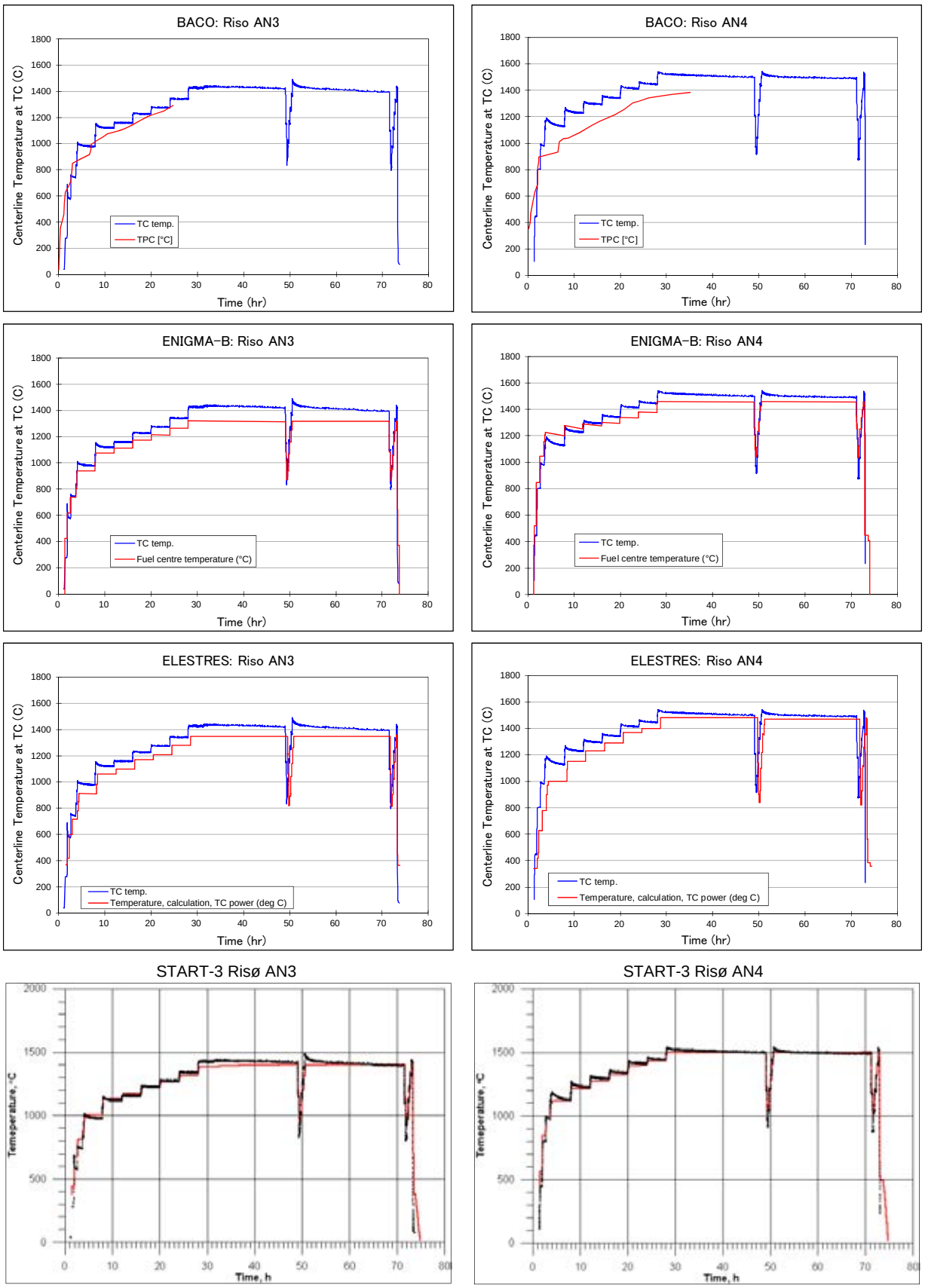

FIG. 39. Fuel centre temperatures calculated for the bump ramps at Risø AN3 and AN4. (cont.)

7.4.3. Fission gas release

The code predictions are shown in Fig. 40.

The fission gas release in these experiments was determined both by PIE measurements as well as on-line pressure measurements which were able to follow the release of gas throughout the experiment. The pressure measurements agree well with the end of life PIE datum.

The experimental pressure measurements show a significant increase in pressure at around 50 hours into the ramp test. At this point there is a power transient, comprising a rapid power drop and return. This feature of fission gas release during a power drop is often observed and is possibly due to mechanical hold up of fission gas in the fuel-clad gap which is able to connect with the plenum region during the power drop. The code predictions generally do not show this sudden increase (though some do) and do not attempt to model such mechanical interactions within the fuel rod. Therefore the predictions tend to show a smoothed release.

The results shown for the START-3 code in Fig. 40 consider another issue with the data; that the pressure measurements commence with a reading of around 5% release. The dotted line in this plot shows an interpretation of what the actual fission gas release kinetics may have been. Further details of the discussion on this topic can be found in the participants' full reports appended to this publication.

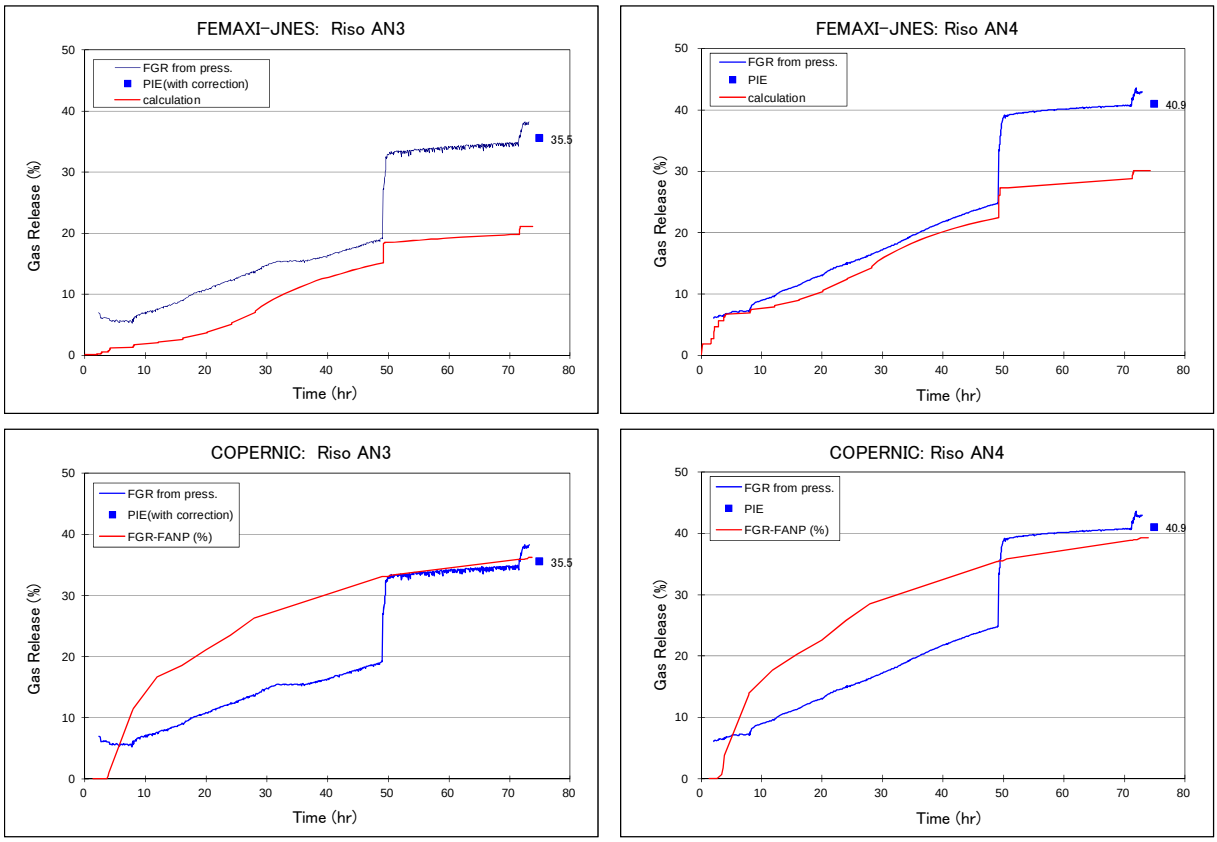

FIG 40. Fission gas release calculated for the bump tests AN3 and AN4 at Risø.

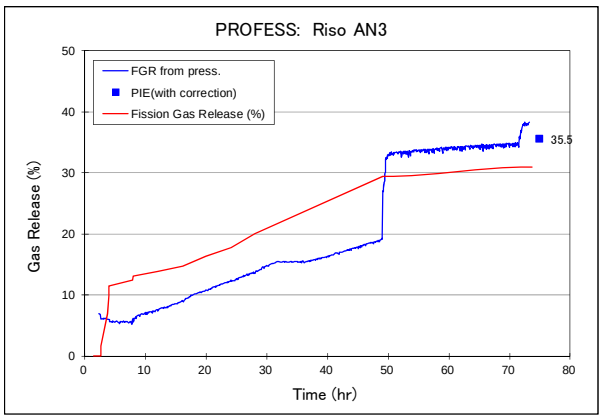

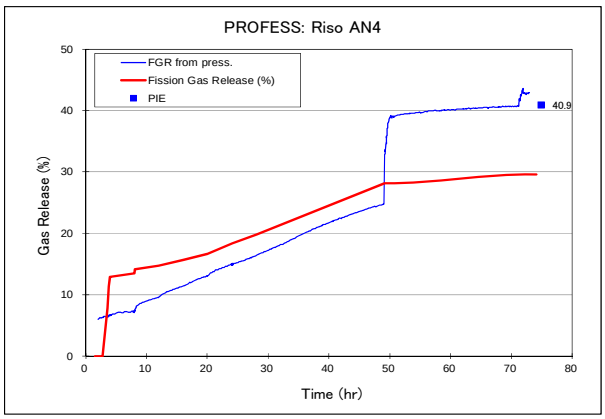

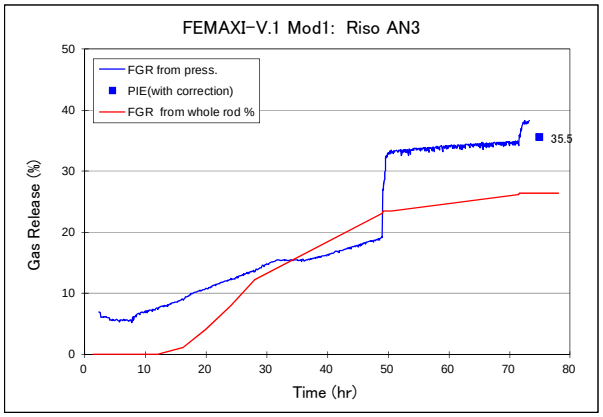

FEMAXI-V.1 Mod 1 Risø AN4

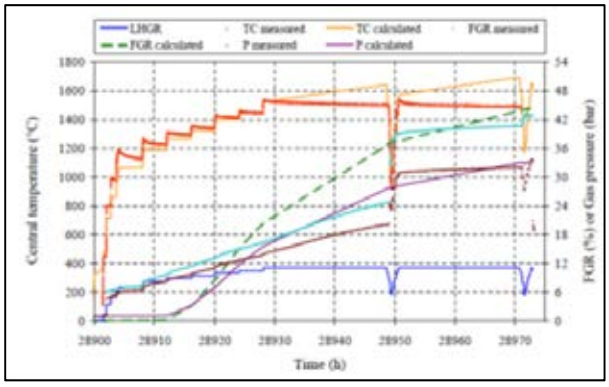

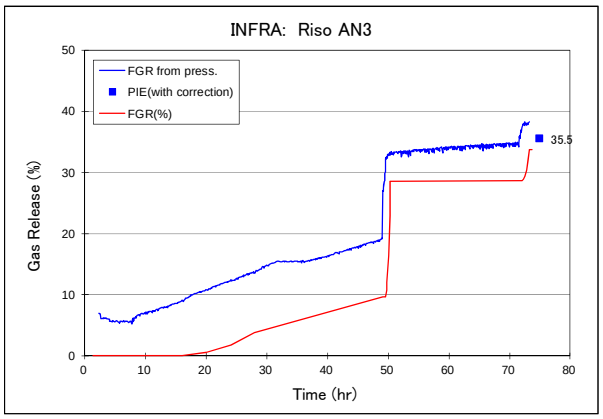

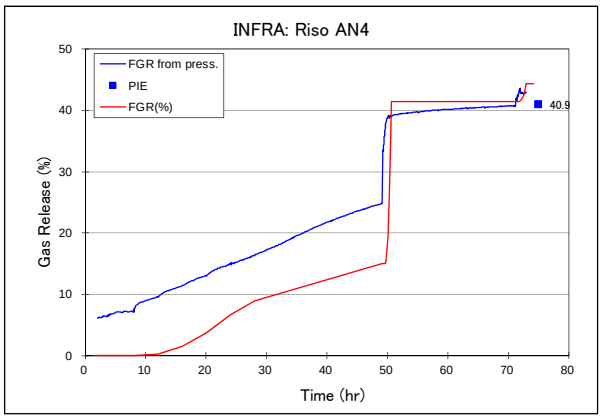

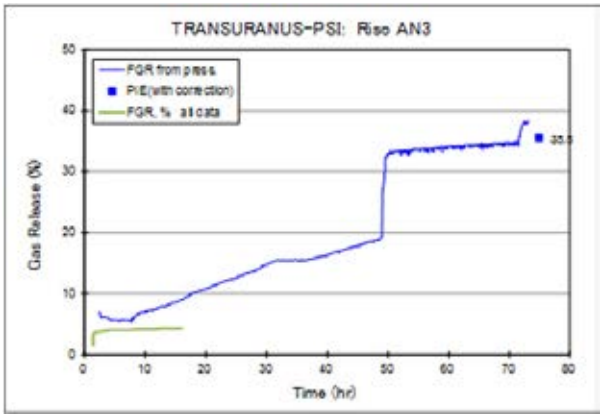

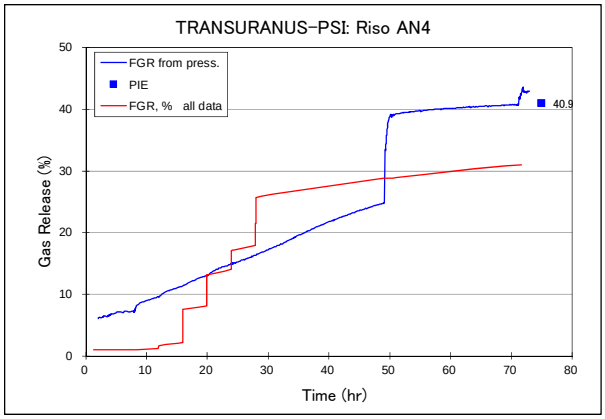

FIG. 40. Fission gas release calculated for the bump tests AN3 and AN4 at Risø. (cont.)

TRANSURANUS: Risø AN3

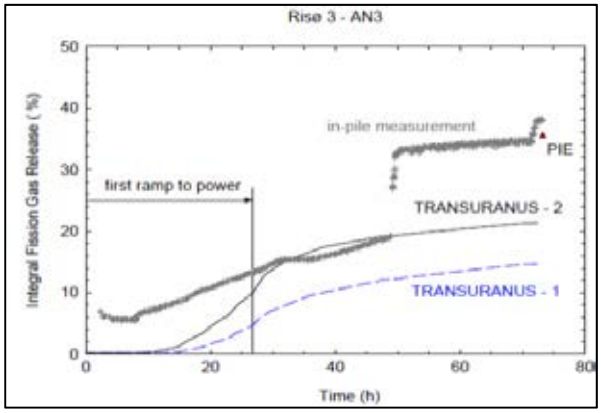

TRANSURANUS Risø AN4

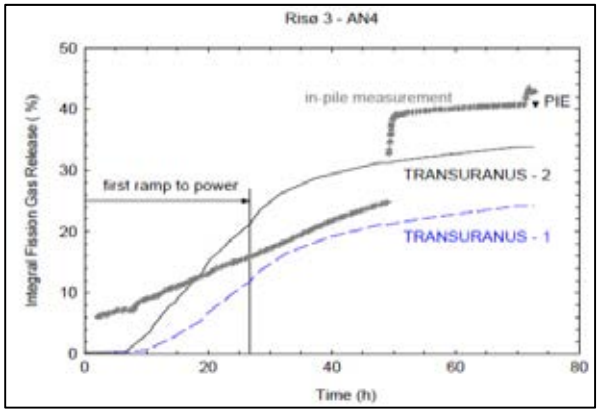

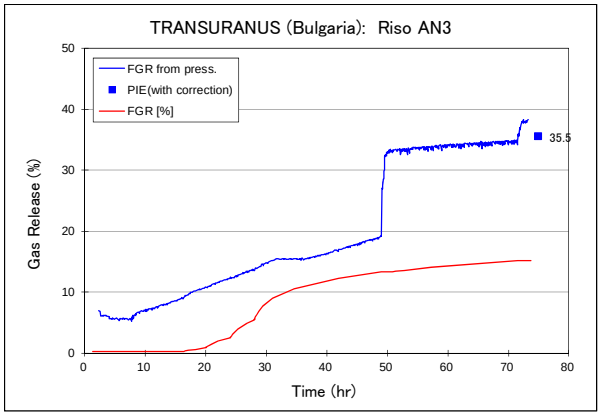

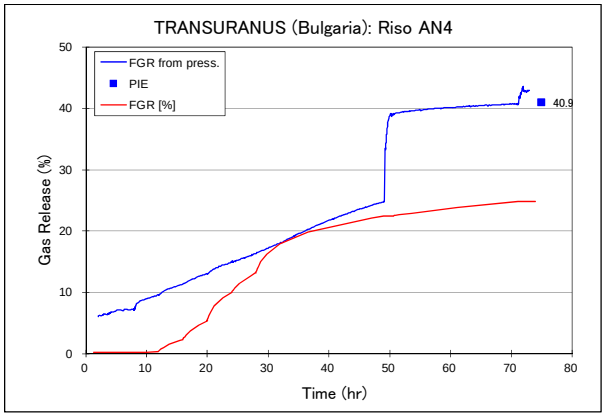

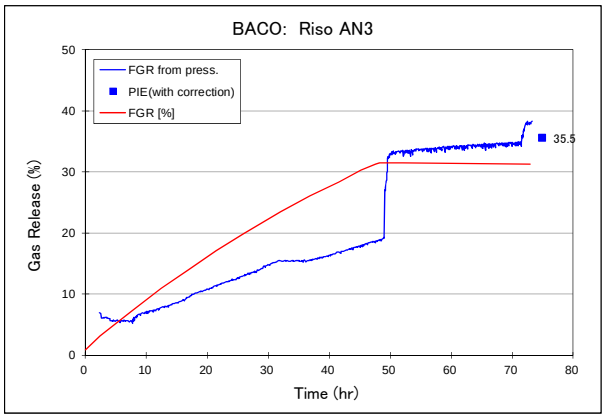

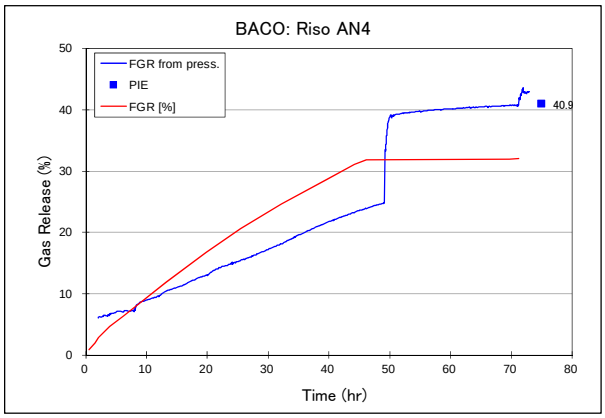

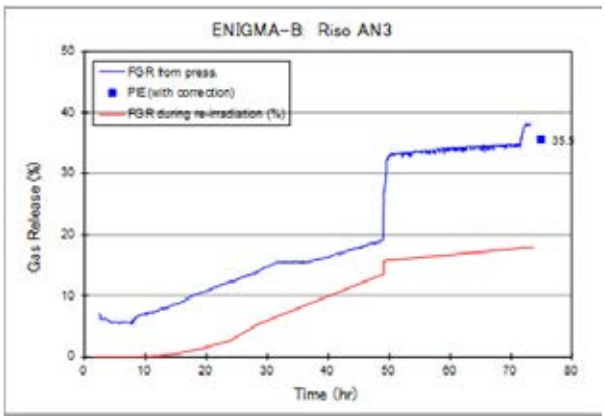

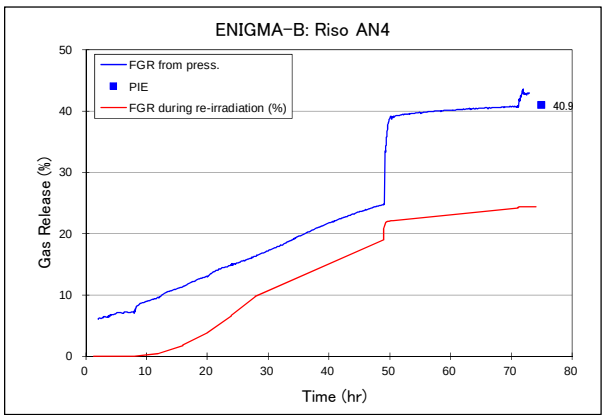

FIG. 40. Fission gas release calculated for the bump tests AN3 and AN4 at Risø. (cont.)

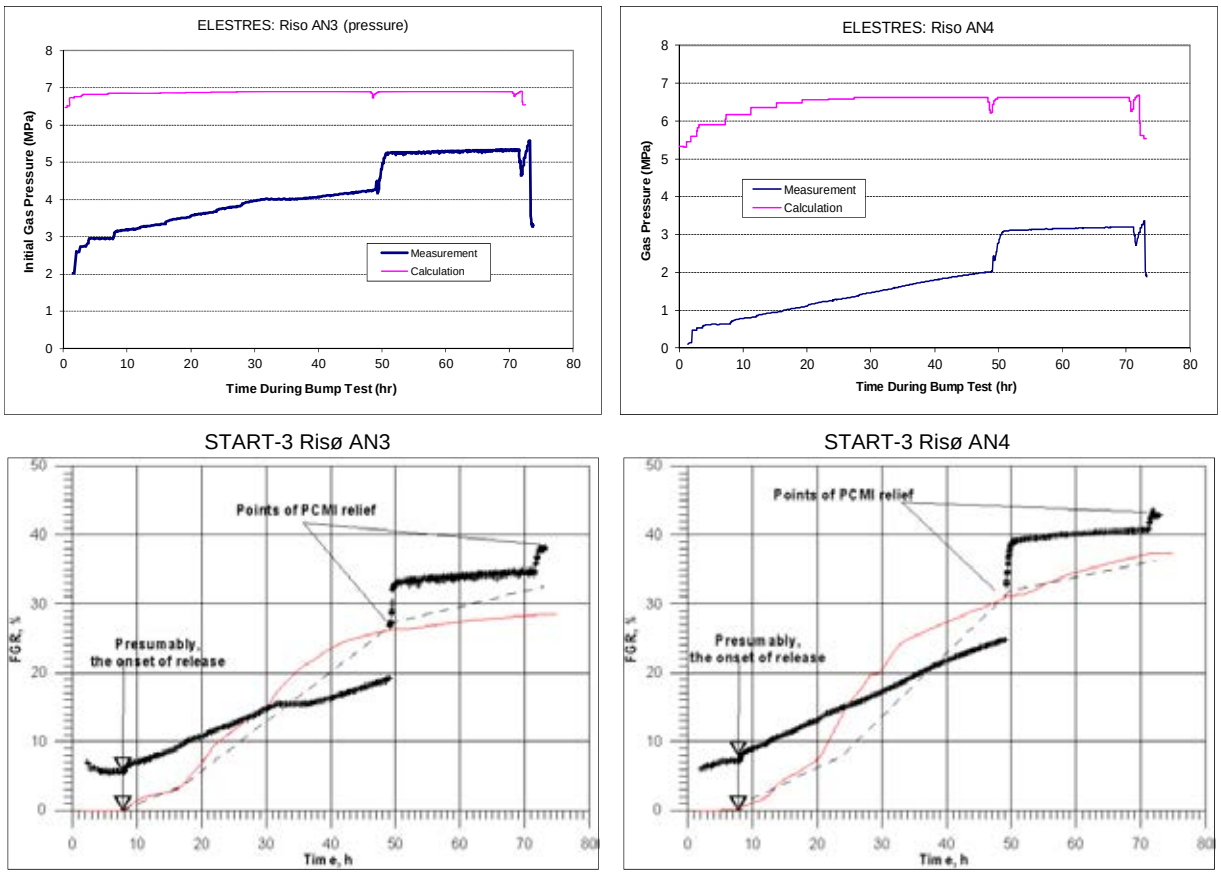

FIG. 40. Fission gas release calculated for the bump tests AN3 and AN4 at Risø. (cont.)

7.5. CASES 16, 17 AND 18: HBEP RODS BK363, BK365 AND BK370

7.5.1. Power history

These were added to the list of priority cases after the 2nd RCM with the specific aim of demonstrating the effect of burnup increasing from 51 MW·d/kgUO_2 (BK370) to 69 MW·d/kg UO_2 (BK365). In addition, EPMA measurements of the radial Pu distribution are available for rods BK365 and BK370. The power history of rod BK365 is shown in Fig. 41.

- The only request was for predictions of EOL FGR values.

The results of the fission gas release predictions are given in Figs 42 and 43.

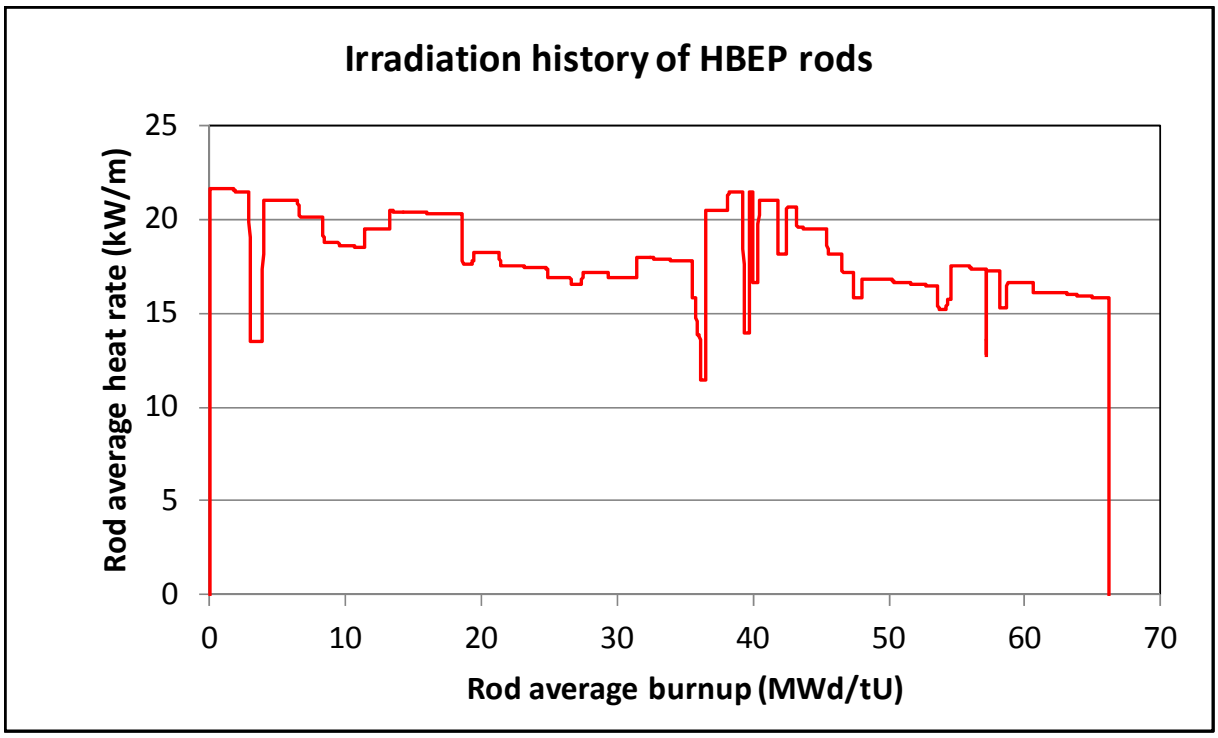

FIG. 41. Irradiation history of the rod BK365.

7.5.2. Fission gas release

Most participants attempted all three rods and the summarized results are shown in Fig. 42. The experimental and calculated results are shown for comparison. Generally the codes reflect the low fission gas release from these rods, due to the low power operation, however there is a general over-prediction of the prioritised case Rod BK365, and few of the modellers reproduced the experimental result of lower release from this rod than from rod BK 370.

Examples of the calculation of the fission gas release in the HBEP rods 363 and 365 showing the burnup dependence of the calculated release are shown in Fig. 43. There is no information on the release rate of fission gas during this experiment, but it is interesting ti note that the majority of the codes showed a gradually increasing release during the irradiation.

There were problems with the calculation of burnup for some codes in this case.

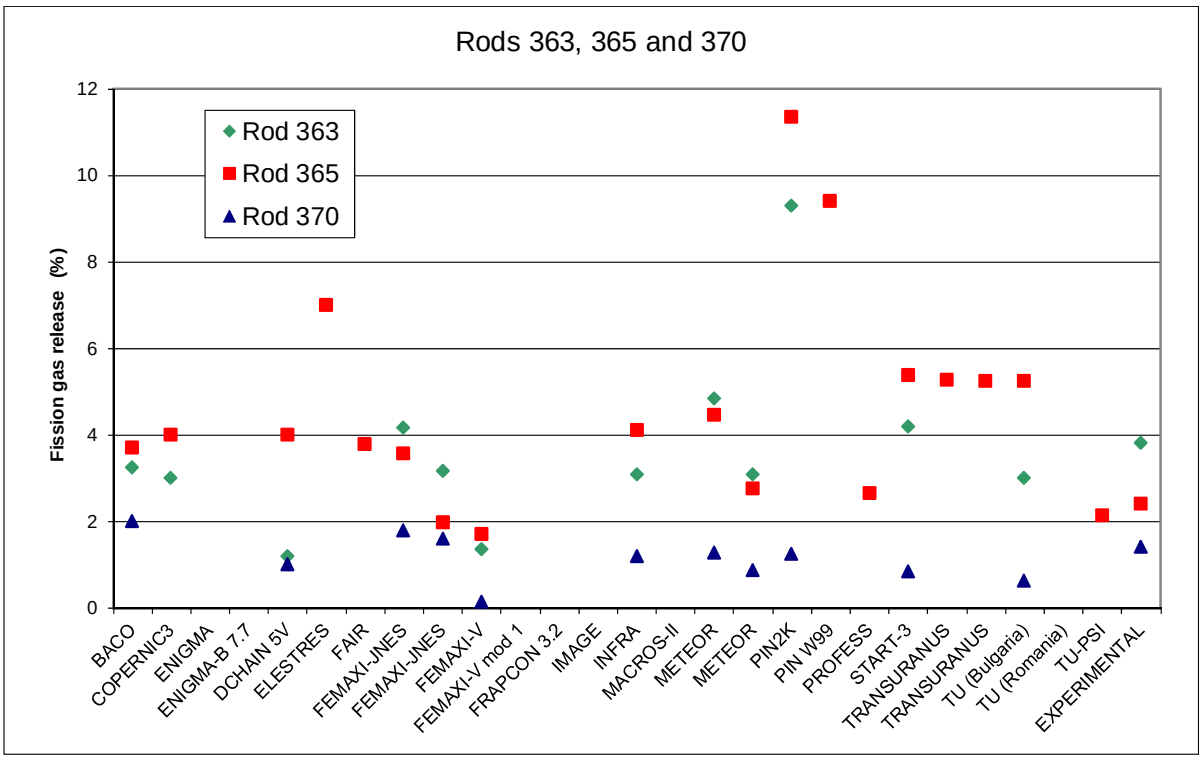

FIG. 42. Predicted fission gas releases for the three HBEP rods 363, 365 and 370. Experimental results are shown on the right of the figure.

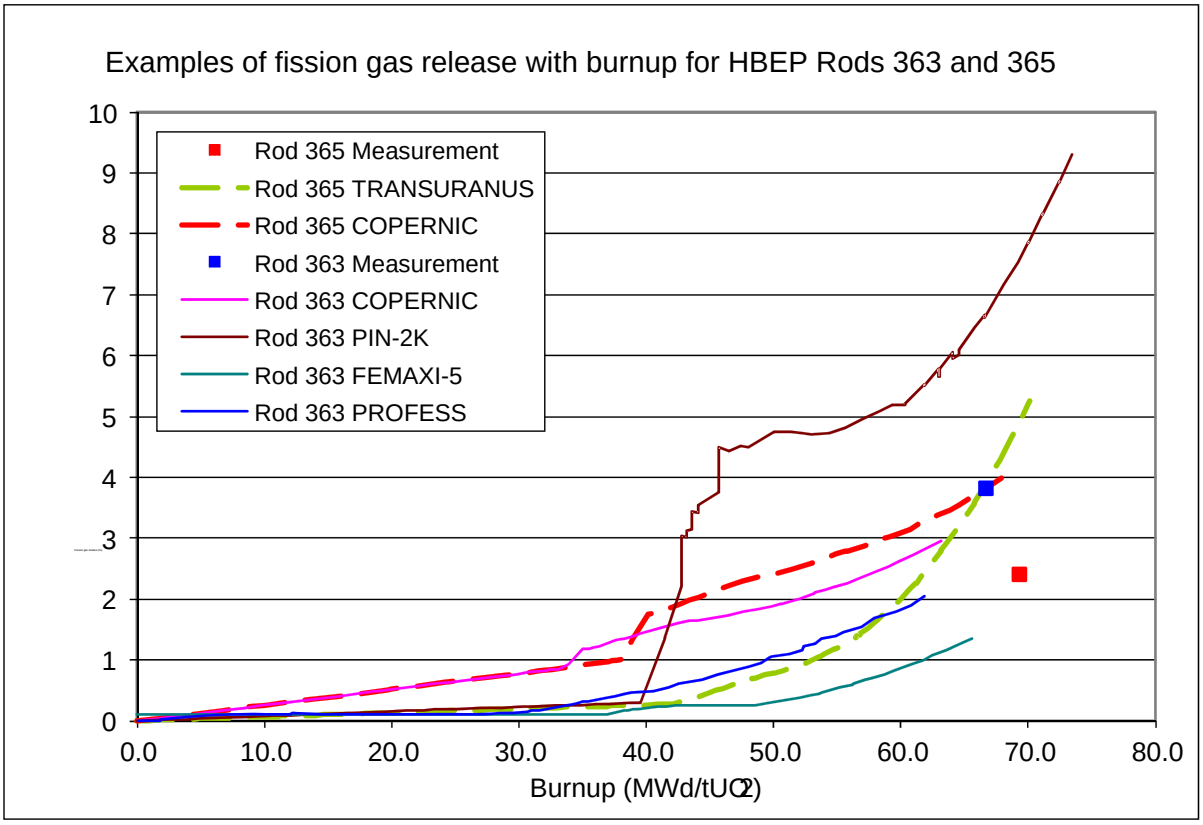

FIG. 43. Examples of the calculation of the fission gas release in the HBEP rods 363 and 365 showing the burnup dependence of the calculated release. There were problems with the calculation of burnup for some codes in this case.

7.5.3. Plutonium distribution

Although it was not a requirement, several codes made predictions of the plutonium profile in the pellet at EOL. This is an important calculation to allow the codes to correctly predict the power distribution in the pellet and hence properly calculate the thermal profile.

Predictions of three of codes showing their plutonium distribution calculations are shown in Fig. 44. The codes match the experimental data fairly well, all showing the significant increase in plutonium content at the pellet edge at high burnup.

Several codes are capable of predicting distributions of xenon and other nuclides in the fuel, and further examples where predictions have been made against the PIE, for this and other cases, can be found in the reports by the participants, which are appended to this publication.

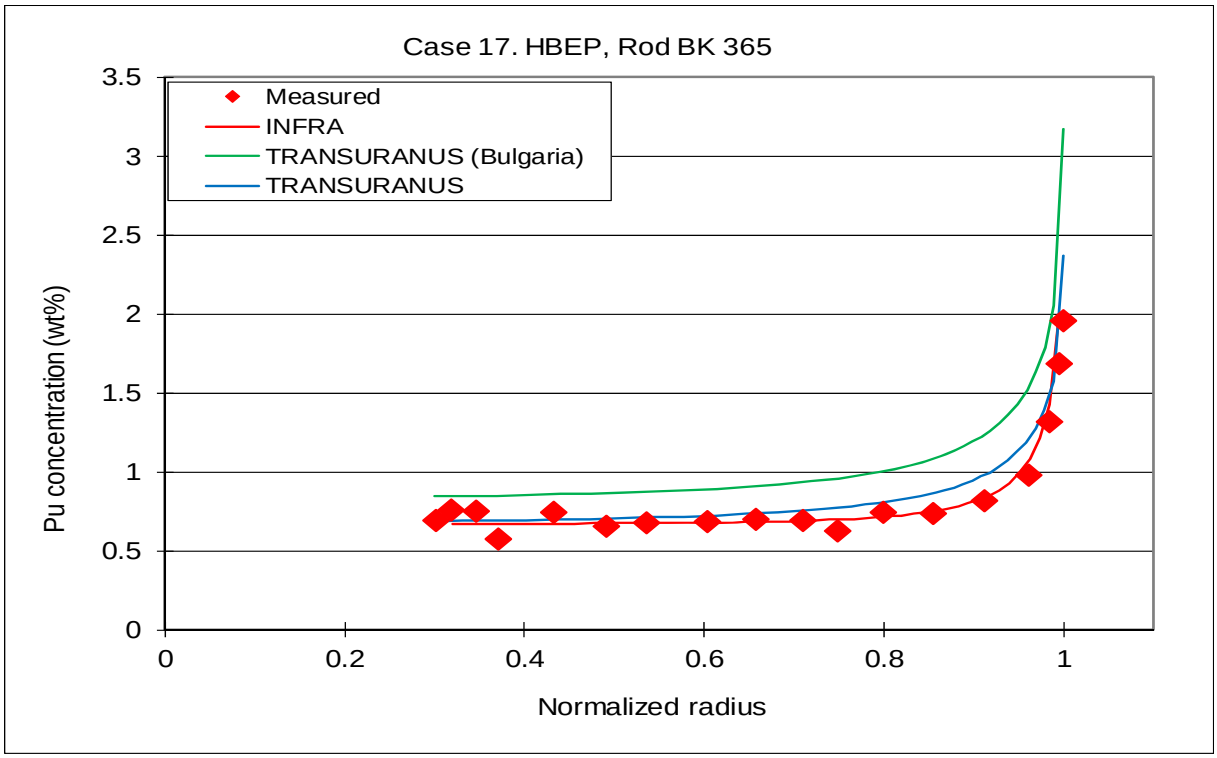

FIG. 44. Plutonium profiles in the HBEP experiment.

7.6. CASES 9–12: KOLA TESTS (WWER-440)

7.6.1. Power history

At the second RCM, the cases 9 and 11 were made priority cases for the participants interested in modelling WWER fuel. The Kola tests were of WWER 440 fuel type, 4.4% ^{235}U enriched with standard Zr1%Nb cladding. The burnups were in the range 44–55 MW·d/kgUO_2

A specific feature of WWER fuel is that the pellets are hollow, which meant that some codes were unable to model their behaviour.

The power history of case 12 (rod 120) is shown in Fig. 45.

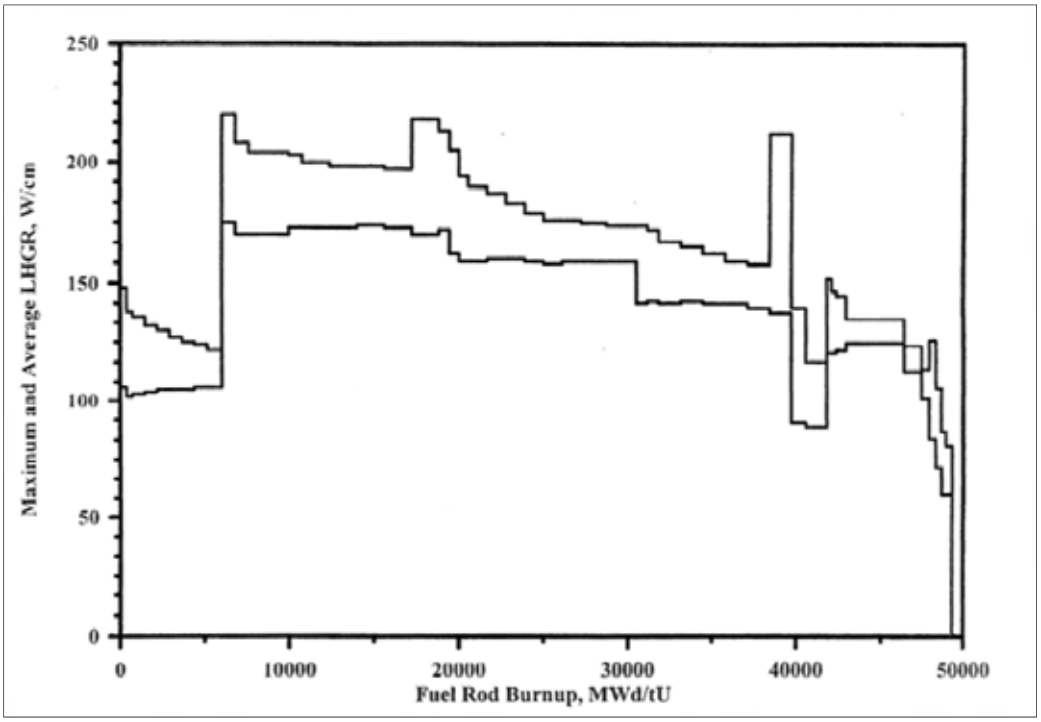

FIG. 45. Power history of rod 120 from the Kola-3 irradiation.

7.6.2. Fission gas release

The code predictions of the measured fission gas release values are shown in Fig. 46. The releases were fairly low and the majority of the predictions correctly model the relative releases between the modelled rods.

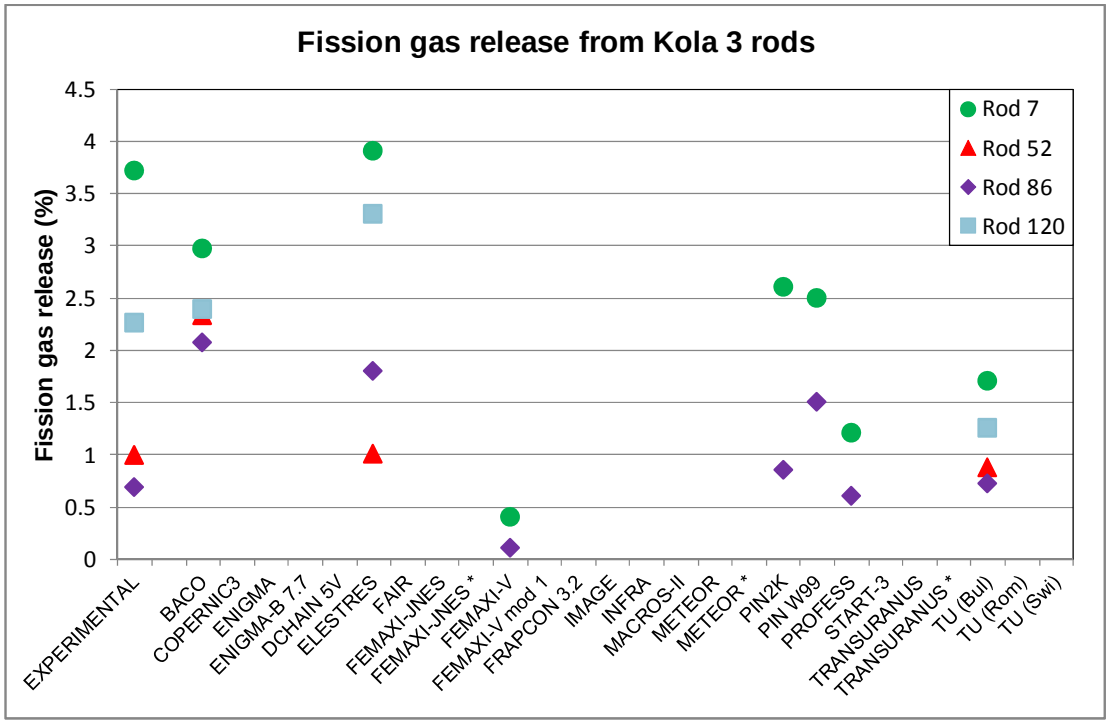

FIG. 46. Fission gas release predictions for WWER-440 fuel rods from Kola 3 NPP.

7.7. OVERALL FISSION GAS RELEASE COMPARISONS

Figures 47 and 48 give the results of an overall comparison of the code predictions and the experimental measurements. These results include all the reported code predictions, not only the priority cases described above. The results are shown as a plot of predicted to measured fission gas release in Fig. 47 and as a ratio of predicted to measured release as a function of burnup in Fig. 48.

The results show that, whilst some codes give excellent results, there is a general under-prediction of the high release measurements (above approximately 10% FGR). However, when the results are plotted as a function of burnup there is no particular trend, and even where there is a systematic under-prediction of the high release experiments, the codes are generally within the usual factor of ×÷2 in predictive capability.

It should be remembered in considering the performance of code predictions against measurements that there is considerable uncertainty in the experimental data. There is typically a 5% uncertainty on the power, which typically translates into a factor of ×2 in FGR, and there are other uncertainties in determining other parameters and the PIE experimental data. The codes are generally validated against a specific dataset available to the developers and this means that the code will be tuned to replicate, as far as possible, the uncertainties in that dataset. When modelling a new dataset, particularly one that is designed to stretch the capabilities of the code, it is to be expected that there will be a scatter both from prediction to measurement and also between the differing codes for a particular case.

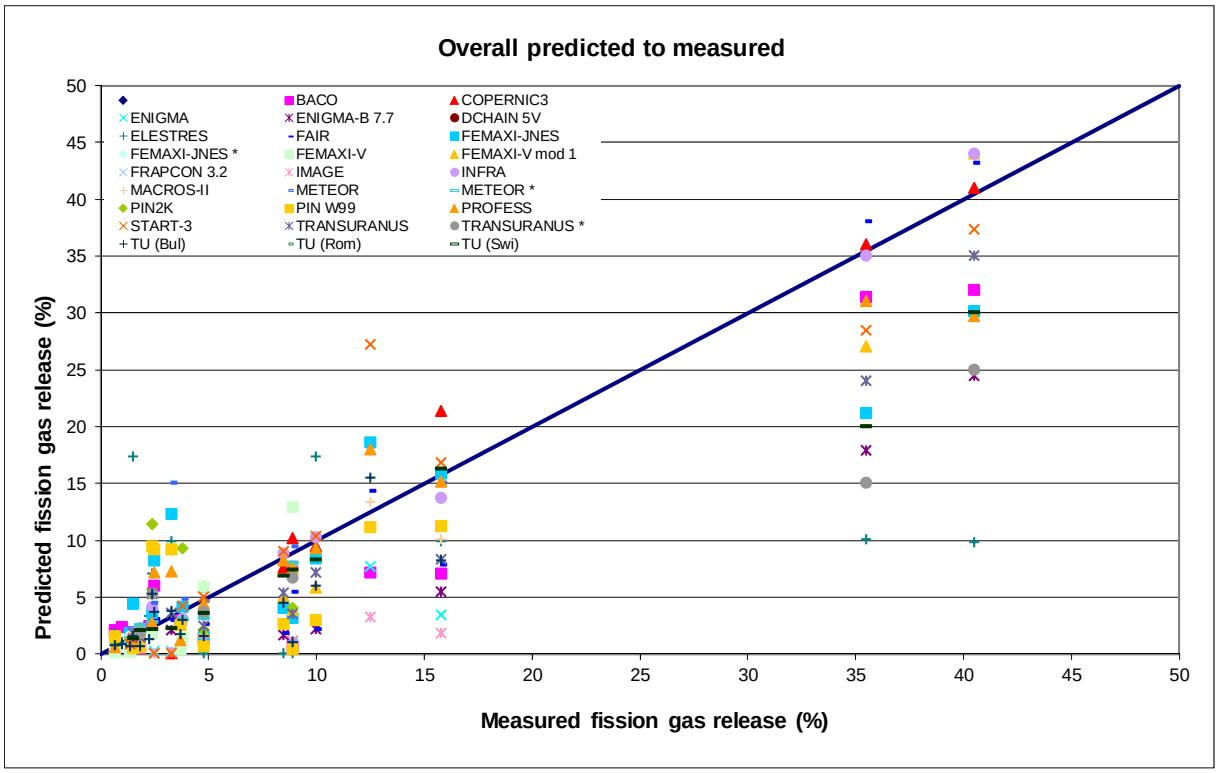

FIG. 47. Overall predicted to measured fission gas release values for all the cases attempted, excluding the idealized cases.

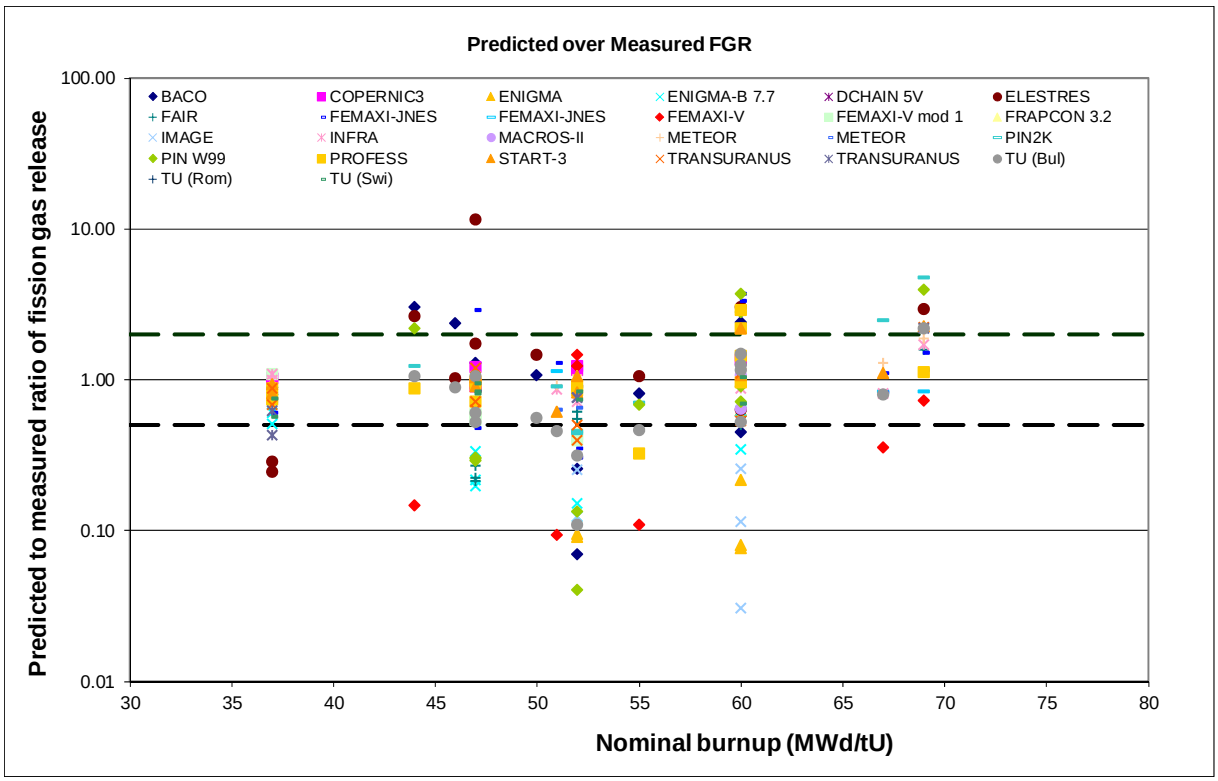

FIG. 48. Overall ratio of predicted to measured fission gas release values as a function of burnup for the 'real' cases.

8. DISCUSSION

8.1. ISSUES RAISED

The modelling of the FUMEX-II priority cases has been carried out by the participating teams of fuel modellers and some overall conclusions can be drawn and some areas noted where further development is still necessary. Some codes performed exceptionally well for most of the cases, but for all there are areas of difficulty where the mechanisms may not be well understood or where a consensus on could not be found.

The following discussion points are listed as of particular interest and were raised during the discussions held at the RCMs and, for many, some of the issues noted in this section are still open. Appendices II and III provide notes of the second and third RCMs and give a brief record of the discussions about the issues between the teams at these two meetings.

8.1.1. Temperature and thermal conductivity degradation

The modelling results show good agreement with fuel centre temperature measurements for both normal operation and during power ramps. All the participants have considered the effect of burnup on the thermal conductivity of UO_2 and that this impairment in heat transport with burnup is necessary to achieve the successful modelling of temperatures.

This result confirms the successful modelling of temperatures that was achieved during the previous FUMEX exercise and extends it to the higher burnups of the present CRP.

8.1.2. FGR: steady state, transient and kinetics of release

With the successful modelling of temperature, it is expected that the predictions of fission gas would improve, and it is clear that the majority of the codes that are making predictions within their validation range do a good job of this. However there is an overall trend of under-prediction of experiments where there is a high level of FGR, though as such levels of release are not usually found in normal operation it may be considered that these values are at the limit of the validation for most codes.

The predictions for total release in a transient are fairly good, though the modelling of the kinetics of release was less successful, with few codes managing to give a good representation of the measured data. The reasons for this will include the operation of mechanisms (such as mechanical hold up of gas within a fuel rod preventing release to a plenum volume) which are currently not modelled, and are possibly too stochastic to be followed and well described in an individual experiment.

8.1.3. FGR: grain size effect

The influence of grain size on FGR is expected to be strong, based on simple diffusion theory. However, during operation many factors can affect a simple model and the use of case 2, which provided strong evidence of a significant grain size effect during a transient release, was a good test for the codes. The predictions showed that the observed ratio of FGR between the large and small grain sized fuel was well modelled, even if the absolute value of release was generally under-predicted, with large differences between codes for the FGR during the base irradiation causing difficulties in interpreting the data.

Overall it is believed that the good predictions of the ratio of FGR between large and small grain size fuel is a good indicator that the correct mechanisms are being modelled.

8.1.4. Rim effect and HBS

One of the main purposes of this CRP was to support the development of modelling of high burnup FGR, as the experimental evidence shows enhancement above that which is predicted from the earlier models. Overall, the codes do not show a trend in under-prediction with burnup (Fig. 48) for the FUMEX-II cases, but this has been achieved through the introduction of many differing approaches which allow an enhancement of FGR at high burnup.

The existence of a HBS at the pellet rim is a feature of high burnup fuel and is first observed at burnups in excess of 40 MW·d/kgU (approximately) and develops as burnup proceeds. It is caused by the enhanced burnup in the pellet periphery due to the buildup of plutonium in this region as burnup proceeds and the power is redistributed through the pellet. The region contains a restructured, fine grain size and a high concentration of fission gas bubbles. However, this simple phenomenological description is not easy to model, and the experimental evidence of fission gas distribution within this region is still open to interpretation.

Several mechanisms and empirical models have been developed by the modellers and there was no consensus between them on how best to describe the development of the HBS or its effect on FGR and mechanical behaviour within their modelling. Details of several of these are given in Sections 6.2.3 and 6.2.4.

8.1.5. Mechanical behaviour

The mechanical behaviour of the fuel is not modelled by all the codes and there were detailed discussions of the effects of gap closure, fission gas swelling, in transients as well as steady state, and the HBS. Pellet-clad bonding was discussed and it was recognised that modelling axial extension during irradiation was an area that needed development.

8.1.6. Other unresolved issues

The participants noted several issues that left unanswered questions. One was the effect of the previous history on transient FGR, where in the HBEP series a ‘hot’ prehistory led to high release whilst a ‘cold’ history gave a moderate enhancement. Another was the overshoot in temperature seen during the Risø ramp tests. Other issues were raised with the data and were resolved following the CRP.

8.2. FUTURE WORK

The CRP FUMEX-II was not designed as a ‘blind’ exercise, the participants were aware of the PIE data from the cases at the outset. This allowed the many codes participating to be developed and tested against the data. This provided an opportunity for continuous development rather than a competitive,

comparative exercise. The discussions raised many topics that will allow the continuation of this process and it is expected that the codes will continue to develop.

The participants did identify specific areas for future development, including:

- RIA and LOCA studies.
- Rod failure from PCMI.
- MOX.
- Gadolinia doped fuel.
- Clad mechanical properties.
- Kinetics of FGR.

9. CONCLUSIONS

Results of code predictions against a set of priority cases show that fuel temperature modelling is much improved since the previous FUMEX CRP. Fuel centre temperature predictions are now generally good, and match the data well, up to burnups of around 60 MW·d/kgU. The agreement is good for both normal operation and during power ramps.

The modelling also shows good agreement for fission gas release at burnups close to current commercial limits (around 50 MW·d/kgU). However, it is recognised that standard models do not account for an increase in fission gas release rates observed at high burnups and the teams have used various options and additional modelling in their codes to try to account for this phenomenon. Three distinct approaches have been tried:

- Allowing fission gas release directly from the rim structure seen at the periphery of pellets at high burnup. Modelling choices include varying the retentive capacity of this region and in determining how to define the extent of the rim region. Evidence for this mechanism comes from the existence of the rim structure, which seems to initiate at the same time as the additional release.
- Allowing release of additional gas from saturated regions of the fuel, where the saturation is temperature dependent and the additional release comes from the pellet interior. Modelling choices here lie in determining the saturation level and the temperature dependence of this effect.
- Allowing an additional burnup dependence on the diffusion and re-solution parameters used in standard models. Release of fission gas is enhanced in the pellet centre with this approach.

Experimental data on fission gas distributions in high burnup have not been sufficiently clear to allow the teams to be able to positively distinguish between these models, though each approach would predict different distributions of retained fission gas. The reason why release from the rim is excluded in the latter two approaches is due to the fact that the available experimental data seem to show significant retention of fission gas in this region. Difficulties in interpretation arise from determining the concentration of fission gas retained in bubbles in the rim structure, which are not well measured by standard electron optical techniques. Additional data together with further interpretation and detailed examination of existing data will help in this regard.

The modellers noted several important issues for high burnup modelling which were addressed during the later stages of the FUMEX-II CRP. These included:

- Accurate calculations of the burnup dependent radial power profile, i.e., plutonium build-up at the rim.
- What is the effect of the HBS at the rim? What is its impact on the thermal performance and FGR behaviour of the fuel rod?

- Is a separate treatment of this HBS region required for successful modelling?
- What are appropriate conditions for the formation of the HBS?
- At what burnup does the enhanced release begin?
- What temperature limits should apply to the models?
- What are the effects of pressure, grain size, dopants or other details of fuel rod manufacture?

The additional priority cases allowed the participants to attempt a consensus on some of these issues. In particular the modelling of the grain size effect would appear to be in reasonable agreement with the scale of the effect in the experimental data.

The modellers found difficulty with the Risø data in particular, with most under-predicting the measured FGR, however it has not yet been possible to discriminate between the models for high burnup release, though detailed examination of the results is continuing. The overall results show no trend in the predictive capability of the codes with burnup, it would appear that all of the modelling approaches tried to date are adequate to explain the high burnup releases available in the CRP list of cases. Whilst some modellers rely heavily on the rim structure to enhance release at high burnup, others do not, and so far there has been no experimental data available to allow discrimination between the competing models in their release predictions, though there is experimental evidence of fission gas retention at the rim.

Not many codes have good mechanical modelling capabilities, and the results that were obtained were limited. Diametral swelling was a difficult area for many codes and their models for this were often very sensitive to small changes in the modelling assumptions. The initial rod elongation in a transient due to PCMI was reasonably well predicted by a few codes, but relaxation of the rod growth was rarely modelled.

APPENDIX

DETAILED DESCRIPTION OF CODES

Where detailed descriptions of the codes have been made available, they are given here in summary form as prepared by the participants and the full descriptions can be found in the participants' reports which are appended to this publication.

INFRA code (Lee)

- 2-stage mechanistic model: grain inside — grain boundary — fuel gap:
  - fission gas generation inside the grain;
  - diffusion to grain boundary to form the surface bubbles;
  - diffusion to grain edge to form the edge bubbles;
  - bubble interconnection to be open to the external space(open bubble);
  - instantaneous release of fission gases in the open bubble;
  - open channel for release of the fission gases diffused to the open bubbles later;
  - open channels or bubbles are accumulated and increases with burnup.
- Characteristics of fission gas release model:
  - burnup-independent diffusion coefficient of fission gas is used;
  - enhanced fission gas release at high burnup is predicted without any burnup enhancement factor;
  - effects of grain size is predicted.

METEOR code (Chen)

Fission gas release model

The fission gas release model was developed by CEA. The model takes into account ejection-recoil, the diffusion of gas atoms in matrix towards the grain boundaries, saturation of grain boundaries and release to free volume.

The rim develops at high burnup and within the temperature range of the fuel. The fission gas release in rim region relates to the population of intra-granular fission gas bubbles. The evaluation of FGR in rim region is related to the change in oxide microstructure as a result of built-up irradiation damage. The code considers the grain subdivision by releasing the energy accumulated in the UO_2 matrix in the microstructure change model. The code also calculates the population of bubbles which develops in the rim, fed by lattice gas atoms and nano-bubbles, preferably through diffusion short circuits formed by the surfaces of the intra-granular faults or small grains. The use of data concerns gaseous porosity in the swelling and the law of fuel conductivity.

It is considered that the crystal lattice builds up energy E^* by distorting the crystal as the result of irradiation defects and fission products which are insoluble in UO_2. At temperature below the 800–900 K range, defects are not very mobile and their elimination in sinks such as grain boundaries cannot offset their production under irradiation.

E^* ($J \cdot m^{-3}$) is given by:

$$E^* = C\,\tau\,f(T),$$

where, C is a proportionality constant, adjustable parameter, τ is burnup (MW·d/kgHM) and $f(T)$ is the ratio of equilibrium values of bubble volume concentration at temperature T and a reference temperature of 573.15 K, which is low enough for the defects to be considered immobile.

When the fuel restructuring process begins, beyond a threshold *Es* (adjustable parameter), the global energy per volume of the system *E* composed of an intact zone and a zone of subdivided grains. The surplus energy d*(E-Es)* is converted into surface energy.

As the restructured fuel fraction is equal to $a_s \times S/3$ (a_s = final small grain radius), the value of the developed surface is obtained by restructuring:

For $E^* \leq Es$,

$S=0$

The model of fission gas release under steady state takes into account the ejection-recoil and the diffusion of gas atoms towards the grain boundaries.

The specific area of the fuel, which changes as a function of temperature and burnup in the fission gas release model is expressed in cm^{-1}.

FEMAXI-JNES code (Kamimura)

The fission gas release model calculates:

- intra-granular diffusion;
- sweep-out of intra granular gas atoms to grain boundary by grain growth;
- trapping of matrix gas into intra-granular bubble;,
- re-solution of intra-granular bubble to matrix by irradiation;
- re-solution of inter-granular bubble into grain interior;
- saturation of inter-granular gas atoms.

START-3 code (Khvostov)

The FGR model is described in full detail in the paper "Development of the Fission Gas Behaviour Model in the START-3 code and its Experimental Support", International Seminar on Fission Gas Behaviour in Water Reactor Fuels, Cadarache, France, 26–29 September 2000, which is included in the annexes to this report

BACO code (Marino)

Fission gas release model:

- empirical (KWU model);
- composed by 2 sub-models:
  - steady state, 2 parts where:
    - fission produced is retained in the UO_2 matrix up to a certain saturation concentration, exciding this concentration the fission gas is collected at the grain boundary;
    - estimation of the fission gas release rate;
  - transient.

TRANSURANUS-PSI (Nordstroem)

Fission gas model, overview

(Based on work by Speight, Turnbull, White and Tucker):

- Spherical fuel grains, where gas as single, freely diffusing atoms.
- On their way out of the grain, gas atoms may become trapped at immobile intra-granular bubbles, or at as-fabricated pores.

- Bubbles grow by absorbing gas before being destroyed by fission fragments (intra-granular re-solution).
- At grain boundary, gas is absorbed into grain boundary bubbles. Interlinkage of the grain boundary bubbles initiates the gas release.
- Because of the re-solution from the grain boundaries back to the grain, grain boundaries act as imperfect sinks for diffusing gas atoms (inter-granular re-solution).
- A model to calculate the gas swept out by the moving grain boundaries during the growth of the equiaxed grains.
- Additionally, the pores which form columnar grains are assumed to sweep out and release 100% of the fission gas.
- Inter-granular gas (gas at the grain boundary):
    - gas flux to grain boundary;
    - atoms per grain boundary bubble.
- Gas release:
    - interlinkage of grain boundary bubbles;
    - total gas release;
    - Gas release from columnar grain area.

ENIGMA-B (Rossiter)

Gas models

The models implemented for the various gases in the fuel rod include:

- fission gas generation (including the isotopics);
- (stable) fission gas release and gas bubble swelling;
- ^{131}I generation and release;
- helium generation and release;
- helium adsorption and re-release;
- release of chemically absorbed nitrogen;
- instantaneous axial gas mixing;
- fuel-clad gap conductance;
- conduction, radiation and empirical components (empirical component takes account of pellet fragment relocation, pellet-clad eccentricity, cladding ovality and pellet wheat-sheaving effects).

Calculation of fission gas release and gas bubble swelling is performed by an integrated model which is described in more detail below. An initial fuel nitrogen content of zero is modelled in all FUMEX-II calculations, so the model for the release of absorbed nitrogen has no effect on the predictions.

Integrated fission gas release and gas bubble swelling model

The integrated fission gas release and gas bubble swelling model is a highly mechanistic model. Both intra-granular and inter-granular bubbles are explicitly modelled. The bubble modelling has been validated against scanning electron microscopy (SEM) and transmission electron microscopy (TEM) images of irradiated fuel.

The following phenomena are simulated in both steady-state and transient conditions (no additional fission gas release is modelled during a transient):

- intra-granular diffusion of single fission gas atoms in solution in the fuel matrix;
- to intra-granular bubbles;
- to inter-granular bubbles on the grain faces;
- directly to free surfaces (where release is instantaneous);
- irradiation induced re-solution of gas atoms in bubbles (no thermal re-solution);
- coalescence and morphological relaxation of grain face bubbles;
- instantaneous venting to the rod free volume of inter-granular bubbles intersecting a grain edge.

Intra-granular diffusion of vacancies to intra-granular bubbles is also modelled. Morphological relaxation (by surface diffusion) and coalescence of inter-granular bubbles must both be considered in order to evaluate the evolution of the bubble morphology. It should be noted that: (a) no explicit burnup dependency of any of these phenomena are assumed; (b) the only mechanisms for release are diffusion of fission gas to free surfaces and venting of grain face bubbles which intersect a grain edge.

The intra-granular diffusion calculations employ a modified three-term Turnbull diffusion coefficient (with no burnup dependent terms). Diffusion to intra-granular bubbles is first calculated (see later). Diffusion to inter-granular bubbles on the grain faces is then evaluated.

The calculation of diffusion to inter-granular bubbles employs the Speight formulation of the Booth solution for a spherical grain [6], where an effective diffusion coefficient equal to the true diffusion coefficient multiplied by the fraction of intra-granular fission gas which is in solution is used and where there is a non-zero gas concentration at the grain boundary due to irradiation induced re-solution of gas in inter-granular bubbles. The fraction of intra-granular fission gas which is in solution is calculated explicitly from the intra-granular bubble modelling, rather than by a trapping probability.

The calculation of diffusion to free surfaces employs the Booth solution for diffusion in a sphere. The sphere radius is such that the surface area to volume ratio (S/V) of the sphere is equal to that of the entire fuel pellet. The fuel pellet S/V is determined empirically such that predicted FGR values for rods irradiated under pre-interlinkage conditions are in good agreement with the measured FGR values. Thus, although gas release due to recoil and knockout of fission gas atoms are not modelled explicitly, their contributions to gas release are, to some extent, implicitly included in the modelling of diffusion to free surfaces.

Intra-granular bubbles are assumed to be continuously nucleated in the wake of energetic fission fragments. The number of bubbles nucleated per fission fragment is considerably smaller than values commonly used, e.g. 24 [8], since only a small sub- population of the as-nucleated bubbles are observed to undergo growth [9]. This growth is assumed to be due to diffusion of both gas atoms and vacancies. Growth competes with irradiation induced re-solution, where size reduction or destruction of bubbles occurs due to ‘chipping away’ by energetic fission fragments. The number of intra-granular bubbles that each fission fragment interacts with is the same as in the commonly used Turnbull model [7]. However, instead of modelling total destruction of each intra-granular bubble that is interacted with, size reduction instead occurs if the bubble volume is equal to or greater than twice a temperature dependent empirical chip volume.

One-off nucleation of inter-granular bubbles is assumed to occur when intra-granular bubbles intersect grain boundaries. Growth of the inter-granular bubbles due to bulk diffusion of fission gas atoms to grain boundaries and grain boundary diffusion of vacancies is modelled. As in the case of intra-granular bubbles, growth competes with irradiation induced re-solution, where size reduction or destruction of bubbles occurs due to ‘chipping away’ by energetic fission fragments. However, in this case a constant, temperature independent, chip volume is assumed. It should be noted that the inter-granular bubble re-solution modelling is incompatible with the Speight model [5]. In the Speight model the flux of gas atoms leaving the grain boundary due to re-solution is directly proportional to the number of gas atoms per unit area of grain boundary (where the constant of proportionality is the re-solution probability). In contrast, in the chip model described above this is not the case.

FAIR code (Sah)

Fission gas release model

Fission gas release model includes release due to thermal diffusion, grain boundary sweeping and rim release. A microstructure based diffusional release model has been incorporated in the code. The main considerations in this model are:

The basic diffusion equation considered in the model is as follows:

$$\frac{\partial c}{\partial t} = D_{gas}\nabla^2 c - gc + bm + \beta$$

where,

D_{gas} is the diffusion coefficient of gas in fuel matrix,
C is the concentration of gas in the grain,
g is the probability of capture of gas by defects,
b is the re-solution probability,
m is the concentration of gas in traps,
β is the rate of generation of fission gas atoms.

Assuming stationary trapping conditions, i.e, gc-bm=0, the diffusion equation can be written as

$$\frac{\partial c}{\partial t} = D_{eff}\nabla^2 c + \beta$$

where

$$c = c(r,t)$$

$$D_{eff} = D_{gas}\frac{b}{b+g}$$

$$b = 2\pi R_f^2 \mu_{ff} F$$

$$g = 4\pi r_b D N_b$$

c is the local gas concentration in the grain,
D_{eff} is an effective diffusion coefficient,
t is time,
r is co-ordinate of spherical grain,
b is the re-solution probability,
R_f is radius of fission spike,
μ_{ff} is length of fission spike,
F is fission rate,
g is capture probability,
r_b is the radius of intra-granular bubbles,
D is the diffusion coefficient of fission gas,
N_b is the number density of intra-granular bubbles.

The above equation is solved numerically with appropriate boundary conditions to get the average concentration of gas in the grain under time varying power condition using algorithm available in literature.

The gas generation rate β is given by following correlation:

$$\beta = \beta(t) = Y.\ \ F$$

where,
Y is the total yield of fission gases Xe and Kr
F is the fission rate

The diffusion coefficients given by Forsberg are used in the model:

Gas release is considered to take place only after a threshold burnup, *Bu*, is reached. The threshold burnup is defined by the following correlation:

$$Threshold \quad Bu = \frac{b\lambda N_{\max}}{2D\phi}$$

where,

b is the re-solution probability from grain boundary (s^{-1}),
λ is the re-solution layer depth (cm),
D is the diffusion coefficient ($cm^2 \cdot s^{-1}$),
N_{max} is the Number of gas atoms per cm^2 area of grain boundary after saturation,
ϕ is the number of gas atom generated per cc per unit burnup.

Resolution probability *b* is taken as a function of fission rate as given by Olander.

Gas is accumulated at the grain boundary also by grain boundary sweeping if grain growth occurs in the fuel. Amount of gas coming to the grain boundary by sweeping is calculated from the grain growth as follows:

$$Sweep \quad gas \quad (atoms/cc) = \frac{a_{new}^3 - a_{old}^3}{a_{new}^3} \times (gas \quad concentration)$$

where *a* is grain radius

Intergranular Bubble Interlinkage

The gas reaching at the grain boundary is considered to form gas bubbles. Bubbles are assumed to have lenticular shape. These bubbles grow in size and cover significant area of the grain face and lead to bubble interlinkage forming a continuous path for gas to be released from the grain boundary.

The gas pressure *P* inside a bubble is balanced by the surface energy and the external hydrostatic pressure acting on the bubble.

$$P = \frac{2\gamma}{r_f} + P_{ext}$$

where,

γ is the free surface energy
P_{ext} is hydrostatic pressure experienced by the bubble
r_f is the radius of curvature of the intergranular bubble

Assuming ideal gas law the number of gas atoms in a bubble required for mechanical equilibrium is given as

$$N = \frac{PV_{gb}}{kT}$$

where,

$$V_{gb} = \frac{4\pi}{3} r_f^3 f(\theta)$$

$$f(\theta) = 1 - 1.5 \ Cos(\theta) - 0.5 \ Cos^3\theta$$

P is the gas pressure inside the bubble,
k is Boltzmann's constant,
T is temperature,
V_{gb} is the volume of the intergranular bubble,

So, the number of atoms in a bubble, N is expressed as

$$N = \frac{4\pi r_f^3}{3kT} f(\theta) \left[\frac{2\gamma}{r_f} + P_{ext} \right]$$

The number of bubbles on the grain boundary for fractional coverage, f_b, is given by

$$N_{gb} = \frac{f_b}{\pi r_f^2 \sin^2 \theta}$$

The number of atoms on the grain boundary at the time of saturation is given by the product of N and N_{gb}:

$$N_{\max} = \frac{4 r_f f(\theta) f_b}{3kTSin^2(\theta)} \left[\frac{2\gamma}{r_f} + P_{ext} \right]$$

The values of γ, k and θ are 0.626 $J \cdot m^{-2}$, 1.38×10^{-23} $J \cdot K^{-1}$ and 50° respectively.

PIN2K and FEMAXI-V codes (Valach)

PIN2K

PIN2K is principally the same as PIN99/w for HiBu (high burnup), which is known from the NEA Data Bank, but a diffusion based FGR model was developed and built into the PIN code.

This mechanistic model has been developed to predict the fission gas release from UO_2 fuels during steady state and transient (limited to ramping during PWR operation) conditions. The model considers the mechanism of diffusion of gas atoms to the grain boundary, trapping of gas atoms by intragranular bubbles, re-solution of gas atoms from these bubbles, sweeping of gas atoms by grain growth, fission gas release due to the intergranular bubble interconnection and micro-cracking during ramp condition. The computer module GASREL written in FORTRAN77 and based on a finite-difference numerical solution was included into the PIN99/w structure and appropriate iteration loops and calls/dimensioning was reprogrammed/innovated. A stand-alone FORTRAN program, GASREL II, was validated on available separate FGR tests and is the standard option in the PIN2K code, with recommended diffusion coefficients and grain boundary saturation values.

FEMAXI-V

FEMAXI-V (ver.1) predicts thermal and mechanical behaviour of a light water reactor fuel rod during normal and transient (not accident) conditions. It can analyze integral behaviour of a whole fuel rod throughout its life as well as the localized behaviour of a small part of fuel rod. Temperature distribution, radial and axial deformations, fission gas release, and inner gas pressure are calculated as a function of irradiation time and axial position. Stresses and strains in the pellet and cladding are calculated and PCMI analysis is performed using FEM. Also, thermal conductivity degradation of pellet and cladding waterside oxidation are modelled.

Heat generation density profile of pellet can be determined by adopting the calculated results of burning analysis code. The gas release model calculates diffusion of gas atoms and their accumulation in bubbles, release and increase in internal pressure of rod. It is possible to allow some materials properties and empirical equations to depend on the local burnup or heat flux, which enables analysis of high burnup fuel behaviour

PIN2K code (Stefanova)

Fission gas release at high burnup

At local burnups higher than 60 MW·d/kgU, formation of the rim structure at the pellet periphery begins and is characterised by submicron grains and increased porosity.

Application of sufficiently simple geometrical relations leads to the following correlation for the athermal local release of gaseous fission products:

$$F_{RIM}(r) = 0 \qquad \text{for } Bu < Bu_0$$

$$F_{RIM}(r) = \frac{Xe_{gen} - \left(Xe(bu_0) + \frac{Bu - bu_0}{Bu_1 - bB_0}\left(Xe_{thr} - Xe(Bu_0)\right)\right)}{Xe_{gen}} \qquad \text{for } Bu_0 < Bu < Bu_1$$

$$F_{RIM}(r) = \frac{Xe_{gen} - Xe_{thr}}{Xe_{gen}} \qquad \text{for } Bu > Bu_1$$

where:
Bu is the local burnup;
Bu_o is theburnup at which the gas release begins;
Xe_{gen} is the amount of Xe produced;
Xe_{thr} is the equilibrium concentration at burnup > $Bu_{1.}$

Model parameters:
Bu_o = 55 MW·d/kg U;
Bu_1 = 100 MW·d/kg U;
Xe_{thr} = 1.1 wt% (0.7 wt%).

The value of 0.7 wt% is included as a conservative estimate.

Post-irradiation examinations have shown that islands of the original fuel structure are present, even in well-developed HBS. In these parts of the fuel fission gas may be released as a result of thermal diffusion. Therefore, a certain function URIM that describes the relative ratio of fully restructured fuel (submicron grains, developed porosity) in the HBS is included into the model.

It is assumed that the development of the fully restructured HBS is completed when local burnup reaches 120 MW·d/kgU.

Thus, the total local gas release can be calculated as follows:

$$F_{tot}(r) = F_{RIM} \cdot U_{RIM} + F_{th} \cdot (1 - U_{RIM})$$

where:

F_{th} is the relative thermal gas release computed according to the usual model.

It was observed that restraining of the HBS formation in normally irradiated PWR fuel rods begins at the temperatures of about 730ºC, and at the temperatures of 1000–1100ºC the fuel structure remains unchanged. This finding is explained by the fact that the thermal gas release prevails at such temperatures and Xe concentration in the matrix sharply decreases. The so-called relative share of fuel matrix, which undergoes structural changes, has been introduced to describe this effect.

Thus, to take into account the temperature dependence of athermal gas release in the HBS, the first part of the equation for URIM should be multiplied by F_{th} It should be emphasised that the surface temperature of WWER-440 fuel does not reach the limiting value, and so this effect does not work.

TRANSURANUS code (van Uffelen)

Fission Gas Release

The standard approach for modelling fission gas release in the fuel performance code TRANSURANUS can be described by four mechanisms that are treated in parallel:

- Release by diffusion.
- Grain boundary sweeping.
- Athermal release during the whole irradiation.
- Athermal release from the high burnup structure (HBS).

Release by diffusion

Following the Booth model, the fuel is assumed to consist of spherical grains. Gaseous fission products are generated uniformly in the grains, migrate to the grain boundaries and are released along the grain boundaries when these become saturated. This leads to a concentration gradient towards the grain boundaries. A diffusion process of the fission products to the grain boundaries is modelled, applying an effective diffusion coefficient that depends on the local temperature:

$$D_{eff} = 5x10^{-8} e^{-\frac{40262}{T}} \quad (\mathrm{m^2 \cdot s^{-1}})$$

For local temperatures below 990 K, a constant is used, implying a minimum effective diffusion coefficient:

$$D_{eff} \geq 1 \times 10^{-25} \quad (\mathrm{m^2 \cdot s^{-1}})$$

At the grain boundaries, the concentration of the fission products is assumed to be limited by a saturation value: $c_b \leq 1 \times 10^{-4}$ μmol·mm^{-2}. When this saturation limit is exceeded supplementary fission gas reaching the grain boundaries is released to the free volume.

Grain boundary sweeping

During normal grain growth, large grains spontaneously grow at the expense of smaller ones. On a microscopic scale the process involves movement of matrix atoms from the convex to the concave side of a curved grain boundary, where the atoms are surrounded by a somewhat larger number of neighbouring atoms. Consequently, the grain boundary, which moves in the direction opposite the net flow of atoms, is displaced toward the centre of curvature of the grains on the convex side of the boundary. From a macroscopic point of view, the driving force for grain growth is the reduction of the free energy of the solid that accompanies the decrease of the area of the grain boundaries it contains.

The grain growth phenomenon affects the fission gas release in three ways. First of all, grain boundary sweeping provides another mechanism for the collection of the fission gas at these internal surfaces from which release can occur, in addition to diffusion as described in the previous section. The collection results from the fact that fission gas is almost insoluble in the fuel matrix, hence the sweeping grain boundary does not redeposit any gas in the newly-formed crystal behind it. The moving grain boundary acts as a fission gas filter. This effect is taken into account by adding a supplementary fractional release term (f) from the matrix to the grain boundaries that is equal to the volume fraction of the fuel swept by the moving boundaries:

$$f = \frac{r_{i+1}^3 - r_i^3}{r_i^3}$$

where the indices i and i+1 refer to the previous and present time, respectively.

The volume fraction swept by the moving grain boundaries corresponds to the volume fraction of the small grains that disappear in favour of the larger ones, which results in the increase of the average grain size. The model for grain growth that is being applied in TRANSURANUS code is based on that of Ainscough [14 in main text].

Secondly, the diffusion distance for the fission gas atoms created in the grains increases. Unlike the first consequence this tends to reduce the release rate. Thirdly, the grain growth also reduces the capacity of the grain boundaries for storing fission gas as their total surface-to-volume ratio is decreasing. The second and third effect were already accounted for in the previous model for thermal fission gas release that was solely based on release by diffusion as described in the previous section.

Athermal release

A temperature-independent (athermal) component of fractional fission gas release ($f_{athermal}$) is calculated, applying the empirical relation recommended by Mr Turnbull in the FUMEX CRP:

$$f_{athermal} = a.Bu$$

Athermal release from the HBS

When the local burnup in the fuel proceeds through an interval of 60–75 MW·d/kgHM, the HBS is formed in the corresponding fuel zones. For a local burnup above Bu_1 = 75 MW·d/kgHM, the model assumes a transfer of a fraction of the fission gas from the grains into the HBS, driven by a burnup dependent rate equation. In agreement with the conclusions of the "International Workshop on the High-Burnup Structure in Nuclear Fuels" held at ITU in June 2004, the fission gas is first retained in the HBS. As soon as the local burnup exceeds an additional empirical threshold (present standard value: Bu_2 = 85 MW·d/kgHM), the HBS is assumed to be saturated, i.e. all additional arriving fission gas is immediately released to the free volume. It should be emphasised, however, that the mechanism of release is not fully understood and the "saturation approach" itself is still a subject of discussion. A number of experiments (e.g. in the High-Burnup Rim Project) show close to 100% retention of fission gas in the HBS up to a burnup of 100 MW·d/kgHM.

REFERENCES

[1] GITTUS, J., MISFELDT, I., KOLSTAD, E., Water-reactor Computer-codes which Model Behaviour During Normal- and Transient-Operation, Consultants Report, IAEA, International Working Group on Water Reactor Fuel Performance and Technology, Proceedings of a Specialists Meeting, Bowness-on-Windermere IWGFTP/**19** (1984) 15–62.

[2] INTERNATIONAL ATOMIC ENERGY AGENCY, Development of Computer Models for Fuel Element Behaviour in Water Reactors, Survey Report, IAEA-TECDOC-415, IAEA, Vienna (1987).

[3] MISFELDT, I., The D-COM blind problem on fission gas release, IAEA, International Working Group on Fuel Performance and Technology for Water Reactors, OECD-NEACSNI/IAEA Specialists' Meeting on Water Reactor Fuel Safety and Fission Product Release in Off-Normal and Accident Conditions, Risø National Laboratory, IWGFTP/**16** (1983) 411–422.

[4] INTERNATIONAL ATOMIC ENERGY AGENCY, International Working Group on Fuel Performance and Technology for Water Reactors, OECD-NEA-CSNI/IAEA Specialists Meeting on Water Reactor Fuel Safety and Fission Product Release in Off-Normal and Accident Conditions, Risø National Laboratory, IWGFTP/**16** (1983).

[5] INTERNATIONAL ATOMIC ENERGY AGENCY, International Working Group on Fuel Performance and Technology for Water Reactors. Water-reactor Computer-Codes and Model Behaviour During Normal- and Transient Operation, Consultants Report, Proceedings of a Specialists' Meeting, Bowness-on-Windermere, IWGFTP/**19** (1984) 63–165.

[6] INTERNATIONAL ATOMIC ENERGY AGENCY, Fuel Modelling at Extended Burnup. A Report of the Co-Ordinated Research Programme on Fuel Modelling at Extended Burnup – FUMEX, IAEA-TECDOC-998, IAEA, Vienna (1998).

[7] OECD/NEA Proceedings of the Seminar on Thermal Performance in Light Water (High Burnup) Fuels, Cadarache, (1998).

[8] OECD/NEA Proceedings of the Seminar on Fission Gas Behaviour in Water Reactor Fuels, Cadarache, (2000).

[9] OECD/NEA Proceedings of the Seminar on Pellet-Clad Interaction in Water Reactor Fuels (PCI-2004), Cadarache, (2004).

[10] VITANZA C., KOLSTAD E., GRAZIANI U., Fission Gas Release from UO_2 Pellet Fuel at High Burnups; ANS Topical Meeting on LWR Fuel Performance, Portland (1979).

[11] OWAKI M. et al., "Development of thermal-mechanical analysis code for high burnup fuel," Nuclear Fuel Behaviour Modelling at High Burnup and its Experimental Support. IAEA-TECDOC-1233, IAEA, Vienna (2000) 375.

[12] LASSMANN K., WALKER C. T., v. d. LAAR J., LINDSTRÖM F., Modelling the High Burnup UO_2 Structure in LWR Fuel, J. Nucl. Mat., Vol. **226**, (1995), 1–8.

[13] RONCHI, C., VAN UFFELEN, P., JONNET, J. International Workshop on the High Burnup Structure in Nuclear Fuels (CD-ROM). S.P.K.04.157/2004. Special publication of the European Commission, Joint Research Centre. RNK: SP-31, Karlsruhe, (2004).

[14] AINSCOUGH J. B., OLDFIELD B. W., WARE J. O., Isothermal Grain Growth Kinetics in Sintered UO_2 Pellets, J. Nucl. Mat., Vol. **49**, (1973), 117–128.

[15] MERTENS L. et al., HBS Development in MOX Fuel. International Workshop on the High Burnup Structure in Nuclear Fuels, (CD-ROM). S.P.K.04.157/2004. Special publication of the European Commission, Joint Research Centre. RNK: SP-31, Karlsruhe, (2004).

[16] LÖSÖNEN P., Proceedings of the International Topical Meeting on LWR Fuel Performance, Park City, UT, (2000).

[17] KINOSHITA M. et al., High-Burnup Rim Project: (III) Properties of rim-structured fuel, International Meeting on LWR Fuel Performance, Orlando (2004), paper 1102.

[18] BERNARD L.C. et al., An efficient model for the analysis of fission gas release, J. Nucl. Mat. **302** (2002) 125–134.

ABBREVIATIONS

BOL	beginning of life
Bu	burnup
BWR	boiling water reactor
CANDU	Canadian type pressurised heavy water reactor (Canadian Deuterium Uranium)
CRP	coordinated research programme
EOL	end of life
EPMA	electron probe microanalysis
FCT	fuel centre temperature
FD	finite difference
FE	finite element
FGR	fission gas release
HBEP	high burnup effects programme
HBS	high burnup structure
HWR	heavy water reactors
IFPE	International Fuel Performance Experiments database.
IWGFPT	International Working Group on Fuel Performance and Technology
LOCA	loss of coolant accidents
LWR	light water reactor
mli	mean linear intercept (technique for grain size determination)
MOX	mixed oxide fuel
MTR	materials test reactor
NSC	nuclear science committee of the OECD/NEA
PCI	pellet clad interaction
PCMI	pellet clad mechanical interaction
PHWR	pressurized heavy water reactor
PIE	post irradiation examination
PWR	pressurized water reactor
RCM	research coordination meetings
RIA	reactivity insertion accidents
WWER	Russian designed pressurised light water reactor
XRF	X ray fluorescence

ANNEX I

FIRST RESEARCH COORDINATION COMMITTEE MEETING ON IMPROVEMENT OF MODELS USED FOR FUEL BEHAVIOUR SIMULATION (CRP FUMEX-II)

16–19 December 2002

This was the first meeting of the FUMEX-II Exercise and its participants. FUMEX-II is a successor to the first FUMEX exercise and takes the form of coordination between a code improvement exercise and the NEA/IAEA International Fuel Performance Experiments (IFPE) database. The dual advantages of this cooperation are:

- Exposure of code developers to a wide ranging database.
- Assistance in qualification of the IFPE database, correction of errors and detection of missing data, brought about by use of the database for comparison of predictions with data by a large number of workers.

The first part of the meeting was devoted to a review and discussion of the IFPE Database with the second part of the meeting devoted to the FUMEX-II exercise and presentations made by participants. The agenda of this four-day meeting is attached to this report.

Following extensive discussion, conclusions and recommendations regarding the IFPE Database can be summarized as follows:

- The interest of the users, not only at this meeting, shows that a continued need exists for the service and functions provided by the IFPE.
- Concerns expressed as to the proper functioning of the IFPE were related to:
    - Funding, resources to maintain/extend/qualify the data base.
    - Procedures for feedback and notification of updates.
- Proposals for improvements included:
    - Extend the description chapters to include more information on uncertainties if available.
    - Models (as such, or correlations for older materials); note however that this suggestion was not unanimously agreed.
    - Data assumed by users to fill gaps in information provided.
    - User experience in general.
    - Alternative (un)condensed histories.
    - IFPE should concentrate on fuels having rod geometry, but inclusion of non-standard fuel variants with this geometry are welcome (e.g. MOX, disprosium doped fuel).
    - Separate effects experiments not closely linked to an irradiation history will be considered on a case by case basis.

The first part of the meeting was concluded by a distribution of a CD-Rom to all participants containing the cases to be used in the FUMEX-II exercise.

From presentations made at the meeting, it was concluded that great progress had been made in code development since the end of FUMEX. Also, it was clear that the first FUMEX exercise had been extremely valuable since many codes had benefited tremendously by having access to the data provided. A questionnaire had been distributed to the 19 participants of the first exercise to provide guidance as to the cases that would further benefit their code development and validation. From the 15 responses received, a list of potential cases was drawn up by a panel of experts at a meeting held in

Vienna 26–29 November 2001; the list of cases is given here in Table I–1. From this list, participants in FUMEX-II were requested to perform calculations for the six cases identified as high priority in Table I–1 and a minimum of a further 4 cases at their discretion. In order to familiarize participants with the cases from the IFPE database, a presentation was made detailing these cases and outlining the particular benefit associated with them.

Subsequent to constructing the list of cases given in Table I–1, it was found that a number of cases were not available. In particular, the CEA GONCOR dataset was not available and data for the HATAC and REGATE experiments were offered as substitutes. These are both cases where fuel had been base irradiated in French commercial reactors before ramping in the CENG Siloe reactor. The data they provided were: fission gas release (FGR), cladding diameter measurements, EPMA of fission product distributions and further PIE. It was agreed that both experiments should be included in the FUMEX-II list of cases and the datasets would be provided to the IAEA by early 2003. It was agreed that REGATE would be a high priority case whilst predictions against HATAC were at participant's discretion.

The original list also included WWER fuel irradiated in the Kola-3 reactor and ramp tested in the MIR test reactor. Unfortunately, agreement had not been obtained for the release of the data from the ramp tests. However, they were considered of importance particularly to participants with WWER codes, therefore they were retained in the list of cases with the hope that release would be achieved within the timescale of the programme.

It has not been possible to obtain real histories and data for RIA and LOCA cases 24 and 25 respectively. It was agreed that these were extremely useful for testing transient codes. Kamimura (NUPEC) and Sartori (NEA) agreed to investigate the possibility of obtaining these data or idealized cases.

Case 26 identified several simplified histories which would test code application to very high burnup, these are:

- 26(1) to define the locus of the centre temperature/burnup threshold for 1% FGR;
- 26(2a) to calculate FGR for an irradiaton history of 15 kW/m constant power up to 100 MW·d/kgU;
- 26(2b) to calculate FGR for an irradiation history of 20 kW/m at BOL falling linearly to 10 kW/m at 100 MW·d/kgU;
- 26(2c) to calculate FGR for an idealized history supplied by BNFL.

At the meeting it was agreed to add a further case 26(2d) to be supplied by FANP which would be an idealized high burnup history for which a range of FGR measurements were available.

It was noted that 5 participants were concerned with the operation of CANDU type reactors and this system was not represented in the FUMEX-II list of cases. Because CANDU elements did not have a plenum, FGR and rod internal pressure was of concern for advanced reactor design and operating regimes. It was agreed that a further two idealized cases were to be included in the list to remedy the omission.

A revised list of cases with new numbering is given in Table I–2; these new numbers supersede those in Table I–1.

The FUMEX-II programme is scheduled to take place within the period 2002 through to 2006 when the final report will be issued. There will be two further RCMs, one in 2004 and the last one in late 2005 or early 2006. It was agreed that there was merit in defining a small number of cases to be tackled by participants as soon as possible with the results communicated to the IAEA by September 2003. In this way, an interim meeting held in conjunction with another meeting, e.g. the PCI workshop to be held at Cadarache, could be used for presentation and a discussion of these findings. The cases agreed were:

- IFA-597 rod 8, thermocouple temperature versus local power in first ramps.
- Risø 3 rod AN3, thermocouple temperature versus local power in first ramps.
- Risø 3 rod AN4, thermocouple temperature versus local power in first ramps.
- Cases 27(1), 27(2a) and 27(2b), FGR versus burnup to 100 MW·d/kgU.

Participants were urged to perform and report these and as many cases as possible if time and effort permitted. The form of the data reply would be either MS EXEL spreadsheets or ASCII files tabulating temperature (°C) versus local power (kW/m) or FGR (%) versus Burnup (MW·d/kgU) as appropriate.

It was agreed that the best method of communication between participants and the IAEA was by means of a group e-mail circulation. In this way, all participants would be kept informed of questions and responses.

Finally, the inter-agency cooperation, with the link between the FUMEX-II CRP and the IFPE as a practical example, was judged to be very useful by the participants of the IAEA-NEA meeting.**List of Actions**

(1) C. Struzik (CEA): To supply datasets for REGATE and HATAC by end of February and March 2003 respectively.
(2) G. Rossiter (BNFL): To supply by end of February 2003 the BNFL specification of the BNFL notional simplified case identified for case 27.
(3) F Sontheimer (FANP): To supply by mid-2003 the FRAMATOME specification for the idealized high burnup dataset identified for case 27.
(4) K. Kamimura (NUPEC): Agreed to contact JAERI to investigate the possibility of obtaining either a ‘real’ or idealized dataset for the RIA case 25.
(5) E. Sartori (NEA): Agreed to investigate the possibility of obtaining a dataset for the LOCA case 26.
(6) M. Tayal (AECL): Agreed to supply by end of May 2003 two notional CANDU cases to investigate the effect of power on FGR.
(7) F. Sokolov (IAEA): To set up an e-mail group “FUMEX-II” as soon as possible to assist communication between participants, each other and the IAEA.
(8) Expert panel: To finalize as soon as possible the specification of the simplified cases in case 27.
(9) Expert panel: To define output requirements and format for submission of predictions of all cases to the IAEA.

TABLE I–1. ORIGINAL LIST OF PROPOSED CASES FOR FUMEX-II

No	Case identification	Measurements made for comparison
1.	Halden IFA 534.14, rod 18	EOL FGR and pressure, grain size 22 μm, Bu ≈ 52 MW·d/kgUO_2
2.	Halden IFA 534.14, rod 19	EOL FGR and pressure, grain size 8.5 μm, Bu ≈ 52 MW·d/kgUO_2
3.	**Halden IFA 597.3, rod 7**	**Cladding elongation, at Bu ≈ 60 MW·d/kgUO_2**
4.	**Halden IFA 597.3, rod 8**	**FCT, FGR at Bu ≈ 60 MW·d/kgUO_2**
5.	Halden IFA 507, TF3	Transient temperature during power increase
6.	Halden IFA 507, TF5	Transient temperature during power increase
7.	GONCOR	FGR and cladding diameter during and after transient at Bu ≈ 48 MW·d/kgUO_2
8.	Kola-3, rod 7 from FA222	FGR, pressure and creepdown at Bu ≈ 55 MW·d/kgUO_2
9.	Kola-3, rod 52 from FA222	FGR, pressure and creepdown at Bu ≈ 46 MW·d/kgUO_2
10.	Kola-3, rod 86 from FA222	FGR, pressure and creepdown at Bu ≈ 44 MW·d/kgUO_2
11.	Kola-3, rod 120 from FA222	FGR, pressure and creepdown at Bu ≈ 50 MW·d/kgUO_2
12.	Risø-3 AN2	Radial distribution of fission products and FGR-EOL, Bu ≈ 37 MW·d/kgUO_2
13.	**Risø-3 AN3**	**FGR and pressure-EOL, FCT, Bu ≈ 37 MW·d/kgUO_2**
14.	**Risø-3 AN4**	**FGR and pressure-EOL, FCT, Bu ≈ 37 MW·d/kgUO_2**
15.	HBEP, rod BK363	FGR-EOL, Bu ≈ 67 MW·d/kgUO_2
16.	HBEP, rod BK365	Fission products and PU distribution, FGR-EOL, Bu ≈ 69 MW·d/kgUO_2
17.	HBEP, rod BK370	Fission products and Pu distribution, FGR-EOL, Bu ≈ 51 MW·d/kgUO_2
18.	TRIBULATION, rod BN1/3	Pressure, FGR, cladding creepdown, Bu ≈ 52 MW·d/kgUO_2
19.	TRIBULATION, rod BN1/4	Pressure, FGR, cladding creepdown, Bu ≈ 51 MW·d/kgUO_2
20.	TRIBULATION, rod BN3/15	Pressure, FGR, cladding creepdown, Bu ≈ 51 MW·d/kgUO_2
21.	EDF/CEA/FRA, rod H09	Fission products and Pu distribution, FGR-EOL, Bu ≈ 46 MW·d/kgUO_2
22.	Kola-3 + MIR test	Temperature during ramp, FGR-EOL, Bu ≈ 55 MW·d/kgUO_2
23	Kola-3 + MIR test	Pressure-EOL, Bu ≈ 55 MW·d/kgUO_2
24.	RIA	to be specified (real data or simplified case)
25.	LOCA	to be specified (real data or simplified case)
26.	**Simplified case**	**Temperature vs. Bu for onset of FGR (draft available)**

Note: the cases of high priority are shown in bold.

TABLE. I–2 REVISED LIST OF CASES

No.	Case identification	Measurements made for comparison
1.	Halden IFA 534.14, rod 18	EOL FGR and pressure, grain size 22 μm, Bu ≈ 52 MW·d/kgUO_2
2.	Halden IFA 534.14, rod 19	EOL FGR and pressure, grain size 8.5 μm, Bu ≈ 52 MW·d/kgUO_2
3.	**Halden IFA 597.3, rod 7**	**Cladding elongation, at Bu ≈ 60 MW·d/kgUO_2**
4.	**Halden IFA 597.3, rod 8**	**FCT, FGR at Bu ≈ 60 MW·d/kgUO_2**
5.	Halden IFA 507, TF3	Transient temperature during power increase
6.	Halden IFA 507, TF5	Transient temperature during power increase
7.	**REGATE**	**FGR and cladding diameter during and after a transient at Bu ≈ 47** MW·d**/kg**
8	HATAC	FGR and cladding diameter during and after a transient at Bu ≈ 49 MW·d/kg
9.	Kola-3, rod 7 from FA222	FGR, pressure and creepdown at Bu ≈ 55 MW·d/kgUO_2
10.	Kola-3, rod 52 from FA222	FGR, pressure and creepdown at Bu ≈ 46 MW·d/kgUO_2
11.	Kola-3, rod 86 from FA222	FGR, pressure and creepdown at Bu ≈ 44 MW·d/kgUO_2
12.	Kola-3, rod 120 from FA222	FGR, pressure and creepdown at Bu ≈ 50 MW·d/kgUO_2
13.	Risø-3 AN2	Radial distribution of fission products and FGR-EOL, Bu ≈ 37 MW·d/kgUO_2
14.	**Risø-3 AN3**	**FGR and pressure-EOL, FCT, Bu ≈ 37 MW·d/kgUO_2**
15.	**Risø-3 AN4**	**FGR and pressure-EOL, FCT, Bu ≈ 37 MW·d/kgUO_2**
16.	HBEP, rod BK363	FGR-EOL, Bu ≈ 67 MW·d/kgUO_2
17.	HBEP, rod BK365	Fission products and PU distribution, FGR-EOL, Bu ≈ 69 MW·d/kgUO_2
18.	HBEP, rod BK370	Fission products and Pu distribution, FGR-EOL, Bu ≈ 51 MW·d/kgUO_2
19.	TRIBULATION, rod BN1/3	Pressure, FGR, cladding creepdown, Bu ≈ 52 MW·d/kgUO_2
20.	TRIBULATION, rod BN1/4	Pressure, FGR, cladding creepdown, Bu ≈ 51 MW·d/kgUO_2
21.	TRIBULATION, rod BN3/15	Pressure, FGR, cladding creepdown, Bu ≈ 51 MW·d/kgUO_2
22.	EDF/CEA/FRA, rod H09	Fission products and Pu distribution, FGR-EOL, Bu ≈ 46 MW·d/kgUO_2
23.	Kola-3 + MIR test	Temperature during ramp, FGR-EOL, Bu ≈ 55 MW·d/kgUO_2
24	Kola-3 + MIR test	Pressure-EOL, Bu ≈ 55 MW·d/kgUO_2
25.	RIA	to be specified (real data or simplified case)
26.	LOCA	to be specified (real data or simplified case)
27	**Simplified case**	**(1) Temperature vs. Bu for onset of FGR**
		(2a) FGR for constant 15 kW/m to 100 MW·d/kgU
		(2b) FGR for 20 kW/m at BOL decreasing linearly to 10 kW/m at 100 MW·d/kgU
		(2c) FGR for idealized history supplied by BNFL
		(2d) FGR for idealized history supplied by FANP
		(3a) FGR for CANDU idealized history
		(3b) FGR for CANDU idealized history

Note: high priority cases are in bold.

ANNEX II

NOTES OF THE SECOND RESEARCH COORDINATION MEETING OF THE FUMEX-II COORDINATED RESEARCH PROJECT, HELD AT HALDEN, NORWAY, 7–10 SEPTEMBER 2004

The meeting was attended by representatives of the 14 fuel-modelling teams which have been participating in the CRP since its inception, as well as three additional teams from Bulgaria, Switzerland and the UK.

Tuesday 7, September

The first day, Tuesday, 7 September, was started with welcomes to the participants from W. Wiesenack, Project Manager of the OECD Halden Reactor Project, which was hosting the meeting and from the traveller on behalf of the IAEA.

Turnbull then gave an overview of the current status of the International Fuel Performance Experimental Database (IFPE) and an overview of the reasons for choosing the priority cases for the FUMEX-2 studies.

J. Killeen gave a report on the discussions held during a FUMEX meeting and the PCI seminar held at Aix-en-Provence in March 2004. The FUMEX meeting had been a consultancy meeting, which had been attended by many, but not all, of the FUMEX participants. There had been discussions on progress, shortfalls in data and the status of the IFPE. Priorities had been discussed, and it was felt that progress was acceptable, and that any additional work should be discussed at the 2nd RCM. A questionnaire was to be circulated to participants to inform discussions at the RCM. The PCI seminar had considered many issues of relevance to fuel modelling, with sessions covering:

- Conditioning of fuel;
- Ramp rate restrictions;
- Low power operation limits;
- Frequent fault (class II) analysis;
- Core design constraints;
- Load follow.

The issues discussed of main interest for the FUMEX-2 Project and which still remain subject to considerable uncertainties, were:

- Rim effect modelling, which included:
  - Swelling;
  - Fission gas release;
  - Interlinkage in the rim zone.
- PCI modelling, which included discussions on:
  - Mechanistic models;
  - Empirical rules;
  - New fuel types.

Sim presented the results obtained with the Canadian ELESTRES code. He explained that the code had been in use for safety assessment of CANDU reactors since 1981. He had not calculated cases that were not directly relevant to CANDU experience or were outside the range of operation expected for the advanced CANDU reactor design. He explained that the low burnup and high ratings of CANDU

plant for which ELESTRES is designed, meant that the code was not an appropriate tool to investigate high burnup BWR/PWR fuel types.

Mr Kim described the results obtained with the INFRA code from the Republic of Korea, including the six priority cases, but not the CANDU cases 27(3). The results were good, but relied in some cases on empirical fitting of a friction parameter to allow modelling of rod elongation of the Halden IFA 597.3 fuel rod 7 (case 3).

Mr Dutta showed the results from the Indian codes FAIR and PROFESS. He demonstrated the graphic capabilities of his code system, which allowed the large volume of code output to be directly visualised in a large number of ways. He noted that his fission gas predictions for the REGATE tests were low.

Mr Marino (Argentina) noted that he had had problems with some predictions with the BACO code, and that he could not get convergence for case 27(2d), the idealized FANP case. These cases are a rather severe test of a code that was not initially set up to consider such extended histories. He said that he found the FUMEX exercise helpful, he had eliminated bugs in the code and was reviewing his fission gas model.

The results presented by Mr Khvostov (Russian Federation) from the START-3 code were generally in good agreement with the experimental data. An important feature of the modelling was the importance of the rim region for fission gas release. His model predicts that the majority of fission gas release can come from the rim in high burnup cases, such as the idealized cases 27(2a) and (2b). Another important issue for his modelling was the power profile during irradiation, and he requested that as much power information as possible should be provided in the data (e.g. neutron spectrum).

Mr Chen from China, did not have results of code calculations to present, so presented details of his model of the temperature response of a fuel element and coolant under transient conditions.

The first day ended with a discussion on the modelling issues arising for CANDU based codes and the CANDU idealized histories. Mr Sim chaired the session and gave an overview of the fuel problems that are of concern to CANDU plant. There is no rim effect due to the low burnups in CANDU reactors. The discussion considered the high temperature creep rates, as CANDU fuel is operated at higher temperatures than are typical for LWR fuel. Discussion of the reasons for the low temperatures predicted for the idealized case 27(1) led to the suggestion that the lack of a re-solution effect in the CANDU codes would lead to over-predictions of low temperature release, which is not a CANDU concern. It was noted that the behaviour of CANDU fuel is similar to fast reactor fuel and that issues such as columnar grain growth need to be modelled. This modelling was seen as of interest to other modellers, and Mr Sim was asked to provide references to details of the modelling for wider distribution.

Clad integrity issues were also discussed as well as models of densification and the importance of densification resistance for CANDU fuel.

Wednesday 8 September

On the Second day, Wednesday, there were further participant presentations. The first was from Mr Rossiter (UK) who described the results from the ENIGMA-B code. Unlike START-3, ENIGMA does not consider gas release to be enhanced from a rim region, the only effect of this region is a thermal effect due to the porosity effect on thermal conduction. He reported that he under-predicted the releases from IFA 597 (cases 3 and 4), end of life releases were correct, but the release from the ramp was too small. There was also some under-prediction for the other priority cases, but the results were shown in the context of the wider calibration data base for ENIGMA, and the results were seen to lie within the expected prediction scatter. Mr Sontheimer commented on the under-prediction of IFA 597, which was also seen in his results, and he pointed out that there had been unusual corrosion reported in the data and that perhaps there had been poor heat transfer in consequence that was not being modelled.

Mr Lemehov from Belgium, reported that he had worked with FRAPCON 3.2, FEMAXI V-1m and MACROS II. The results from the MACROS code were the main ones presented, as FEMAXI was not well suited to dealing with refabricated fuel rods. His results included a lot of detailed predictions for

the location of fission gas within a pellet and for the isotopic composition of the released gas. He stated his conviction that there was no additional gas release from a rim region, noting experimental results for the isotopic composition of released gas that supports a theory of fission gas release from the pellet centre, not its edge. This initiated a discussion, and alternative views of the inferences to be made from the experimental data were expressed.

Mr Moizumi of Japan presented results from FEMAXI-JNES. The code tended to over-predict the temperatures for the experimental cases, and the model of heat transfer through xenon gas was thought to be a possible candidate and was being reconsidered. The predictions for the simplified cases were good and the code overall gave good results with a revised fuel thermal conductivity model. There was seen to be a need to improve the PCMI modelling to improve predictions of clad deformation during ramps.

Mr Valach (Czech Republic) presented the PIN Micro code. He reported that he had had difficulties with numerical stability and he had needed to use fine meshes to ensure convergence. He had carried out considerable fine tuning of the diffusion coefficient used in the code and the results fitted the experimental data reasonably well, though he was unable to complete the BNFL simplified case, 27(2c), due to numerical instabilities at the high burnups.

During discussions, Mr Sontheimer reminded participants that the issue of rim porosity was very important in the understanding of the results from the RISO rods. The porosity was observed to be very high and this may be a reason why so many participants underestimated centre temperatures with these rods during the ramps.

At the end of the morning, by common consent, the agenda was altered and the discussion session was changed from QA issues to be a first discussion on rim effect modelling. Mr Sontheimer led the discussion and created a tabulation, which was used as a basis for debate. Participants described how their codes set about modelling the phenomenon, and a wide range of ideas were evident. These descriptions were put into the table to allow an overview to be obtained.

The afternoon session started with further participant reports. Mr Elenkov (Bulgaria) had calculated 13 cases, including the priority cases, with a WWER version of TRANSURANUS. In particular, he had focussed on calculations of the Kola cases (cases 9, 10, 11 and 12). The results gave a slight under-prediction of the gas release. Mr Lemehov commented that there was a problem with TRANSURANUS for WWER fuel in that the burnup is calculated incorrectly due to neutron spectrum effects and that therefore the fission gas release will also be incorrect. Mr Schubert was asked to clarify the issue.

Ms Paraschiv (Romania) described the DCHAIN-5V code, it included grain boundary sweeping and had a more sophisticated model for fission gas release than TRANSURANUS, though TRANSURANUS was used to provide the thermomechanical input. The thermal modelling was therefore similar to TRANSURANUS, but the fission gas releases were different and generally a little higher, fitting the data better. This presentation highlighted two different reported results for the fractional fission gas release from the IFA 597.3 rod 8 (16% and 20%). Mr Turnbull agreed to investigate the discrepancy.

Mr Nordstroem (Switzerland) presented the results obtained with the PSI version of TRANSURANUS. This version includes its own gas release model, but relies on the standard TRANSURANUS for the thermomechanical calculations. The model was developed for sphere-pac fuel and requires more development, especially for pellet fuel. The gas release model included grain boundary sweeping of fission gas, as well as columnar grain growth, but no athermal gas diffusion or rim effect are used. The code was tested against the idealized cases only and gave reasonable results.

Mr Kelppe (Finland) presented the results from ENIGMA 5.9B, which he said had been performing well for ten years with low burnup fuel, but did not give good results at high burnup. Very low fission gas release was predicted and the practical option had been taken to include an enhancement factor at high burnup.

The day ended with a second discussion session on the rim effect and how it is modelled. Mr Sontheimer again led the discussion. There was debate about the HBEP rod BK365 and details of the

power history for this rod. It was seen as a good experiment for additional modelling. There was a further robust exchange of views about the rim effect. It was noted that there was a distinctive increase in fission gas release from high burnup fuel, which could be roughly characterised as 3% FGR for fuel at 80 MW·d/kgU at below 20 kW/m, 10% FGR if the rating was between 20 kW/m and 25 kW/m and up to 40% FGR at higher ratings up to around 100 MW·d/kgU. These additional releases coincided with the appearance of the rim structure in Post Irradiation Examination studies. At least four distinctly different approaches to modelling the effect of enhanced release at high burnup were apparent Firstly some modelled significant additional release from the rim and fuel surface, with the majority of the "additional" release coming from this region. Others treated high burnup fuel as having exhausted a solubility limit, which ensured an additional release from regions where gas generation was high whilst, others treated the rim region as a thermal barrier leading to increased temperatures and release. Finally there were simple empirical enhancement factors applied for high burnup fuel. There was discussion of what experimental data could be found to help, and IFA 665 at Halden was discussed. This experiment is intended to go to 100 MW·d/kgU with a possible extension to 120 MW·d/kgU.

Thursday 9 September

On the third day, Thursday 9September, Mr Wiesenack gave a presentation of the instrumentation and experimental facilities used at the Halden Reactor. After his talk, there were the last three participant presentations. Mr Schubert presented the work done by the TRANSURANUS development team. He said that there was an empirical approach to the rim effect, which was a function of burnup. There was a threshold at 60 MW·d/kgU followed by saturation of gas in the lattice at around 85 MW·d/kgU and release. There is no grain size modelling at high burnup, though there was some evidence that a large grain size delayed the onset of the high burnup structure. TRANSURANUS was predicting clad lift off for the BNFL simplified case, 27(2c), and under-predicted the FANP case, 27(2d) and the Risø cases (14 and 15) by around a factor of 2.

Mr Sontheimer then presented the results obtained from a development version of the Framatome-ANP code, which is still to be named. His code did not model enhanced release from a rim region, all release is assumed to come from the pellet centre, and he believed that the experimental data on fission gas distributions supported this approach. Release in this model is normal thermal diffusion with an additional release due to the assumption of a burnup and temperature dependent solubility limit of fission gas, additional gas generated in such regions is assumed to be released immediately. For high burnups, around 30% of the total calculated release comes from the additional, solubility limit term. The code predictions were good for the simplified cases, particularly so for the FANP case, 27(2d), which was derived from real fuel histories that were used to help develop the code. There was a small overprediction for the IFA 597 cases (cases 3 and 4), but the code generally gave good predictions for both the simplified cases and the real experimental cases.

Finally Ms Stefanova gave results for Bulgarian versions of the PIN code PINw99 and PIN2k. Results were presented for the simplified cases, excluding the CANDU cases, and for the Kola and REGATE cases. The results were generally reasonable, particularly for the WWER data, but the code could not give a value for the BNFL case, 27(2c), due to thermal feedback problems.

The fourth discussion session was chaired by Mr Rossiter, who gave a short presentation to highlight the issues that are current for ramps and PCI. He highlighted the various options open to improve ramp performance, which include new fuel and cladding materials, which would be a challenge for fuel modelling. There was a good debate on issues such as delayed hydrogen cracking of fuel rods and which irradiated materials properties should be used. The CANDU participants noted that there was a lot of PCI modelling required for licensing with a plastic strain limit below 1%.

In the afternoon a technical visit was made to the Halden reactor project to allow the participants to observe the instrumentation and experimental facilities.

Friday morning, 10 September

The final session on Friday morning, 10 September was devoted to summarizing the current status of the CRP and discussions as to what work should be completed before the CRP concluded. Mr Killeen presented some summary slides, showing the combined results from many participants for several of

the priority cases. This highlighted areas where there are wide differences in code predictions and it is possible to see the effect of some of the models discussed earlier in the week on the predictions, for example, different codes using similar modelling assumptions for the high burnup region tending to give similar predictions.

Mr Killeen also summarized the discussion sessions, noting that the CANDU session had highlighted:

- high power for CANDU fuel,
- no plenum,
- low burnup,
- fission gas re-solution was not a CANDU issue,
- high temperature models included:
  - columnar grains,
  - grain boundary sweeping,
- clad integrity - CANDU uses collapsible cladding,
- asymmetric temperature profiles occur in candu,
- densification resistance of fuel is a key parameter.

So far comparative data is not available, but idealized cases look very useful to assure code capability at high powers and those participants who had not yet attempted the CANDU cases were encouraged to do so.

The sessions on high burnup issues had highlighted:

- Rim modelling was a key issue and there was a lot of disagreement on its effect.
  - What is the rim? Temp and BU definition.
  - Releases a fraction of the gas?
  - Releases over-saturated gas?
  - Does not release gas?
- Temperature modelling has improved, but:
  - what is the degradation of thermal conductivity at very high burnup?
- Evidence is still required to help discriminate between models:
  - experimental evidence is still not definitive,
  - experiments suggest that the rim zone retains gas, but alternative explanations of the observed isotopic ratios and EPMA are tenable.

The discussion on PCI raised issues that:

- data requirements remain important,
- it is difficult to extrapolate modelling to new materials,
- there is no full understanding as to why some fuel types seem to be PCI resistant.

Mr Killeen concluded by presenting the timescales and work requirements to ensure that all participants have completed their studies and are able to report fully at the final RCM in December 2005.

Mr Schubert and Mr Turnbull then chaired the discussion, with Mr Schubert presenting a few slides to start the debate. He noted that fuel temperatures are, in general, well predicted, which is a great improvement from the results obtained during FUMEX CRP. It is important to calculate a burnup dependent radial power profile, so as to determine the Pu build-up at the pellet rim and hence the local

power, but questions remained on the effect of this region and if separate treatment was needed. Also it was necessary to model the conditions for the formation of the rim structure, considering issues such as burnup, temperature limits, pressure, grain size, dopant or other features.

At high burnup, data show an up-swing of fission gas release at high burnup which correlates reasonably well with the observation of the onset of the rim region. Four approaches to modelling this up-swing were discussed:

(1) Fission gas release contribution directly from the rim:

- what is the magnitude of this contribution?

(2) Burnup dependent diffusion parameters for fission gas release:

- diffusion coefficient,
- irradiation re-solution.

(3) Limiting saturation concentration of Xe in the matrix that is burnup and temperature dependent.

(4) The rim structure acts as a thermal barrier, increasing central temperatures and release.

The result was that two distinct trends were seen in the predictions. Models that released gas from the rim zone tended to predict release in excess of 1% (The Vitanza criterion) when a particular burnup was reached, independent of temperature, whilst other models predicted a Vitanza criterion curve that gave a monotonic decrease in the fuel temperature at which 1% release was found as a function of burnup. There was a discussion of the usefulness of the Vitanza threshold at high burnups, where there is a lot of recoil and knock-out which give a high contribution to the 1% release criterion. Suggestions were made to review the calculations for the priority case 27(2b), 15 kW/m constant power, and see if it is possible to separate out the components of the code predictions to help to derive an alternative to the Vitanza threshold for high burnup use, if appropriate.

There was much discussion about the nature of the rim region and how it should be addressed, whether there was bonding or how fuel surface roughness could be modelled, what was the effect of the solid fission products on the bubble surface energy and if the rim should be treated as a porous material, or as a solid with pores. Mr Schubert agreed to make available material from the recent meeting at Karlsruhe, concerning the rim region.

Mr Sontheimer noted that the idealized FANP case, 27(2d), was in fact an idealized history of real fuel rods and the quoted fission gas release values were obtained from high burnup rods. He was asked if it would be possible to release further high burnup data. It was also noted that Halden had some high burnup data from IFA 515, a low temperature experiment, but this data may not be able to be released at the present.

Additional cases from the FUMEX list of cases were identified as useful in helping to allow the modellers to discriminate which would be a good approach to modelling high burnup. In particular it was suggested that cases 1, 2 and 17 were well suited and it was agreed that these should be priority cases for the next period of the CRP. For the WWER modellers, cases 9 and 11 were identified as priorities.

The next topic for discussion was that of PCI which is seen as difficult to treat, and it was suggested that at the present it was best to use empirical models of swelling and densification and validated correlations.

Actions and outstanding queries from the discussions

- Mr Turnbull agreed to confirm the measurement of fission gas release from IFA597.3 rod 8.
- Mr Sim was asked to provide information on the columnar grain growth models used in CANDU modelling for circulation to participants.

- Mr Schubert was asked to clarify how TRANSURANUS calculated burnup for WWER reactor types, as there are spectrum issues that lead to incorrect burnup and hence gas release predictions.
- Mr Schubert agreed to arrange for the proceedings of the rim effect meeting held at Karlsruhe to be circulated.
- Mr Killeen to talk to Mr Sontheimer about the possibility of the release of additional fission gas measurements from high burnup fuel.
- Mr Killeen to talk to Mr Wiesenack about releasing data from IFA 515.

New priority cases to be modelled before the end of FUMEX-II

(1) IFA 535, FUMEX-II cases 1 and 2. The intention here is to investigate the effect of differing grain size.
(2) HBEP rod BK365, FUMEX-II case 17. This is a good high burnup case (the other HBEP rods, cases 16 and 18 are also considered useful. To be done if practicable).
(3) For WWER modelling FUMEX-II cases 9 and 11 (Kola assembly FA222) are recommended.

ANNEX III

NOTES OF THE THIRD RESEARCH COORDINATION MEETING OF THE FUMEX-II COORDINATED RESEARCH PROJECT, HELD IN VIENNA, 5–8 DECEMBER 2005

OPENING AND PRESENTATIONS

The meeting was attended by all the participating teams.

Mr Ganguly welcomed the participants on behalf of the IAEA.

Mr Turnbull introduced the technical discussions. He noted that the first FUMEX exercise had been a "blind" exercise, and that it had led to the establishment of the IFPE database. FUMEX-II included some 26 cases from the IFPE database. He provided a brief overview of the cases, in particular he discussed:

- IFA 597, 60 MW·d/kgU, low rated with HBS at the rim. Rod 9 failed early, so rods 7 and 8 were taken to higher powers. Rod 8 had a PIE FGR of 15.8%, clad elongation was measured for rod 7.
- Risø AN3 and AN4 provided a comparison between Xe and He fill gas at 36 MW·d/kgU. The test rods were step ramped to 40 kW/m. FGR was measured at operating temperature. The rods had a closed gap, but the Xe filled rod was hotter.
- Case 27 provided several idealized cases to test the Vitanza threshold and the high burnup response of the codes.

Questions were raised about details of the tests, such as the existence of an oxide layer on the REGATE rods and how the 5% gamma heating should be accounted for in defining LHR.

The participants then gave their presentations, starting with Mr Sah from India. He described his code, PROFESS, and the results obtained. He highlighted that he over-predicted temperatures, but was better with the ramps. He had had difficulties with the definitions of burnup and as there was no fuel creep model in his code he found difficulties with some of the dimensional changes. He noted that the temperatures of the FUMEX-II cases were low compared with CANDU experience and his high temperature models were not invoked.

This presentation initiated some discussion on the AN3 and AN4 tests and it was asked why the temperature rise at the end of AN3 but not AN4. Gap contamination was considered as a possible cause.

Mr Kelppe described the ENIGMA5.9 code used in Finland. It was not good at low powers for burnups in excess of 40 MW·d/kgU and he used an empirical FGR model to increase the predictions to get nearer to the measurements. He noted that he had used FRAPCON as well with the FUMEX-II data sets. His colleague Ms Kekkonen described the new code IMAGINE that was also used in Finland and has a mechanistic FGR model. She presented a limited set of results.

The Russian START-3 code was described by Mr Khvostov. He said that there were improvements in the thermal conductivity degradation and radial power models as a result working with the FUMEX cases. The model for gas swelling had been developed before the current CRP, but the FUMEX-II data was valuable in verification and validation. Improvements in the code as a result of FUMEX-II included thermal analysis, radial power distribution and pellet clad contact modelling. He noted a strong effect of oxide thickness and he modelled a significant level of FGR from the HBS at low temperatures.

Mr Chen described the Chinese METEOR code, which was much improved from the previous RCM. He described a stored energy model to explain the formation of the HBS. METOER struggled with numerical stabilities with transient cases and could not handle re-instrumented rod cases. He also had problems with some EOL burnup predictions.

Mr Passage discussed the PINw99 model, where the rim model was empirical. He noted that it was a simple code and not suitable for transient modelling and there was no restart capability to allow work with re-instrumented rods.

The Belgian representative, Mr Sobolov, said that he used three codes; FRAPCON 3.2, a commercial code, FEMAXIV.1 a relatively old version and MACROS-II a quasi- steady state code. Mr Sobolov has tuned the codes to give best predictions of the FUMEX-II cases and achieved best results with the MACROS code.

Mr Elenkov from Bulgaria was involved in developing TRANSURANUS for WWER applications and discussed the effects of the gas swelling models in temperature modelling.

Mr Zymak from the Czech Republic described the use of FEMAXI and PIN2K. He had concerns with the quality of the HBEP data following his comparison of the rods BK 365 and BK 363. He carried out a sensitivity study on the initial gas pressure and plenum dimensions that suggested that the difference between the rods was simply due to the irradiation history and not the fill gas. He noted that the codes had been improved by the FUMEX-II exercise, but the FGR model still needed development.

Mr Nordstroem from Switzerland was also working with TRANSURANUS and was developing a new FGR model. His model was originally developed for Sphere-pac fuel and had been validated against Swiss data. The code does not predict the burst release seen in some cases, but does provide reasonable results for the bump tests.

The Argentinian code, BACO, was presented by Mr Marino. It is a PHWR code validated to 14 MW·d/kgU and he wanted it to be developed for the advanced PHWR fuel, CAREM, being developed in Argentina with a target burnup of 40 MW·d/kgU. The FGR model is empirical and he is using 3-D modelling techniques for temperature and dimensional studies.

The TRANSURANUS code is managed by the European Commission and Mr van Uffelen discussed the work being done to validate the code for use with WWER fuel. He said that there was a new FGR model that was not yet implemented. He noted that there were some difficulties with the restart option in the code. In the FUMEX-II cases the FGR predictions of standard TRANSURANUS were generally low and additional modelling was being considered. He wanted to improve the mechanical modelling as well, and he was using an unrestrained swelling model, modified from MATPRO-11. He also noted concerns with the oxide layer in the REGATE test causing difficulties.

Mr Sontheimer described the AREVA code, COPERNIC. He said that it was validated with a huge commercial database of 2000 rods and PIE. His FGR model for high burnup is based on a xenon concentration limit in the fuel that allows release when exceeded.

The ENIGMA-B code of the UK was presented by Mr Rossiter. The code has no specific high burnup or failure model, relying on mechanistic modelling.

DISCUSSION

Following the presentations, Mr Turnbull chaired a discussion session, discussing each priority case in turn.

27(1) The Vitanza threshold.

This is an engineering limit, based on a wide range of data from the Halden database.

The code developers noted that INFRA had a two stage FGR model that takes time to release gas at low burnup. The release from the HBS becomes significant due to the high concentration of gas there and athermal release with a high diffusion coefficient. FRAPCON also uses athermal release from the HBS and gets a predicted FGR of 1% at a fixed burnup, independent of temperature. There was a long discussion on release from the rim and many codes used information of the rim structure and extent to understand the high releases seen at high burnup. It was noted that the FGR was very sensitive to gap conditions, and other issues such as grain boundary sweeping or hydrostatic stress were also important. Different approaches were taken with grain boundary sweeping, it was noted that grain growth reduced the surface area of the grain boundaries in the fuel, which would decrease the capacity

to store gas, and it was explained that typically around 20% of the fuel volume could be swept by grain boundary movement. Other codes did not use such a mechanism.

The discussion moved to the issue of whether the rim region releases a significant quantity of gas. There were many different views. There is enough gas generated in the rim region in HBS to be able to make a large contribution to overall FGR. Different estimates of the potential release of this gas were around 10–20%, though one code modeller used a mechanistic model for this region and used the observed grain subdivision as an effective enhanced diffusion coefficient and could release a lot of gas with this model. Other possible physical effects that were postulated included a reverse flow of gas from this region to the pellet interior, percolation theories, re-solution, and chemical diffusion. There was no agreed reason to explain even the morphology of the HBS gas bubbles (which are spherical). The experimental data of gas measurements made at the rim was generally agreed to show that the gas was mostly retained within the HBA and was not significantly released, but there were dissenting views which had a different interpretation of the data.

A PHWR modeller noted that at low burnups, the Vitanza threshold did not represent the data and perhaps a limit of 1500°C should be recommended.

Mr Turnbull asked if there should be a uniform value for the diffusion coefficient and what it should be. The modellers used different values, and where there is an understanding that three terms (normal diffusion, athermal and irradiation enhanced) are most likely to exist, many modellers did not use all three terms at all times.

There was concern that the FGR predictions were generally good at low releases but did under-predict at high release values. This led to further discussion of the HBS and its possible impact on properties deeper within the pellet.

Case 27(2) simplified LWR cases

Several codes were not able to reproduce the increase in FGR at the end of the FANP idealized case, for example, TRANSURANUS was only able to get good agreement by including large rim release. Codes that gave good releases included COPERNIC (which is validated against such data) which has a concentration limit in the fuel matrix, and codes that specifically included release from the rim.

HBEP

Mr Sontheimer noted that the HBEP rods were interesting, the power histories gave different high burnup enhancement of FGR; a hot history gave a large enhancement whilst a cold history gave a moderate enhancement. He was asked if his saturation effect was equivalent to an irradiation enhanced diffusion, but Mr Sontheimer noted that strange EPMA profiles were seen after ramps which suggest that the two effects are not equivalent.

Some modellers had problems with the value given for the burnup of the BK rods. It was noted that there were discrepancies in the one data diagram from Batelle. This raised further concerns with the definition of power, Halden always used thermal power–the power through the clad.

REGATE

There was concern with the oxide profile in this experiment. Mr Sontheimer advised that it had arisen from the base irradiation of the segmented rods. There was secondary ridging and the role of the dishes in the pellets needed to be modelled. The release from the transient caused much discussion, some modellers got reasonable results, but others believed that they needed a new transient model, most considering that the transient release was from the grain boundary inventory and that something more than diffusion was required. There was discussion on the effect of HBS, even though there was no evidence of HBS in the pellet body at this burnup it was postulated that pre-HBS grain ghanges can affect high temperature behaviour. Some modellers asked for further detail from the experiment, such as the fast flux, the definition of the grain size–believed to be mean linear intercept–and its distribution.

AN3, AN4

The main interest lay in the temperature overshoots during the step power ramp in these tests. Mr Rossiter said that he could predict some overshoots based on gap closure effects. Mr Sontheimer noted that a large amount of HBS at the rim could have some effect. Mr Turnbull noted that the gap had closed and that the temperatures were very high.

IFA 597

The neutron flux was not given for this experiment. There were also other queries about the data. Ms Paraschiv noted that the heavier rod was quoted as having the lower density, Mr Turnbull believed that the data was accurate.

SUMMARY

Each participant was asked to summarize what had been achieved in the CRP and what further work was necessary.

Mr Elenkov noted big progress since FUMEX CRP, with new models and results , but there were still serious problems; for example why does HBS occur and there is a need to study MOX fuels.

Mr Sim was grateful for the excellent data which was good to allow modelling of integral behaviour. He was interested in separate effects, thermal conductivity, bubble size and grain boundary micro-cracking. He would like to see experimental data on gap size and felt that Gd_2O_3 doped fuel needed modelling.

Mr Sontheimer was very pleased with the results; they provide a good complement to their larger database. There were good data for thermal performance and FGR. For dimensional changes there are bigger uncertainties; bonding, dishing, hour-glassing etc. He has mostly diameter measurements for power rods and the axial measurements are more difficult. He noted that the porosity structures are different at high burnup.

Mr Sah said that FUMEX-II had helped the development of PROFESS. He was interested in the effect of high burnup and the HBS and its effect on FGR. He was interested in detailed microstructural information, particularly on bubble morphology and distribution. He suggested that India might offer some data to allow modelling of PHWR fuel. He listed areas where he needed data to help improve the code, including fuel creep and swelling. He was interested in transient data and MOX fuel.

Mr Kamimura had three requests; one for swelling, ramp and RIA data at above 55 MW·d/kgU, a second for hydrogen data to allow study of cladding phenomena resulting in hydride reorientation and cladding failure. Finally he was interested in MOX fuel, particularly to look at plutonium distribution.

Mr Marino was interested in fuel failures which are due to PCMI. He wanted a future CRP to study clad mechanical properties.

Ms Paraschiv was grateful for the opportunity to work with TRANSURANUS.

Mr Khvostov also noted huge improvements in the codes between FUMEX and FUMEX-II CRPs. For the future he would like to see single effect studies and would like more simplified cases to help understand the effect of the HBS on thermal and mechanical behaviour.

Mr Nordstroem noted that for normal operation the codes are now satisfactory. He had an interest in cladding and LOCA/RIA studies.

Mr van Ufellen noted that FUMEX-II did not include blind cases. He was interested in developments in PCI, LOCA, gadolinia and MOX fuel, but noted that there were other programmes in Europe on MOX and other issues.

Mr Zymak reminded the group that his country had both PWR and WWER reactors and needed to be able to model both types.

Mr Lee said that modelling was about understanding; it was advanced–but not enough. The data provided was good but need more understanding of high burnup behaviour. For FGR he would like

more data, but noted that transient modelling was not required as such operation was not allowed. PCMI was his main problem with enhanced swelling and a bonding layer.

Mr Chen was very positive about FUMEX-II. He had gained a lot of information on heat transfer and the parameters for grain growth. Most of his results were over-predictions. FUMEX-II was important for PCI failure threshold modelling. He was not able to model refabricated rods. He was interested in MOX fuel.

Mr Kelppe liked the simplified cases and noted that not all codes had reached maturity for steady state conditions. He was not interested in MOX, but was in bubble distribution and PCI modelling looking at the boundary conditions. He thought he may need 2-D and 3-D modelling for stress corrosion cracking.

Mr Sartori talked about the IFPE database. There was a lot of information on bubble distributions, particularly form the UK CAGR programme with much information on bubble densities and the response to irradiation conditions. Two MOX datasets were available, one from Argentina and one failed rod from France. There is a Halden solid vs. hollow pellet experiment on MOX fuel that will go to the database. Further, the PRIMO data and ATR data from INL will be available shortly. On gadolinia, he was hoping to obtain release of IFA 585 from Halden. The HATAC data is now available.

There was a discussion of the reporting of FUMEX-II. Issues to be noted included:

- code descriptions,
- end of life statistics,
- note that codes are tuned to a database,
- ensure consistency of presentation of results,
- discuss improvements,
- note that the scatter between codes is improving,
- note that a final FGR does not require the kinetics to be correct,
- simplified cases are very beneficial,
- separate out PHWR codes due to their extreme extrapolations,
- structure report case by case but discuss topics including:
    - pressure dependence,
    - rim growth,
    - Xe/He mixing,
    - effect of rim on swelling,
    - FGR enhancement at high burnup as a function of power history,
    - grain size >50µm is outside range,
- check data issues with REGATE,
- discuss HBS,
- do not “rank” codes.

Open questions included:

- the rim effect and HBS,
- transient release – where does the gas come from? Grain boundary, cracking, sweeping, columnar grain growth?
- definition of power, to include decay heat for transient modelling,
- QA of data in IFPE, concerns with rod II2 from Risø (cf. AN3 and AN4).

TABLE 1 VALIDATED USE OF THE FUMEX-II CODES

Code	Validated to rod average burnup (MW·d/kgU)	Note (target burnups in MW·d/kgU)
BACO	45	60
COPERNIC	100	local burnup
DCHAIN-V	60	
ELESTRES	20	35
ENIGMA5.9 (WWER440 and PWR)	50	65
ENIGMA-B	60	MOX development
FEMAXI	60	
FEMAXI-JNES	60	70
FRAPCON5.2	60	
INFRA	100	development
MACROS	60	
METEOR	<70	
PIN and FEMAXI (WWER)	60	
PINw99	57	
PROFESS	20	need 27 and WWER capability
START-3	70	80
TRANSURANUS	60	75 development
TRANSURANUS-PSI	50	FGR benchmarked

CONTRIBUTORS TO DRAFTING AND REVIEW

Chen, P.	China Institute of Atomic Energy, China
Elenkov, D.	Institute for Nuclear Research and Nuclear Energy, Bulgaria
Kamimura, K.	NUPEC, Japan
Khvostov, G.	A.A. Bochvar Res. Institute of Inorganic Materials, Russian Federation
Kushwaha, H.S.	BARC, India
Lee, C.B.	Korea Atomic Energy Research Institute
Marino, A.	CNEA, Argentina
Nordstroem, A.	PSI, Switzerland
Paraschiv, A.	Institute for Nuclear Research, Romania
Ranta-Puska, K.	VTT, Finland
Rossiter, G.	BNFL, United Kingdom
Sah, D.N.	BARC, India
Sobolov, V.	Nuclear Research Centre SCK CEN, Belgium
Sontheimer, F.	FRAMATOME ANP GmbH, Germany
Stefanova, S.	Institute for Nuclear Research and Nuclear Energy, Bulgaria
Tayal, M.	AECL, Canada
Turnbull, T.	Consultant, United Kingdom
Valach, M.	Nuclear Research Institute, Rez, Czech Republic
van Uffelen, P.	JRC Institute for Transuranium Elements, European Commission
Wiesenack, W.	Halden Reactor Project, Norway

Consultants Meetings

Vienna, Austria: 16–19 December 2002, 5–8 December 2005;
Halden, Norway: 7–10 September 2004;
Aix-en-Provence, France: 9–11 March 2004

IAEA
International Atomic Energy Agency

Where to order IAEA publications

In the following countries IAEA publications may be purchased from the sources listed below, or from major local booksellers. Payment may be made in local currency or with UNESCO coupons.

AUSTRALIA
DA Information Services, 648 Whitehorse Road, MITCHAM 3132
Telephone: +61 3 9210 7777 • Fax: +61 3 9210 7788
Email: service@dadirect.com.au • Web site: http://www.dadirect.com.au

BELGIUM
Jean de Lannoy, avenue du Roi 202, B-1190 Brussels
Telephone: +32 2 538 43 08 • Fax: +32 2 538 08 41
Email: jean.de.lannoy@infoboard.be • Web site: http://www.jean-de-lannoy.be

CANADA
Bernan Associates, 4501 Forbes Blvd, Suite 200, Lanham, MD 20706-4346, USA
Telephone: 1-800-865-3457 • Fax: 1-800-865-3450
Email: customercare@bernan.com • Web site: http://www.bernan.com

Renouf Publishing Company Ltd., 1-5369 Canotek Rd., Ottawa, Ontario, K1J 9J3
Telephone: +613 745 2665 • Fax: +613 745 7660
Email: order.dept@renoufbooks.com • Web site: http://www.renoufbooks.com

CHINA
IAEA Publications in Chinese: China Nuclear Energy Industry Corporation, Translation Section, P.O. Box 2103, Beijing

CZECH REPUBLIC
Suweco CZ, S.R.O., Klecakova 347, 180 21 Praha 9
Telephone: +420 26603 5364 • Fax: +420 28482 1646
Email: nakup@suweco.cz • Web site: http://www.suweco.cz

FINLAND
Akateeminen Kirjakauppa, PO BOX 128 (Keskuskatu 1), FIN-00101 Helsinki
Telephone: +358 9 121 41 • Fax: +358 9 121 4450
Email: akatilaus@akateeminen.com • Web site: http://www.akateeminen.com

FRANCE
Form-Edit, 5, rue Janssen, P.O. Box 25, F-75921 Paris Cedex 19
Telephone: +33 1 42 01 49 49 • Fax: +33 1 42 01 90 90
Email: formedit@formedit.fr • Web site: http://www. formedit.fr

Lavoisier SAS, 145 rue de Provigny, 94236 Cachan Cedex
Telephone: + 33 1 47 40 67 02 • Fax +33 1 47 40 67 02
Email: romuald.verrier@lavoisier.fr • Web site: http://www.lavoisier.fr

GERMANY
UNO-Verlag, Vertriebs- und Verlags GmbH, Am Hofgarten 10, D-53113 Bonn
Telephone: + 49 228 94 90 20 • Fax: +49 228 94 90 20 or +49 228 94 90 222
Email: bestellung@uno-verlag.de • Web site: http://www.uno-verlag.de

HUNGARY
Librotrade Ltd., Book Import, P.O. Box 126, H-1656 Budapest
Telephone: +36 1 257 7777 • Fax: +36 1 257 7472 • Email: books@librotrade.hu

INDIA
Allied Publishers Group, 1st Floor, Dubash House, 15, J. N. Heredia Marg, Ballard Estate, Mumbai 400 001,
Telephone: +91 22 22617926/27 • Fax: +91 22 22617928
Email: alliedpl@vsnl.com • Web site: http://www.alliedpublishers.com

Bookwell, 2/72, Nirankari Colony, Delhi 110009
Telephone: +91 11 23268786, +91 11 23257264 • Fax: +91 11 23281315
Email: bookwell@vsnl.net

ITALY
Libreria Scientifica Dott. Lucio di Biasio “AEIOU”, Via Coronelli 6, I-20146 Milan
Telephone: +39 02 48 95 45 52 or 48 95 45 62 • Fax: +39 02 48 95 45 48
Email: info@libreriaaeiou.eu • Website: www.libreriaaeiou.eu

JAPAN
Maruzen Company, Ltd., 13-6 Nihonbashi, 3 chome, Chuo-ku, Tokyo 103-0027
Telephone: +81 3 3275 8582 • Fax: +81 3 3275 9072
Email: journal@maruzen.co.jp • Web site: http://www.maruzen.co.jp

REPUBLIC OF KOREA
KINS Inc., Information Business Dept. Samho Bldg. 2nd Floor, 275-1 Yang Jae-dong SeoCho-G, Seoul 137-130
Telephone: +02 589 1740 • Fax: +02 589 1746 • Web site: http://www.kins.re.kr

NETHERLANDS
De Lindeboom Internationale Publicaties B.V., M.A. de Ruyterstraat 20A, NL-7482 BZ Haaksbergen
Telephone: +31 (0) 53 5740004 • Fax: +31 (0) 53 5729296
Email: books@delindeboom.com • Web site: http://www.delindeboom.com

Martinus Nijhoff International, Koraalrood 50, P.O. Box 1853, 2700 CZ Zoetermeer
Telephone: +31 793 684 400 • Fax: +31 793 615 698
Email: info@nijhoff.nl • Web site: http://www.nijhoff.nl

Swets and Zeitlinger b.v., P.O. Box 830, 2160 SZ Lisse
Telephone: +31 252 435 111 • Fax: +31 252 415 888
Email: infoho@swets.nl • Web site: http://www.swets.nl

NEW ZEALAND
DA Information Services, 648 Whitehorse Road, MITCHAM 3132, Australia
Telephone: +61 3 9210 7777 • Fax: +61 3 9210 7788
Email: service@dadirect.com.au • Web site: http://www.dadirect.com.au

SLOVENIA
Cankarjeva Zalozba d.d., Kopitarjeva 2, SI-1512 Ljubljana
Telephone: +386 1 432 31 44 • Fax: +386 1 230 14 35
Email: import.books@cankarjeva-z.si • Web site: http://www.cankarjeva-z.si/uvoz

SPAIN
Díaz de Santos, S.A., c/ Juan Bravo, 3A, E-28006 Madrid
Telephone: +34 91 781 94 80 • Fax: +34 91 575 55 63
Email: compras@diazdesantos.es, carmela@diazdesantos.es, barcelona@diazdesantos.es, julio@diazdesantos.es
Web site: http://www.diazdesantos.es

UNITED KINGDOM
The Stationery Office Ltd, International Sales Agency, PO Box 29, Norwich, NR3 1 GN
Telephone (orders): +44 870 600 5552 • (enquiries): +44 207 873 8372 • Fax: +44 207 873 8203
Email (orders): book.orders@tso.co.uk • (enquiries): book.enquiries@tso.co.uk • Web site: http://www.tso.co.uk

On-line orders
DELTA Int. Book Wholesalers Ltd., 39 Alexandra Road, Addlestone, Surrey, KT15 2PQ
Email: info@profbooks.com • Web site: http://www.profbooks.com

Books on the Environment
Earthprint Ltd., P.O. Box 119, Stevenage SG1 4TP
Telephone: +44 1438748111 • Fax: +44 1438748844
Email: orders@earthprint.com • Web site: http://www.earthprint.com

UNITED NATIONS
Dept. I004, Room DC2-0853, First Avenue at 46th Street, New York, N.Y. 10017, USA
(UN) Telephone: +800 253-9646 or +212 963-8302 • Fax: +212 963-3489
Email: publications@un.org • Web site: http://www.un.org

UNITED STATES OF AMERICA
Bernan Associates, 4501 Forbes Blvd., Suite 200, Lanham, MD 20706-4346
Telephone: 1-800-865-3457 • Fax: 1-800-865-3450
Email: customercare@bernan.com · Web site: http://www.bernan.com

Renouf Publishing Company Ltd., 812 Proctor Ave., Ogdensburg, NY, 13669
Telephone: +888 551 7470 (toll-free) • Fax: +888 568 8546 (toll-free)
Email: order.dept@renoufbooks.com • Web site: http://www.renoufbooks.com

Orders and requests for information may also be addressed directly to:

Marketing and Sales Unit, International Atomic Energy Agency
Vienna International Centre, PO Box 100, 1400 Vienna, Austria
Telephone: +43 1 2600 22529 (or 22530) • Fax: +43 1 2600 29302
Email: sales.publications@iaea.org • Web site: http://www.iaea.org/books

12-30461